Order Number 9009761

Protein effects on a model for the activation of a serotonin receptor

Mercier, Gustavo Alberto, Ph.D.

City University of New York, 1989

U·M·I
300 N. Zeeb Rd.
Ann Arbor, MI 48106

PROTEIN EFFECTS ON A MODEL FOR THE ACTIVATION OF A SEROTONIN RECEPTOR

by

GUSTAVO A. MERCIER

A dissertation submitted to the Graduate Faculty in Biomedical Sciences in partial fulfillment of the requirements for the degree of Doctor of Philosophy, The City University of New York.

1989

This manuscript has been read and accepted for the Graduate Faculty in Biomedical Sciences in satisfaction of the dissertation requirement for the degree of Doctor of Philosophy.

July 18, 1989
Date

Dr. Harel Weinstein
Chair of Examining Committee

July 18, 1989
Date

Dr. Terry A. Krulwich
Executive Officer

Members of the Examining Committee:

Dr. Jack P. Green

Dr. Roman Osman

Dr. J. B. A. Ross

Dr. Michael Zerner
Chemistry Department
University of Florida
Gainesville, Florida

THE CITY UNIVERSITY OF NEW YORK

ABSTRACT

PROTEIN EFFECTS ON A MODEL FOR THE ACTIVATION OF A SEROTONIN RECEPTOR

by

Gustavo A. Mercier

Advisor: Dr. Harel Weinstein

A proton transfer (PT) triggered by a ligand interacting with the receptor had been suggested as the initial step in the activation of a serotonin (5-HT) receptor. A new strategy is introduced to evaluate, in the absence of the three dimensional structure of the receptor, the role of the receptor in modulating the activation mechanism. The strategy consists of using proteins of known structure as receptor models to study the **effects of the receptor environment** on the process of activation. **Actinidin**, a sulfhydryl proteinase, satisfied the criteria as a model receptor in which to study the effects from the protein environment of the 5-HT/LSD receptor (also known as the 5-HT_{1a} receptor). The results from computations of the PT from His 162 to Cys 25 showed that the electrostatic effect from the protein raises the energy barrier and lowers the driving energy for the proton transfer. This result constitutes a desirable property of the model; otherwise, the receptor would be activated in the absence of agonists. The protein effect results from the interaction with the proton donor and acceptor groups as they changed due to the PT, and not from a direct effect on the proton along its path. Different structural

elements in actinidin contribute differently to this interaction. The largest helix, A1, opposes the PT through the effect of its helix dipole. The charged residues (i.e. elements of primary structure) in helix A3 favor the PT, and mask the effect of its helix dipole (i.e. from its secondary structure) which opposes the transfer. Steric effects in the activation process were evaluated by using the indole of Trp 184 which is oriented over the hydrogen bonded system of Asn 182 and His 162. Steric hindrance in the protein restricts the orientation that ligands could assume above this hydrogen bonded system. The orientation favored by actindin was close to the one that allowed 5-HT to activate the model receptor through a PT. In this orientation other congeners of tryptamine also lower the barrier and increase the driving energy for PT with a rank order that appears to correlate with the intrinsic efficacies of the drugs, as expected from receptor theory. The heuristic model for the activaton of a 5-HT receptor suggests that ligands overcome the electrostatic effects from the receptor structure that stabilize the "inactivated" form of the receptor while the steric effects in the binding pocket can select the proper orientation for the ligand so that activation can occur.

ACKNOWLEDGEMENTS

Many individuals contributed to my doctoral training, and I am grateful for their support and guidance. Drs. Weinstein and Osman were instrumental in the development of this thesis. Dr. Ross, as the only experimentalist in my thesis committee, provided his unique perspective to the work. The members of the laboratory have been many and through their kind ears and many questions they contributed to my education. I would like to thank them, but particularly Drs. Rubenstein, Dijkman, Pardo, and Mazureck. You certainly challenged my wits! I also thank Drs. Green and Krulwich who allowed me to come to Mount Sinai under a Medical Scientist Training Program fellowship from the National Research Service Award Program of the National Institute of Health (5-T32-GM7280-08). Through its financial support, this award made my M.D.-Ph.D. training possible.

It is a real burden to finish a thesis without the help of non-scientist. The secretaries of the department of Physiology and Biophysics welcomed this very demanding pharmacology student with open arms. Gloria and Maria in the Graduate School office were always very helpful and on time with my checks! Ms. Maureen Reek as a friend and administrator of the department of Physiology and Biophysics never hesitated to lend her hands and ears, particularly when I was going bananas.

I would also like to give my deepest thanks and appreciation to my parents and siblings because they have been most helpful, patient and supportive during the many years of my M.D.-Ph.D. training. To my girlfriend, Alice, I give a big hug and kiss. She proofread parts of my thesis, and was instrumental in my success during my third year of medical school with her support and advice. She made third year fun and easy. I would also like to thank the many friends who helped me during all these years. The list is too lengthy and I risk missing names, but you know who you are.

Numerous computational resources were available to me. Without these my work would have never started. A generous grant of computer time from the University Computer Center of the City University of New York is gratefully acknowledged. Some of the curve fitting and data analysis was done on the PROPHET computer system - a national computer resource sponsored by the NIH through the division of Research Resources. Some of the computations for the thesis were done at the Cornell National Supercomputer Facility, Center for Theory and Simulation in Science and Engineering which is funded, in part, by the National Science Foundation, New York State, and IBM Corporation. Similarly, I would like to acknowledge the generous computer time provided by the Department of Biomathematics of the Mount Sinai School of Biomedical Sciences of the City University of New York, and the Cray computer time provided by the Pittsburgh Supercomputer Center, a national supercomputer facility sponsored by the National Science Foundation.

Some of the work in this thesis has been published already. I would like to thank the Elsevier Science Publishers, Physical Sciences and Engineering Division for allowing the reproduction of the text and tables in chapter 2. This work is to be published in the book Quantum Chemistry: Basic Aspects, Actual Trends which is edited by R. Carbo, 1989. The IRL Press, a division of the Oxford University Press, is also acknowledged for granting permission to reproduced the text and tables in chapter 4. The work in this chapter was published in Protein Enginnering, 2: 261-270, 1988.

TABLE OF CONTENTS

LIST OF TABLES

LIST OF FIGURES

CHAPTER 1

BACKGROUND AND SCOPE

The application of tools from molecular biology and modern biochemistry to pharmacology have opened new prospects in the efforts to understand receptor function and to design new agents with specific biologic activity. In recent years, through the application of recombinant DNA technology and advances in biochemistry, it has been possible to isolate membrane bound receptors, characterize their primary structure, and reconstitute the receptors in either artificial membranes or in such systems as the frog oocyte or mammalian cell lines (Stevens, 1985; Dixon et al., 1986; Kubo et al., 1986; Gocayne et al., 1987; Grenningloh et al., 1987; Kobilka et al., 1987; Leung et al., 1987; Masu et al., 1987; Marx, 1987; Schofield et al., 1987; Stevens, 1987; Trowbridge, 1987; Bunzow et al., 1988; Fargin et al., 1988; Julius et al., 1988; Kobilka et al., 1988; Lester, 1988; Hartig, 1989; Prichett et al., 1988). These approaches have opened the door for the study of structure-function relationships in membrane-bound receptors. Such work is expected to complement the structure-activity studies that traditionally have occupied pharmacologists' minds. Unfortunately, structure-activity and structure-function studies have been hindered by the lack of structural information on the membrane-bound receptors at the atomic level. This lack of structural information has made these studies dependent upon the pharmacology

of drug-receptor interactions. For example, inferences from drug-receptor theory have been particularly important because they provide a framework for the classification of the receptors and their ligands. This classification has provided the information necessary for identifying from among the newly isolated membrane-bound proteins the receptors with pharmacologic activity without which it would be impossible to initiate structure-function studies of these receptors. Also, drug-receptor theory together with the chemical basis for the biological activity of ligands has justified the search for chemical properties of the ligands, i. e. the molecular determinants, which are responsible for their biological activity. The extension of inferences from the biochemistry of enzyme-substrate interactions to the structure-activity and function studies of receptors has been justified insofar as the receptor macromolecules are proteins (Goodford, 1980; Lipscomb, 1981; Weinstein et al., 1985).

In the efforts to design ligands with specific biological activity a strategy aimed at identifying the molecular determinants responsible for ligand **binding** and receptor **activation** has been formulated which did not require a priori knowledge of the receptor structure. To identify the molecular determinants responsible for binding a series of compounds with known affinities to the receptor would be analyzed for commonalities in the chemical properties that may explain their different reactivities. The common properties would represent a putative set of molecular determinants that would be tested experimentally for their relevance to ligand binding by using them to predict the rank order of affinities for compounds not in the original

series. The application of theoretical chemistry and computational simulations would then permit the expression of the molecular determinants responsible for binding in terms of reactivity criteria, e.g. electrostatic potentials, which are **different** from the chemical structure of the ligands. The newly acquired information would lead to new classes of ligands because the reactivity criteria may be met by compounds that belong to chemical classes different from the ones used to identify the molecular determinants. More important is the ability to apply the chemical intuition derived from bio-organic chemistry to identify biochemically relevant species that would match the molecular determinants, hence identifying models for the receptor site that would be capable of binding the ligands. This would be extremely useful in pharmacology where the chemical nature of the binding sites in membrane bound receptors is currently unknown. Computational simulations would then be used to test the suggestions from chemical intuition and to identify the changes on the model binding site upon ligand binding. Such changes would form the basis for an activation process that would be characterized through further simulations, and later tested experimentally. In this way the molecular determinants for the activation process would be identified. Once the molecular determinants for binding and activation are known, the design of agonists and of antagonist would be easier because the former would be expected to satisfy both set of determinants while the latter only would satisfy the binding criteria.

The implementation of the strategy described above for the design of new biologically active compounds would strain the limits of

theoretical chemistry and computational power because it demands the simulation of both electronic mechanisms inside proteins and of dynamics in systems which are membrane-bound and surrounded by polyelectrolytes in an aqueous environment. It is also at the limits of current experimental technology because the strategy merges the application of molecular biology with the pharmacologic experiments described in receptor theory in an effort to test models for the receptor site which are congruent with the molecular determinants for binding and activation. The rewards from a successful application of this strategy would extend beyond the mere generation of new ligands; that is, a deeper understanding of the chemical basis for cell physiology could be expected. Thus, it would not be surprising to find that such strategy has been implemented already in the design of new drugs for the H2 and the 5-HT receptors. The details of this strategy, including the application of proteins as models for receptors systems, could be illustrated with the work done on the 5-HT receptor.

In the four decades since the discovery of serotonin (5-HT) numerous receptor subtypes for the endogeneous ligand have been described. These receptor sites are the target for a variety of ligands that span many different chemical classes (Arvidsson et al., 1986; Middlemiss et al., 1986; Peroutka, 1988). This result is consistent not only with the description of many subtypes of the receptor, but also with the idea introduced above that the molecular determinants responsible for binding and activation may be satisfied by molecules with different structure. The 5-HT receptor subtype that also binds d-LSD, a receptor relabeled 5-HT_{1a} under the newer classification

schemes (Peroutka, 1988), has been the focus of the heuristic approach described above with the goal of identifying those molecular determinants.

Work on the structure-activity of ligands active at the 5-HT/LSD receptor has been initiated by selecting series of congeneric drugs with varying activity at the receptor site (Green et al., 1976). In addition, studies designed to investigate the consequences of substrate binding to enzyme systems have been initiated in an effort to use enzymes as models for the receptor. The use of enzymes or soluble proteins as models for receptors has been discussed in the literature (Goodford, 1980; Goodford et al., 1980; Weinstein et al., 1985). Inasmuch as receptors are proteins, such studies are particularly appropiate because the 3-D structure of many enzymes are known and descriptions at the detailed atomic level of their catalytic activity exist for some systems. Similar information is not available for receptors at the present time. Indeed, the work with enzymes has proven useful because it has guided the choice of congeneric drugs, as well as the interpretation of the structure-activity studies using these compounds. It is noteworthy that analysis of enzyme-substrate interactions has shown that the affinity constant measured by pharmacologists through binding experiments not only reflects the local interactions at the binding site which are of interest in structure-activity studies, but also include the free energy spent in the global motions of the protein initiated by binding of the ligand (Liebman and Weinstein, 1985). Therefore, it has been necessary to limit the choice of congeneric drugs to those with similar molecular volume to minimize differences

in the molecular motions initiated by binding, thus focusing on differences in affinity that reflect mostly differences in the local interactions with the unknown binding site in the receptor. A series of hydroxylated derivatives of tryptamine have satisfied this criterion thus forming a set of congeneric drugs used in a wide range of structure-activity studies (Weinstein et al., 1976; Green et al., 1976; Reggio et al., 1981; Weinstein et al., 1981b; Mazurek et al., 1984; Shenker et al., 1985; Shenker et al., 1987; Weinstein et al., 1987).

The application of chemical intuition and concepts from enzymology have restricted the choice of chemical properties of the congeneric drugs that have been considered relevant to the binding event. One such property is based on electrostatic forces which are important in the chemical reactivity of many compounds including enzyme mediated catalysis (Warshel, 1981a; Weinstein et al., 1981a). The molecular electrostatic potential (MEP) represented such molecular property. It can be computed for the congeners and analyzed as an indirect measure of the ability of these drugs to undergo a favorable electrostatic interaction with the receptor (Weinstein et al., 1976; Weinstein and Osman, 1977; Weinstein et al., 1978a,b; Weinstein et al., 1981a,b). When the ethylamine side chain of 5-HT with its cationic head group was extended so as to match the MEP of 5-HT with that of d-LSD, a topological relationship between the head group and the MEP over the indole was generated. The cationic head group, the MEP over the indole portion of 5-HT, and their topologic relationship had become the molecular determinants that successfully predicted the rank order of affinities for the congeneric compounds

and for compounds from other chemical classes not included in the original set (Reggio et al., 1981; Mazurek et al., 1984; Weinstein et al., 1987). Finally, the molecular determinants had proved useful as tools for drug design by introducing an "electrostatic orientation vector" which was generated from the MEP (Weinstein et al., 1981a,b). This construct allowed for the quick evaluation of whether compounds could bind avidly or poorly to the receptor. Indeed, the MEP of d-LSD permitted the identification of a double bond in the ergoline structure as equivalent to the 5-hydroxy group in its contribution to the "electrostatic orientation vector". Reduction of the double bond eliminated the vector and rendered the resulting compound inactive (Weinstein et al., 1981b). The value of the electrostatic orientation vector in drug design was two-fold: it reflected reactivity properties without reference to the chemical structure, and its limitations had been illuminated because the physical basis for its predicting power were known. When determinants are expressed in terms different from the chemical structure, there is hope for generating new and structurally different active compounds. Moreover, when the limitations of these determinants are understood, they are likely be used judiciously in the drug design effort.

Though the molecular determinants for binding at the 5-HT/LSD receptor had predictive power, it was necessary to test their contribution to a chemical process relevant to binding. Such testing would rule out the possibility that these determinants represented an ad hoc set of properties with predictive power, but irrelevant to any mechanistic hypothesis that attempted to explain the binding event.

Three observations led to choosing imidazolium as model receptor site in which to do this test. First, the recognition elements represented electrostatic properties (Weinstein and Osman, 1977; Weinstein et al., 1978a,b; Weinstein et al., 1981a,b). Second, the experimental data indicated that stacking complexes existed between imidazolium and indole (Shinitzky and Katschalski, 1968), the principal functional group in 5-HT. Third, the imidazolium group was in the side chain of histidine, an amino acid present in the active site of many enzymes. Simulations designed to explore the stacking interaction between the indole portion of 5-HT and other congeners and imidazolium revealed that specific orientations were preferred by energetic criteria and that the stabilization energy was mostly electrostatic, i.e. polarization, in nature (Weinstein and Osman, 1977; Weinstein et al., 1978a,b; Osman et al., 1981; Osman et al., 1985; Osman et al., 1980; Osman et al., 1987). Application of the electrostatic orientation vector concept showed that it had predictive power with respect to the mutual orientation between the imidazolium and the 5-HT congeners in the stacking complexes (Weinstein and Osman, 1977; Weinstein et. al., 1978a,b). With the orientation of 5-HT as the preferred orientation for binding, the imidazolium model was capable of discriminating between the different congeners in a fashion consonant with their interaction with the receptor. Thus, the results formed a rationale for the success of the molecular determinants in predicting the rank order of affinities. This indicated that these determinants may be the basis for a mechanistic hypothesis which would explain the binding event.

Once a mechanistic hypothesis for receptor binding was available it was possible to explore the consequences of receptor binding as required by the heuristic approach described above. An analysis of the electronic distribution of the receptor model, i.e. imidazolium, upon stacking with 5-HT revealed that one of the N--H bonds was weakened. Such weakness suggested a change in proton affinity of one of the nitrogen atoms. Therefore, it was possible that a proton transfer from imidazolium to an acceptor may form the basis for an activation mechanism (Osman et al., 1985; Osman et al., 1987). Again knowledge from the biochemistry of enzymes indicated that such a process was not unreasonable; that is, many enzymes are involved in acid/base catalyzed reactions where proton transfers are necessary. The imidazole group of His is an active participant in many of these proteins. Thus, a proton transfer model was constructed (PTM) which contained an imidazolium with a proton acceptor (Osman et al., 1987). The latter was mimicked by ammonia, but was not necessarily limited to this functional group. Simulations were done to explore the ability of the PTM to respond to stacking of 5-HT (Osman et al., 1987). 5-HT showed similar orientations over the PTM as those described for the interaction with imidazolium alone. In addition, it lowered the barrier to proton transfer and increased its driving energy, i.e. the difference in energy between products and reactants. Though the PTM was constructed from specific molecules, the concept of a proton transfer triggered by the drug as an activation mechanism was independent of the specific nature of the donor and acceptor groups. Indeed, when the language of theoretical chemistry is used, the activation mechanism is represented by a favorable potential surface for proton

transfer that is generated in the presence of the agonist. The ability to represent the activation process in such terms (i.e. different from the structure) is particularly important in light of the lack of knowledge regarding binding sites. Moreover, the construction of the PTM, and the generation of a mechanistic hypothesis for the activation of the receptor, introduced new tools for drug design by having a model that should discriminate between ligands that activate the receptor (i.e., the agonist) and those that do not (i.e. the antagonist).

The initial simulations of the activation mechanism were done in vacuum. Under such conditions, steric and electrostatic effects from the receptor structure were excluded. An evaluation of the molecular determinants relevant to the activation process indicated that such effects from the protein environment may contribute to modulate the activation event initiated by the ligand. For example, it is known that hydrogen bonds such as the one present in the PTM are stable due to electrostatic interactions between the molecules. In the PTM the position of the proton is changed upon interaction with 5-HT because the latter stabilizes through electrostatic interactions the transition state and the products of the proton transfer (Osman et al., 1987). In addition, simulations of the catalytic activity of enzymes has shown that strong electrostatic fields can be generated by the protein structure in the region of the active site (Allen, 1981; Warshel and Levitt, 1976; Warshel, 1981; Warshel and Russell, 1984; Warshel et al., 1988). Thus, it has been appropriate to consider such **electrostatic effects** on the activation mechanism. Similarly, **steric effects** from the protein would severely hinder the set of possible orientations that the

ligand may achieve around the PTM. The orientations bear importance because it is well known that electrostatic interactions are dependent on the orientation between the molecules. Though in the initial simulation of the activation process the orientations were limited to a plane over the imidazolium ring, it has been more realistic to identify the degree of steric restriction within an environment that is akin to the receptor-macromolecule. An example of such environment would be the protein structure of a soluble enzyme that already includes within its structure the elements of the PTM interacting with an analog of 5-HT such as the indole group present in the side chain of Trp. Ideally, steric effects should be evaluated in the actual protein of interest, but this is impossible at the present time. Only the primary sequence of a few 5-HT receptors is known. No knowledge exists of either their three dimensional structure or of the region of the active site (Fargin et al., 1988; Julius et al., 1988; Prichett et al., 1988; Hartig, 1989).

Actinidin, a sulfhydryl protease, satisfies the requirements needed to evaluate the electrostatic and steric effects of receptor-macromolecule over the activation model for the 5-HT-LSD receptor. This protein not only includes the appropriate juxtaposition of groups that generate the PTM interacting with the indole of Trp, but it also contains a variety of alpha helices in different orientations. Alpha helices have unique electrostatic properties. These structure are believed to be present in a variety of membrane bound receptors including the 5-HT receptor subtypes (Hartig, 1989). **This thesis attempts to explore electrostatic and steric effects that a protein**

structure may have on the activation mechanism using actinidin as the test system. This study utilizes the heuristic strategy described to identify molecular determinants responsible for binding and activating the 5-HT-LSD receptor. The protein effects are explored in terms of both the secondary and tertiary enzyme structure, e.g. the alpha helices. Such structures are known to be present in many proteins including the receptor of interest (Richardson, 1981; Marx, 1987; Hartig, 1989). It is hoped that the results may be extended to the specific receptor since it is assumed that effects that arise from an element of structure are retained when the same element is present in other protein systems. This assumption is based on the premise that the effects from a given structural element originate from properties that are inherent to its structure, and not only from the individual elements that compose it. Also, it is assumed that the contributions from constitutive elements can be discriminated from the contributions of the assembled structure. This approach does not aim at identifying local interactions such as the oxyanion hole described for the serine proteases (Hwang and Warshel, 1988), but aims at long-range effects, from larger elements of the protein structure.

CHAPTER 2

ELECTROSTATIC COMPUTATIONS: METHODOLOGY AND BASIS SET DEPENDENCE

2.1 INTRODUCTION

Hydrogen bonded systems and proton transfer reactions, such as the one in the PTM, have been the subject of extensive investigations with theoretical methods (for a review, see Scheiner et al., 1986), because of their multiple forms of involvement in biologic processes. In addition to their putative role in receptor activation, these systems are involved in both the catalysis of bond cleavage (Fersht, 1985; Polgar and Halasz, 1981; Stryer, 1981) as well as synthesis, of, for example, adenosine triphosphate (ATP), a source of energy for cells (Hinkle and McCarty, 1978). However, due to the magnitude of the molecules in biologic systems, computational studies of hydrogen bonding and proton transfers in these systems have primarily utilized semiclassical approximations rather than full quantum mechanical descriptions (Drummond, 1986; Tapia and Johannin, 1981; Thole and van Duijnen, 1983a; Warshel and Levitt, 1976). In these approximations only the hydrogen bonded system of

interest is described quantum mechanically by the introduction of a molecular Hamiltonian. A considerable fraction of the macromolecule, usually referred to as the **environment**, is represented by a collection of point charges, dipoles and atomic polarizabilities (Tapia and Johannin, 1981; Thole and van Duijnen, 1983a; Warshel and Levitt, 1976; Warshel, 1981b; Tapia and Goscinski, 1975; Thole and van Duijnen, 1980). The part of the system described quantum mechanically, usually referred to as the **quantum motif**, is coupled to the classical description of the environment by several schemes based on classical electrostatics (Tapia and Johannin, 1981; Tapia and Goscinski, 1975; Thole and van Duijnen, 1980). Electrostatic and polarization energies of interaction between the quantum motif and the environment are usually reported from such studies, but little is known about the basis set dependence of the energy values.

This chapter describes in detail the methodology used to compute the electrostatic interaction between the protein environment in the enzyme actinidin and a model of the PTM found in the active site of this enzyme. The method is an application of the Variation-Perturbation Theory of Group Functions introduced by McWeeny (McWeeny and Sutcliffe, 1976). The theory is modified to consider the interaction between one group represented by quantum mechanics and another described as a collection of point charges and polarizable points. Thus, it follows the same spirit of the semiclassical approach described above. No effort is made to justify the use of the semiclassical approach or its application within the Theory of Group Functions because this has been amply discussed in the literature and

its value has been well established (Drummond, 1986; Warshel and Russell, 1984; McWeeny and Sutcliffe, 1976). Instead, this chapter describes a perturbation formalism for the calculation of such an interaction and reports on the bias introduced by the basis set representation of the quantum motif. This bias has remained largely unexplored within the semiclassical approaches described above. Such an evaluation is reported here from calculations of electrostatic and polarization energies of interaction between a hydrogen bonded cationic quantum motif and a protein environment represented by point charges and atomic polarizabilities. The system was chosen to model the amino acids in the active site of actinidin, the sulfhydryl proteinase which is being studied as a model for the receptor of the neurotransmitter serotonin.

2.2 METHODS

2.2.1 STRUCTURES AND GEOMETRIES

The coordinates for the [NH_3...H^+...H_2S] complex were constructed from the imidazolium/methanethiol complex which models the side chains of His 162 and Cys 25 in actinidin (E. C. 3.4.22.14 ; Brookhaven Protein Data Bank file 2ACT) (Baker, 1980; Bernstein et al., 1977). The C_3 axis of ammonia was aligned with the ND1-HD1 bond and one hydrogen was placed in the plane cutting perpendicular to the imidazolium plane and containing the C_3 axis. The carbon atom of methanethiol (CG) was replaced by a hydrogen atom. The internal

coordinates for the hydrogen atoms of ammonia are those of an ammonium molecule optimized with the STO-3G basis set. The coordinates for the proton at the three points of extremum (HM1, HTS, HM2) in the proton transfer energy curve, as well as those of the second hydrogen in H_2S at the same points (HSM1, HSTS, HSM2), were taken from the corresponding structures calculated for the larger imidazolium/methanethiol complex representing the two residues in the protein, His 162 and Cys 25 (for details see chapter 3). The proton transfer energy curve for the larger complex was previously computed using the gradient methods and the several basis sets implemented in the Gaussian 82 system of programs (as detailed in chapter 3). In the computations of the imidazolium/methanethiol complex, the critical points were determined by optimizing the proton and the hydrogen atom bonded to sulfur while the remaining atoms were held fixed. The first and second minima on the proton transfer energy curve are labeled M1 and M2, respectively. The transition state, which was optimized under the constraint of one negative eigenvalue in the Hessian matrix, is labeled TS. The position of the optimized atoms showed little dependence on basis sets, even after considering computations that included extensive basis sets. Figure 2-1 shows the complex $[NH_3...H^+...H_2S]$, and Table 2-1 reports the coordinates of the complex in angstroms.

2.2.2 COMPUTATIONAL DETAILS

The electrostatic interaction energy between the ammonium/hydrogen sulfide complex and the residues in the active site of actinidin was computed by using a classical representation for the side chains. Using the program HYDRO from M. Levitt, hydrogen atoms were added to the residues Gln 19, Asn 182, and Trp 184 in the coordinates of 2ACT. Point charges were assigned to the atoms from a library generated with the Mehler-Paul basis set (Mehler and Paul, 1979). The point charges were constructed through a dipole preserving population analysis (Thole and van Duijnen, 1980) for fragments consisting of the atoms in the backbone and the side chains. The method guarantees that the first and second moments of the continuous electron charge distribution of the fragments computed with that basis set will be reproduced by the point charges. Isotropic atomic polarizabilities were assigned from a library in a modification of the original HONDO program (Dupuis et al., 1976), which contains the Direct Reaction Field Hamiltonian method (Thole and van Duijnen, 1980). These polarizabilities were derived through a fitting procedure described by Thole (Thole, 1981), and are expected to reproduce the molecular polarizability for the fragments in the environment.

The electrostatic interactions between the quantum motif and the environment were calculated with the computational scheme described below. The formal development of the scheme is based on

the Variation-Perturbation Theory of Group Functions given by McWeeny and Sutcliffe (McWeeny and Sutcliffe, 1976).

2.2.3 COMPUTATIONAL FORMALISM

(from Mercier et al., 1989)

Consider two molecular systems A (e.g. quantum motif) and B (e.g. macromolecular environment), each described by a wavefunction from the solution to the separate electronic Schroedinger equations:

$$H_A|\psi_A\rangle = E_A|\psi_A\rangle \quad ; \quad H_B|\psi_B\rangle = E_B|\psi_B\rangle \qquad (1)$$

If the molecules interact in a weak complex so that charge transfer between A and B can be neglected (i.e. exchange interactions are negligible), the Hamiltonian for the combined system may be written

$$H = H_A + H_B + H_{AB} \qquad \text{so that} \qquad H|\Psi\rangle = E|\Psi\rangle \qquad (2a);\ (2b)$$

where $|\Psi\rangle$ is the antisymmetrized product of the individually antisymmetrized group functions ϕ_A and ϕ_B describing the perturbed subsystems A and B, respectively

$$|\Psi\rangle = A'|\phi_A\phi_B\rangle \qquad (2c)$$

A' is the antisymmetrizer operating between group functions for A and B.

Following the Variation-Perturbation Theory for group functions [24], with A and B representing the two groups, the total energy of the system is written in terms of the self energies of the component groups in the complex, and an interaction term:

$$E = \langle \phi_A | H_A | \phi_A \rangle + \langle \phi_B | H_B | \phi_B \rangle + \langle \Psi | H_{AB} | \Psi \rangle \qquad (3)$$

If the individual group functions in equation 2c are single determinant wavefunctions such as those computed through the Hartree-Fock approximation, the interaction term may be written as

$$E_{AB} = \langle \Psi | H_{AB} | \Psi \rangle = E^J_{AB} + E^K_{AB} \qquad (4)$$

where E^J_{AB} is the coulombic interaction energy and E^K_{AB} is the exchange interaction energy.

When B is a very large system such as a protein, it may be represented classically by a collection of point charges and atomic polarizabilities. This representation is expected to reproduce the electrostatic properties of B in the absence and presence of the perturbation introduced by A, when E^K_{AB} can be neglected. The approximation is especially useful if the main interest is in the properties of the system A and its perturbation by B. Using the classical representation of B, the total energy for the AB complex can be approximated by a self consistent energy E^{SC}

$$E^{sc} = \langle \phi_A | H_A | \phi_A \rangle + \tfrac{1}{2} \int \rho'_B V_B \, d\tau + E^{cc}_{AB} \qquad (5)$$

where $|\phi_A\rangle$ is a wavefunction for A after the mutual perturbation of A and B has taken effect. The second term in the expansion of E^{sc} is the self energy of the classical system B, written in terms of ρ'_B, the charge distribution of B prior to any perturbation from A (i.e. the real charge distribution of classical electrostatics) and V_B which is the total potential from the real (i.e. unperturbed) and induced (i.e. perturbed) charge distributions of B acting on ρ'_B. E^{cc}_{AB} is the classical coulombic energy of interaction between A and B after perturbation. As shown below, equation 5 leads to a variational-perturbation scheme analogous to the one introduced by McWeeny and Sutcliffe [23] that generates a self-consistent charge distribution for the AB complex within the classical representation of B.

2.2.4 THE E^{cc}_{AB} TERM

From classical electrostatics, the coulomb interaction term between A and B components of the system will have the form

$$\begin{aligned} E^{cc}_{AB} &= \tfrac{1}{2} \int \rho'_B V'_A \, d\tau + \tfrac{1}{2} \int \rho'_A V'_B \, d\tau \\ &\quad + \tfrac{1}{2} \int \rho'_A V''_B \, d\tau + \tfrac{1}{2} \int \rho'_B V''_A \, d\tau \\ &= \int \rho'_B V'_A \, d\tau + \tfrac{1}{2} \int \rho'_A V''_B \, d\tau + \tfrac{1}{2} \int \rho'_B V''_A \, d\tau \end{aligned} \qquad (6)$$

where V'_A and V'_B are the electrostatic potentials produced by the unperturbed charge distributions ρ'_A and ρ'_B, and V''_A and V''_B are the potentials from the perturbed charge distributions ρ''_A and ρ''_B. The induced charge distributions ρ''_A and ρ''_B in A and B, respectively, are produced by the mutual perturbation of A and B. The perturbed terms come from the effect of A on the polarizabilities $\{\bar{\alpha}_k\}$ of B and the difference between $|\psi_A\rangle$ and $|\phi_A\rangle$ of A, defined in equations 1 and 2c, respectively. Equation 5 may thus be rewritten as:

$$E^{sc} = \langle\phi_A|H_A|\phi_A\rangle + \tfrac{1}{2}\int \rho'_B(V'_B + V''_B)\,d\tau + \int \rho'_B V'_A\,d\tau + \tfrac{1}{2}\int \rho'_A V''_B\,d\tau + \tfrac{1}{2}\int \rho'_B V''_A\,d\tau \qquad (7)$$

2.2.5 SELF-CONSISTENT COMPUTATION OF THE CHARGE DISTRIBUTION OF AB

Use of equation 7 to compute the energy of the AB complex, requires the wavefunction of the perturbed system A, $|\phi_A\rangle$, and ρ''_B. ρ''_A is then computed from the difference between the charge distributions calculated from the unperturbed wavefunction $|\psi_A\rangle$ and from $|\phi_A\rangle$. The calculation of $|\phi_A\rangle$ can be accomplished with the variation-perturbation scheme of McWeeny and Sutcliffe (McWeeny and Sutcliffe, 1976) modified to consider only electrostatic interactions between A and B. In this scheme, a solution for the energy and charge distribution of the AB system is obtained by variationally solving for a new group function for A when perturbed by the group function of B. The perturbation terms consist of coulombic

and exchange operators averaged over the group function of B. The new group function for A yields a perturbation for B. This perturbation is used to obtain a new charge distribution in B. Thus, a solution to equation 3 is computed through an iterative scheme that involves the variational solutions for perturbed group functions. A similar iterative scheme when both A and B are represented classically has been used by others (Warshel and Russell, 1984; van Belle et al., 1987).

For the semiclassical AB system considered here, the iterative scheme is accomplished by introducing successive perturbations in the electronic molecular Hamiltonian for A, and by polarizing the charge distribution of B. These perturbations have their origin in the average charge distributions of A and B. For A the electrostatic effects from B are introduced in the Hamiltonian given in equation 1

$$H_A^{(i)} \left| \psi_A^{(i)} \right\rangle = E_A^{(i)} \left| \psi_A^{(i)} \right\rangle \tag{8a}$$

where

$$H_A^{(i)} = H_A^{(i-1)} + \int \frac{\rho_B^{(i-1)}}{\left| \vec{r} - \vec{r}_B \right|} d\tau_B \qquad i \geq 1 \tag{8b}$$

and

$$H_A^{(0)} \equiv H_A \qquad i = 0 \tag{8c}$$

The classical charge distribution of B is iteratively modified by the field from A so that

$$\rho_B^{(i)} = \rho_B^{(i-1)} + \rho''^{(i)}_B \qquad i \geq 1 \tag{9a}$$

with

$$\rho_B^{(0)} \equiv \rho'_B + \rho''_B \qquad i = 0 \tag{9b}$$

and

$$\rho''^{(i)}_B = \rho''_B[|\psi_A^{(i)}\rangle] \qquad i \geq 0 \tag{9c}$$

The term $\rho''_B[|\psi_A^{(i)}\rangle]$ denotes a functional dependence of $\rho''^{(i)}_B$ on the wavefunction for A in a manner defined by equation 14, through the average value of the operator $\vec{F}$ (equation 16).

Solution of equation 8a leads to a new $\rho_B^{(i)}$ through 9a-9c and a new Hamiltonian through 8b-8c. The perturbed wavefunction for A is computed iteratively

$$|\phi_A\rangle \equiv |\psi_A^{(i=\infty)}\rangle \tag{10a}$$

and ρ''_A and ρ''_B are calculated from the differences

$$\rho''_A = \rho_A^{(i=\infty)} - \rho'_A \tag{10b}$$

$$\rho''_B = \rho_B^{(i=\infty)} - \rho'_B = \rho''^{(i=\infty)}_B \tag{10c}$$

These can then be used in equation 7 to compute the total energy

Note that the resulting Hamiltonian in 8a is linear. Thus, it is different from the Hamiltonian suggested by Tapia and Johannin (Tapia and Johannin, 1981) for similar semiclassical computations. The Hamiltonian in 8a would be identical to the Interaction Field Modified Hamiltonian introduced by Weinstein and coworkers (Weinstein, 1977) if the charge distribution of B were computed from the antisymmetrized wavefunction of B. In the scheme described above, the perturbation of B by A occurs only through the average electrostatic properties of A and not through the properties of the instantaneous charge distribution of A as it occurs in the Hamiltonian suggested by Thole and van Duijnen (Thole and van Duijnen, 1980). This difference alleviates the convergence problems associated with a wrong initial charge distribution, and eliminates spurious energy terms (i.e the dispersion-like term associated with the Direct Reaction Field formalism [Thole and van Duijnen, 1982]). For i=0 and a point charge distribution for B, the Hamiltonian in 8b reduces to a Hamiltonian used by Umeyama for similar computations (Umeyama et al., 1984).

2.2.6 THE ITERATIVE ALGORITHM

The practical implementation of the algorithm presented above requires some approximations in the perturbation term of equation 8a. Because in the systems of interest (e.g. proteins) the B part is a large

molecule, a multipole expansion centered on the atomic nuclei is used to obtain the potential terms V'_B and V''_B. The expansion is truncated at the dipolar term:

$$\int \frac{\rho(\vec{r}')}{|\vec{r} - \vec{r}'|} d\tau' = \sum_k \frac{Q_k}{|\vec{r} - \vec{r}_k|} + \frac{\vec{M}_k \cdot (\vec{r} - \vec{r}_k)}{|\vec{r} - \vec{r}_k|^3} + \dots \qquad (11)$$

The unperturbed charge distribution of B is usually computed from a wavefunction. The dipolar term of equation 11 is collapsed into a point charge representation. The generation of such point charges can be achieved through a scheme developed by Thole and van Duijnen (i.e. the dipole preserving point charges) (Thole and van Duijnen, 1983b). Because B is too large for quantum mechanical computations, the point charges are computed from the wavefunction of fragments of B. The charge distribution from the combination of the fragments is an approximation that lacks the mutual polarization of the fragments obtained when a full SCF computation of B is feasible. In our scheme, this polarization is approximated by allowing the point charges of the fragments to interact with the atomic polarizabilities to generate induced dipoles that represent the intrafragment polarization. In such computations, the effective polarizability tensor of Thole and van Duijnen (Thole and van Duijnen, 1980) together with the modified dipole interaction tensor of Thole (Thole, 1981) are used to generate a self-consistent charge distribution for B that includes of the dipole preserving point charges and the induced dipoles that represent the intrafragment polarization. Thus, the potential from the charge

distribution of B before the external perturbation by A, is computed from

$$\int \frac{\rho'_B}{|\vec{r} - \vec{r}_B|} d\tau_B \approx \sum_{k \in B} \frac{q_k}{|\vec{r} - \vec{r}_k|} + \frac{\vec{m}_k \cdot (\vec{r} - \vec{r}_k)}{|\vec{r} - \vec{r}_k|^3} \qquad (12)$$

The potential that results from the polarization of B due to the charge distribution of A (i.e. $\rho''_B[|\psi_A^{(1)}\rangle]$) in equation 9c can also be expanded in a multipole expansion centered on the atoms of B.

$$\int \frac{\rho''(\vec{r}')^{(i)}}{|\vec{r} - \vec{r}'|} d\tau' = \sum_k \frac{\vec{M}_k^{(i)} \cdot (\vec{r} - \vec{r}_k)}{|\vec{r} - \vec{r}_k|^3} + \frac{1}{2} \frac{(\vec{r} - \vec{r}_k)^T \cdot \overline{W}_k^{(i)} \cdot (\vec{r} - \vec{r}_k)}{|\vec{r} - \vec{r}_k|^5} + \cdots \qquad (13)$$

No zeroth order term exists because the interaction between A and B is assumed not to induce any net charges in B. The multipolar expansion is truncated at the induced dipole term. The superscript (i) reflects the fact that the dipoles are induced by the i-th iteration in the calculation of the perturbed wavefunction of A according to the set of equations 8 and 9. These induced multipoles are generated by the average charge distribution of A as required in the variation-perturbation scheme. Thus, assuming linear response, the potential from the polarization of B due to A is approximated by

$$\int \frac{\rho''^{(i)}_B}{|\vec{r} - \vec{r}_B|} d\tau_B \approx \sum_{k \in B} \frac{\left(\{\bar{A}^{-1} + \bar{T}\}^{-1} \cdot \langle \vec{F} \rangle^{(i)}\right) \cdot (\vec{r} - \vec{r}_k)}{|\vec{r} - \vec{r}_k|^3} \qquad (14)$$

where the term $\{\bar{A}^{-1} + \bar{T}\}^{-1}$ is the effective polarizability of Thole and van Duijnen (Thole and van Duijnen, 1980), represented as a 3nX3n supermatrix with n as the number of polarizable points in B. Following the notation of Thole and van Duijnen, the first term of the effective polarizability contains the isotropic atomic polarizabilities, α_k, of B :

$$\bar{A} = \begin{bmatrix} \bar{a}_1 & & 0 \\ & \ddots & \\ 0 & & \bar{a}_n \end{bmatrix} \text{ where } \qquad \bar{a}_k = \begin{bmatrix} \alpha_k & & 0 \\ & \alpha_k & \\ 0 & & \alpha_k \end{bmatrix} \qquad \text{(15a);(15b)}$$

and the second term contains the dipole interaction tensors (i.e. the negative of the dipole field tensors), $\bar{\beta}_m^k$, where k and m denote the coupled induced dipoles:

$$\bar{T} = \begin{bmatrix} 0 & \bar{\beta}_1^2 & \cdots & \bar{\beta}_1^n \\ \bar{\beta}_2^1 & 0 & & \vdots \\ \vdots & & \ddots & \bar{\beta}_{n-1}^n \\ \bar{\beta}_n^1 & \cdots & \bar{\beta}_n^{n-1} & 0 \end{bmatrix} \qquad \text{(15c)}$$

where

$$\bar{\beta}_m^k = \left(\bar{I} - 3\frac{(\vec{r}_m - \vec{r}_k) \cdot (\vec{r}_m - \vec{r}_k)^T}{|\vec{r}_m - \vec{r}_k|^2} \right) \cdot \frac{1}{|\vec{r}_m - \vec{r}_k|^3} \qquad \text{(15d)}$$

The operator $\vec{F}$ in equation 16 is a 3nX1 column vector composed of the field operator:

$$\vec{F} = \begin{bmatrix} \vec{f}_{1A} \\ \vdots \\ \vec{f}_{kA} \\ \vdots \\ \vec{f}_{nA} \end{bmatrix} \quad \text{where} \qquad \vec{f}_{kA} = \frac{\vec{r}_k - \vec{r}}{|\vec{r}_k - \vec{r}|^3} \qquad \text{(16a) ; (16b)}$$

The term $\langle \vec{F} \rangle_A^{(i)}$ is the expectation value of the components of $\vec{F}$ computed using the $|\psi_A^{(i)}\rangle$ wavefunction.

In summary, the perturbing term in equation 8b is approximated by

$$\int \frac{\rho_B^{(i)}}{|\vec{r} - \vec{r}_B|} d\tau_B \approx \int \frac{\rho_B^{(i-1)}}{|\vec{r} - \vec{r}_B|} d\tau_B - \langle \vec{F}^T \rangle^{(i)} \cdot \{ \bar{\Lambda}^{-1} + \bar{T} \}^{-1} \cdot \vec{F} \qquad i \geq 1 \quad ; \text{ and defined as}$$

$$\sum_{k \in B} \frac{q_k}{|\vec{r} - \vec{r}_k|} + \frac{\vec{m}_k \cdot (\vec{r} - \vec{r}_k)}{|\vec{r} - \vec{r}_k|^3} - \langle \vec{F}^T \rangle^{(0)} \cdot \{ \bar{\Lambda}^{-1} + \bar{T} \}^{-1} \cdot \vec{F} \quad \text{for } i = 0 \qquad (17)$$

The symmetry properties of the effective polarizability matrix and the definition of $\vec{F}$ have been used to write the induced dipole term in supermatrix notation.

2.2.7 IMPLEMENTATION OF THE ITERATIVE ALGORITHM

For an illustration of the use of the above algorithm to compute the electrostatic interactions, the calculation for the hydrogen bonded complex NH_4/H_2S and its environment in actinidin was limited to i=0 and i=1 (the latter including only the point charge perturbation), the side chains of Gln 19, Asn 182, Trp 184. Equation 8a was solved using the HF-SCF-LCAO approximation with the STO-3G, 6-31G, and 6-31G** basis sets (Hehre et al., 1972; Hehre et al., 1970; Hehre et al., 1969; Francl et al., 1982; Hariharan and Pople, 1972). The polarization from the quantum motif was small for the cationic hydrogen bonded complex, even with the most extensive basis set (see RESULTS, below), and no attempts were made to continue the iterations. Accordingly, the energy calculation following equation 7 is reduced to

$$E^{SC(0)} = \langle \psi_A^{(0)} | H_A^{(0)} | \psi_A^{(0)} \rangle + \tfrac{1}{2} \int \rho'_B V'_B \, d\tau_B \; - \; \tfrac{1}{2} \vec{F}'^{T}_{B} \cdot \{ \bar{\Lambda}^{-1} + \bar{T} \}^{-1} \cdot \langle \vec{F} \rangle_A^{(0)}$$

$$+ \sum_{k \in B} q_k \cdot \left\langle \frac{1}{|\vec{r}_k - \vec{r}|} + \sum_{l \in A} \frac{Z_l}{|\vec{r}_k - \vec{r}_l|} \right\rangle_A^{(0)}$$

$$- \sum_{k \in B} \vec{m}_k \cdot \left\langle \frac{\vec{r}_k - \vec{r}}{|\vec{r}_k - \vec{r}|^3} + \sum_{l \in A} \frac{Z_l \cdot (\vec{r}_k - \vec{r}_l)}{|\vec{r}_k - \vec{r}_l|^3} \right\rangle_A^{(0)} \; - \; \tfrac{1}{2} \langle \vec{F}^T \rangle_A^{(0)} \cdot \{ \bar{\Lambda}^{-1} + \bar{T} \}^{-1} \cdot \langle \vec{F} \rangle_A^{(0)} \tag{18}$$

The six terms in equation 18 respectively represent the self energy of the unperturbed system A (EA), of the unperturbed system B (EB), the polarization contribution to the self energy of B (SELF B), the

contributions from the point charges (VxQ) and the dipoles induced through the intrafragment polarization (FxM), and the contribution from environment to the interaction polarization energy (IND B).

At the zeroth order level, there is no contribution to E^{sc} from the polarization of the quantum motif by the environment (i.e. IND A), and the self energy of A in equation 18 corresponds to the unperturbed energy of the quantum motif. The polarization contribution from the quantum motif (IND A) was estimated by one step in the iterative algorithm. This energy term, which corresponds roughly to the fifth term in equation 7, is computed from the difference in the wavefunction computed at i=1 and i=0 with only point charges included in the perturbation for i=1

$$\frac{1}{2}\int \rho'_B V''^{(1)}_A d\tau =$$

$$\frac{1}{2}\sum_{k\in B} q_k \cdot \left[\left\langle \frac{1}{|\vec{r}_k - \vec{r}|} + \sum_{l\in A}\frac{Z_l}{|\vec{r}_k - \vec{r}_l|}\right\rangle^{(1)}_A - \left\langle \frac{1}{|\vec{r}_k - \vec{r}|} + \sum_{l\in A}\frac{Z_l}{|\vec{r}_k - \vec{r}_l|}\right\rangle^{(0)}_A\right]$$

$$-\frac{1}{2}\sum_{k\in B} \vec{m}_k \cdot \left[\left\langle \frac{\vec{r}_k - \vec{r}}{|\vec{r}_k - \vec{r}|^3} + \sum_{l\in A}\frac{Z_l(\vec{r}_k - \vec{r}_l)}{|\vec{r}_k - \vec{r}_l|^3}\right\rangle^{(1)}_A - \left\langle \frac{\vec{r}_k - \vec{r}}{|\vec{r}_k - \vec{r}|^3} + \sum_{l\in A}\frac{Z_l(\vec{r}_k - \vec{r}_l)}{|\vec{r}_k - \vec{r}_l|^3}\right\rangle^{(0)}_A\right]$$

(19)

2.3 RESULTS

Table 2-2 lists the stabilization energy of the $[NH_4/H_2S]$ complex as a function of the basis set, at the critical points on the

potential energy curve for proton transfer. The zero point is the energy of an ammonium/methanethiol complex at infinite separation, calculated in the geometries obtained from an STO-3G optimization of the components. With all the basis sets, the complex is stable only when the proton lies on the ammonia side. The 6-31G** results fall between the values computed with the minimal and split valence basis sets. This result is independent of the choice of the critical point on the proton transfer energy curve (i. e., M1, TS, and M2).

Table 2-2 also shows the energy barriers (i.e. TS-M1 and TS-M2) for the proton transfer between the ammonia and the hydrogen sulfide, as well as the driving energy for proton transfer (i.e. M1-M2). The proton transfer from NH_3 to H_2S is largely unfavorable, as shown by the large barriers for transfer and the unfavorable driving force for transfer from the ammonia side. With the most extensive basis set, the barrier for transfer is 55.0 kcal/mol from the ammonia side, and 10.5 kcal/mol from the hydrogen sulfide side. These values lie between those computed for the minimal and split valence basis sets. The STO-3G basis set underestimates and the 6-31G basis set overestimates the barrier from the ammonia side. The trend is reversed for the barrier from the hydrogen sulfide side where the minimal basis set overestimates, and the split valence underestimates the results from the largest basis set used.

Table 2-3 shows the basis set dependence of the electrostatic interaction energies computed as described in the methods section. Several features are noteworthy. *First*, the polarization energy of the quantum motif (i.e. IND A) is significantly smaller than the unperturbed interaction energy (i.e VxQ plus FxM) and the polarization energy of the environment (i.e. IND B). This result holds even with the most extensive basis set. The magnitude of IND A is nearly constant across each one of the critical points with any given basis set, and the changes upon addition of polarization functions are small and within the variations observed across the basis sets for the larger VxQ, FXM, and IND B energies at any given critical point. *Second*, the induction contribution to the self energy of the environment (SELF B) is small, and insensitive to the position of the proton. *Third*, the total unperturbed interaction energy and its individual components change very little upon expansion of the basis set. All the values are within 0.9 kcal/mol for the VxQ term and within 0.1 for the FxM term. As expected, the major term in the unperturbed interaction energy comes from the interaction with the point charges (i.e. VxQ). Finally, the contribution from the B component, the environment, to the interaction polarization energy (i.e. IND B) is as large as the VxQ term, and these two terms have the largest dependence on the position of the proton. As is the case for the VxQ term, the three basis sets tested yield very similar IND B values (i.e. within 0.1 kcal/mol) for each of the critical points.

2.4 DISCUSSION

Scheiner reported the proton transfer energy curve for the ammonium/hydrogen sulfide complex (Scheiner, 1984). In the fully optimized complex, the hydrogen bond is essentially linear, with the proton lying clearly on the ammonia side. The optimized N--S distance is 3.35 A which is close to the 3.32 A distance in our complex constructed from the model for His 162 and Cys 25 in actinidin. The major difference between the fully optimized complex and the one calculated here is the angular orientation between the C_3 axis and the internuclear axis connecting N and S. This angle is 55.5 degrees in our complex and reflects the angular restriction imposed by the protein. This angle is essentially zero in the complex reported by Scheiner. The corresponding angles for the C_2 axis of hydrogen sulfide in both complexes are rather similar: 65.8 degrees for the complex computed here, and 70.7 degrees for that reported by Scheiner.

As expected from previous work on the angular dependence of the proton transfer energy curve in hydrogen bonded systems (Scheiner et al., 1986), the discrepancy in geometry makes the barriers and driving energies computed from our complex different from Scheiner's values. At the 4-31G* level, the barrier for proton transfer in the linear hydrogen bond between ammonium and hydrogen sulfide is 30.4 kcal/mol when the N--S distance is fixed at 3.35 A; the proton transfer from S to N has a barrier of 1.7 kcal/mol.

The hydrogen bonding energy of such a complex is 13.9 kcal/mol., and the energy difference between the endpoints is 28.7 kcal/mol.. The corresponding values for the angular complex, computed with the 6-31G** basis set, are 55.0 kcal/mol for the barrier from the ammonia side and 10.5 kcal/mol for the barrier from the sulfur side. The stabilization energy of the complex is 6.3 kcal/mol., and the end points of the proton transfer are separated by 44.5 kcal/mol.. Some of the discrepancies, such as the difference between the stabilization energy and the hydrogen bonding energy, can be attributed to the lack of full optimization in the computations done with the complex of Figure 2-1, but others, like the differences in the barrier from the ammonia side and in the energy between the end points, can be rationalized by considering the charge/dipole model for the stabilization of the end points of proton transfer developed by Scheiner (Scheiner et al., 1986). According to this model, the angular dependence of the interaction energy between the molecules in a cationic hydrogen bonded complex is dominated by the charge/dipole interaction, and the proton will be positioned so as to maximize this energy term in the complex. In the ammonium/hydrogen sulfide complex the dipole from ammonia orients with the C_3 axis and the dipole from hydrogen sulfide orients with the C_2 axis (See Figure 2-1). The angular distortion in the C_3 axis of ammonia with respect to the internuclear axis N--S in the complex computed here causes a reduction in the electrostatic stabilization energy in the ammonia/hydrogen sulfide cation form (i.e M2) of the complex compared to the undistorted complex computed by Scheiner. Because the C_2 axes of the complex computed

here and the undistorted one are similarly oriented with respect to the internuclear axis N--S, the charge/dipole interaction in the ammonium/hydrogen sulfide form (i.e. M1) of the complexes will be similar. Thus, with M2 higher and M1 at about the same energy level, the energy difference between M2 and M1 will be larger in the angular complex than in the undistorted complex. A similar explanation applies to the discrepancy between the energy barriers for transfer from the ammonia side because the TS complex resembles the ammonia/hydrogen sulfide cation form (i.e. M2), and is thus higher in energy than the TS of the undistorted form.

Scheiner et. al. (Scheinter et al., 1986; Scheiner et al., 1985; Szczesniak and Scheiner, 1985) have performed calculations on the effect of point charges on the energy for proton transfer in hydrogen bonded complexes. Extreme sensitivity was observed for the barriers and driving energies, such that proton transfers that may not occur normally, could be forced with the appropriate field. In addition, it was shown that the effect of ions on the Hartree-Fock proton transfer energy curve was well reproduced by point charges substituting for the ions (Scheiner et al., 1985). These results suggested that the major effects of ions on the proton transfer were through their electrostatic effect. In addition, it suggested that in computations of the reaction coordinate for proton transfers in the catalytic site of enzymes the interaction between a quantum mechanically described catalytic site ,i.e. the quantum motif, and the large polypeptide environment surrounding it may be adequately described by just considering the electrostatic effects of this environment on the quantum motif as

described above in the Methods section of this chapter. This seems particularly valid when doing calculations at the Hartree-Fock level since recently Liang and Lipscomb have shown that the electrostatic energy between complexes composed of ionic elements makes up as much as 95 percent of the SCF energy (Liang and Lipscomb, 1986). With this in mind, many investigators have introduced and used computational methodologies in which the numerous atoms in a macromolecule are represented as point-charges and point-polarizabilities and the quantum mechanical description is limited to atoms involved in the hydrogen bonded system of interest (Allen, 1981; Drummond, 1986; van Duijnen et al., 1985; van Duijnen et al., 1982; van Duijnen et al., 1980; van Duijnen et al., 1979; Tapia and Goscinski, 1975; Tapia and Johannin, 1981; Tapia et al., 1985; Thole and van Duijnen, 1980; Thole and van Duijnen, 1983a; Umeyama et al., 1984; Warshel, 1981b; Warshel and Levitt, 1976; Warshel and Russell, 1986; Warshel and Weiss, 1980). The basis set dependence of these approaches has never been reported.

The results suggest that the electrostatic interaction energy between the collection of point charges and polarizable points with the quantum motif is adequately represented even at the minimal basis set level. No further improvement of the unperturbed interaction energy (i.e. the sum of VxQ and FxM terms as shown in Table 2-3) is achieved by expanding the basis set. The polarization of the quantum motif understandably is more sensitive to the basis set. But for a cationic hydrogen bonded complex the split valence level is sufficient to achieve the results obtained in computations that include

polarization functions on all the atoms. Interestingly, this energy term is rather small and constant at the extrema of the proton transfer energy curve. Possibly, this is because the environment is far away, and the proton transfer involves a rather small rearrangement of the net charge, i.e., the displacement of a positive charge across 1 angstrom. Previous work suggests that most of the polarization energy will come from the hydrogen bond (Holmes et al., 1985), but this is included in the quantum mechanical calculation and, is thus, appropriately described.

TABLE 2-1. Coordinates for the NH_4/H_2S complex (in angstroms), in the coordinate system of actinidin in file 2ACT of the Brookhaven Protein Data Bank.

Atom	X	Y	Z
ND1	60.021	23.883	16.079
SG	60.507	20.605	16.260
H2	59.359	23.201	16.510
H3	60.461	24.462	16.828
H4	59.501	24.504	15.420
H2S	60.495	20.687	17.586
HM1	60.710	23.288	15.592
HSM1	59.532	19.707	16.168
HTS	60.323	22.286	16.025
HSTS	59.231	20.239	16.083
HM2	60.355	22.012	16.010
HSM2	59.225	20.259	16.050

TABLE 2-2. Stabilization energies [a], barriers, and driving energies for the ammonium/hydrogen sulfide complex (in kcal/mol).

Critical Point	STO-3G	6-31G	6-31G**
M1	-4.6	-11.5	-6.3
TS	42.0	58.3	48.7
M2	29.0	52.4	38.2
TS-M1	46.6	65.4	55.0
TS-M2	13.0	5.9	10.5
M2-M1	33.6	59.5	44.5

[a] Zero energy is the isolated ammonium and hydrogen sulfide molecules. Ammonium: -55.86885 a.u., STO-3G; -56.51315 a.u., 6-31G; -56.54223 a.u., 6-31G**. Hydrogen sulfide: -394.31163 a.u., STO-3G; -398.62646 a.u., 6-31G; -398.67492 a.u., 6-31G**.

TABLE 2-3. Electrostatic interaction energy [a] (in kcal/mol) of the complex of NH_4/H_2S with the environment represented by the side chains of Gln 19, Asn 182, and Trp 184 in actinidin.

Critical Point	Energy	STO-3G	6-31G	6-31G**
M1	SELF B	0.9	0.9	0.9
	VxQ	-5.1	-5.3	-5.2
	FxM	0.9	0.9	0.9
	IND B	-5.2	-5.0	-5.1
	Total	-9.4	-9.4	-9.4
	IND A	0.0	-0.2	-0.1
TS	SELF B	0.8	0.8	0.8
	VxQ	-4.8	-5.4	-4.6
	FxM	0.8	0.9	0.8
	IND B	-3.3	-3.5	-3.4
	Total	-7.3	-8.0	-7.2
	IND A	0.0	-0.1	-0.1
M2	SELF B	0.7	0.8	0.8
	VxQ	-4.4	-4.9	-4.0
	FxM	0.8	0.8	0.8
	IND B	-2.9	-3.1	-3.0
	Total	-6.5	-7.2	-6.2
	IND A	0.0	-0.1	-0.1

[a] The components of the E^{sc} interaction energy are defined in the text.

Figure 2-1. NH_4/H_2S complex oriented as in actinidin (see text).

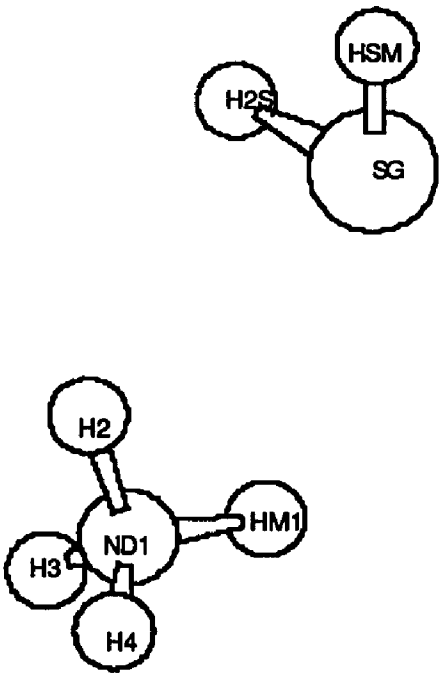

CHAPTER 3

ELECTROSTATIC EFFECTS ON A MODEL PROTON TRANSFER PROCESS INSIDE A PROTEIN

3.1 INTRODUCTION

To identify the molecular determinants that may be relevant to ligand recognition and receptor activation at the 5-HT/LSD receptor subtype, we have followed the heuristic approach described in chapter 1, Background and Scope (Weinstein et. al., 1987; Osman et al., 1987). This approach consists of an analysis of the molecular properties common to ligands of the receptor, and the introduction of models with complementary properties and capable of responding once ligands are recognized (i.e. the PTM).

Inasmuch as the proton transfer event of the activation model (PTM) occurs inside a protein, the energetics of such a transfer are modulated not only by the ligands (Osman et al., 1987), but also by the protein environment, and especially by the electrostatic effects which are already known to be pivotal in enzyme catalysis (Fersht, 1985; Warshel, 1981a; Warshel and Russell, 1984). Because the structure of the 5-HT/LSD receptor is not yet known, this study chooses an enzyme as the heuristic model in which to explore the electrostatic

effects from the receptor on the model for activation. An important consideration in using the heuristic approach is that contrary to enzyme catalysis where the polypeptide structure is expected to aid the steps in the reaction coordinate of the catalytic mechanism, the polypeptide structure of a heuristic model for a receptor would be expected to hinder those steps that lead to receptor activation. Otherwise, the polypeptide structure would trigger a response in the *absence* of the ligands that are responsible for receptor activation. Through a search procedure of the Protein Data Bank (PDB) (Bernstein et al., 1977), the enzyme actinidin (E. C. 3.4.22.14) was identified as a suitable model of the protein environment. It incorporates amino acid residues that can sustain the proposed mechanism of receptor activation and contains multiple helices in a variety of orientations. To make possible the generalization of the inferences from this model to the structure (presently unknown) of the 5-HT/LSD receptor, the electrostatic effects of the protein structure of actinidin on the proton transfer between the His 162 and Cys 25 residues in the active site were computed and analyzed in terms of contributions from constitutive elements of the structure of the enzyme (Mercier et al., 1988a; Mercier et al., 1988b).

3.2 THEORETICAL APPROACH

3.2.1 PROTEIN SELECTION AND CONSTRUCTION OF QUANTUM MOTIF

The coordinates available in the Brookhaven Protein Data Bank (PDB) (Bernstein et al., 1977) were searched for protein structures which contained an arrangement of chemical groups compatible with the Proton Transfer Model (Osman et al., 1985; Osman et al., 1987). Because the proposed recognition site is an imidazolium with hydrogen bond attachments to a neighboring proton acceptor group, a computer program was written to scan the PDB for putative hydrogen bonding groups in the vicinity of the ND1 and/or NE2 atoms in the imidazole ring of His residues. The nitrogen, oxygen, and sulfur atoms of the side chain residues of Ser, Cys, Tyr, Asn, Asp, Glu, Gln, Lys, Arg, and His were flagged when located within 4.1 A of an ND1 and/or NE2 atom. The requirement for a Trp residue positioned in a stacking conformation in proximity to the imidazole rings of the His was added to the search criteria in order to simulate a 5-HT congener, i.e. the ligand, interacting with the proton transfer model, i.e. the receptor. This was accomplished by merging the results of the first scan with those kindly provided by Dr. Dave Roberts who had scanned the PDB for indole/imidazole interactions.

Because none of the known neurotransmitter receptor sequences suggests the presence of metals (Dixon et al., 1986; Gocayne et al, 1987; Grenningloh et al., 1987; Hulme and Birdsall, 1986; Julius et al., 1988; Kobilka et al., 1987; Kubo et al., 1986; Marx, 1987; Masu et al., 1987; Schofield et al., 1987; Stevens, 1987; Trowbridge, 1987) metalloproteins were excluded from the two data sets, and their intersection was visually inspected for the simultaneous occurrence of optimal hydrogen bonding distances between the His and the side chain residues with putative hydrogen bonds, as well as near optimal stacking interaction between the imidazole ring of the His and the indole ring of Trp. Actinidin (E.C. 3.4.22.14), a sulfhydryl proteinase, emerged as a good candidate in which all the criteria were fulfilled. The specific grouping identified in file 2ACT of the PDB (Baker, 1980; Baker et al., 1981; Bernstein, 1977) consisted of His 162 which is in near stacking conformation with the indole ring of Trp 184 and has a putative hydrogen bond to Cys 25 and Asn 184. These residues (See Figure 3-1.) are also considered as the main components of the active site for the enzymatic activity of actinidin (Baker, 1980; Brocklehurst et al., 1981; Lowe and Whitworth, 1974; Polgar and Halasz, 1982) .

3.2.2 STRUCTURE AND ENERGIES OF THE ISOLATED QUANTUM MOTIF

The potential energy curve for proton transfer between ND1 and SG was constructed from quantum mechanical calculations of the isolated proton transfer model consisting of the side chains of His 162

and Cys 25 modeled by imidazolium and methanethiol, respectively. This model corresponds to an inactive form of the enzyme found at low pH. The choice of the model follows the requirements imposed by the proton transfer model (PTM) proposed from studies of recognition and activation of the 5-HT/LSD receptor (Osman et al., 1985; Osman et al., 1987). The coordinates of the imidazolium/ methanethiol complex according to the coordinate system of the protein data bank file are listed in Table 3-1. The imidazolium geometry corresponds to an STO-3G optimized structure with the heavy atoms superimposed onto the side chain of His 162. The methanethiol geometry corresponds to that of the side chain of Cys 25 in the crystal structure of actinidin, with the methyl hydrogens placed with the use of the program HYDRO of M. Levitt. To obtain the methanethiol, the C alpha of Cys 25 was replaced by a hydrogen with a C-H distance of 1.10 Å, the experimental value reported for methanethiol (Mitchell and Cross, 1958). No superposition of the heavy atoms in an optimized methanethiol structure was attempted because the solution would not be unique. The CB and SG atoms in the methanethiol group of Cys form a straight line and the superposition of two straight lines has an infinite number of solutions due to the rotation axis colinear with the superposition lines. Nevertheless, the methanethiol structure of Table 3-1 was checked against the experimental and computed structures (Gordon et al., 1982; Pietro et al., 1982) and no major discrepancies were found. The intermolecular orientation of the molecules is very similar to the one found in the PDB coordinate file for the side chains of His 162 and Cys 25.

Ab initio quantum mechanical calculations at the LCAO-MO-SCF Hartree-Fock level of approximation were performed with the Gaussian 82 (Binkley et al., 1982) systems of programs. Three basis sets were used as described below including the STO-3G (Hehre et al., 1970; Hehre et al., 1969), the 6-31G basis sets (Francl et al., 1982; Hehre et al., 1972), and the 6-31G* basis set (Binkley et al., 1980; Francl et al., 1982; Gordon et al., 1982; Hariharan et al., 1972). Correlation energy contributions were computed to the MP3 level in the Moller Plesset perturbation procedure (Moller and Plesset, 1934) available in Gaussian 82.

The reaction coordinate for the energy curve for the transfer of 1HD1 consisted of the ND1--1HD1 distance. In the computations, the angle and dihedral angles determining the position of 1HD1 and all the internal coordinates of HSG were optimized with the gradient method in Gaussian 82 because the hydrogen bond between ND1 and SG was not linear (See Figure 3-3.) (Binkley et al., 1980; Binkley et al., 1982); all other internal coordinates were kept fixed. The critical points (i.e., the minimum near ND1, termed M1, the transition state, termed TS, and the minimum near SG, termed M2) were calculated by full optimization of the internal coordinates of 1HD1 and HSG. In this optimization, the transition state was constrained to have one negative eigenvalue in the matrix of force constants. Optimizations were done with the STO-3G and 6-31G basis sets; single point calculations at the 6-31G geometries were done with the 6-31G* basis set.

The simulated proton transfer is from imidazolium to methanethiol and not from methanethiol to imidazole. The latter model consists of a neutral system that changes into a zwitterion upon proton transfer, and is the model used in studies of the catalytic activity of actinidin. The proton transfer process I studied consists of a cationic hydrogen bond and involves a charge redistribution in the proton donor and acceptor upon transfer of the proton. This process is consistent with the model for the activation mechanism of the serotonin receptor studied (Osman et al., 1987).

3.2.3 COMPUTATIONS WITH THE QUANTUM MOTIF EMBEDDED IN ACTINIDIN

The protein environment was represented by a collection of point charges and polarizabilities centered on the atoms. The point charges are from a data base generated with the Mehler-Paul basis set (Mehler and Paul, 1979), using a population analysis of the Hartree-Fock SCF wavefunction that preserves the first and second moments of the charge distribution (Thole and van Duijnen, 1983b). The atomic polarizabilities are from a library in the program HONDO modified to solve the Direct Reaction Field Hamiltonian (Thole and van Duijnen, 1980). These polarizabilities were derived through a fitting procedure as described by Thole (Thole, 1981). They are expected to reproduce the polarizabilities of the fragments composed of the backbone and the

side chain atoms in the amino acid residues in actinidin. All atoms in the protein were treated explicitly.

In the PDB data set, some atoms have two sets of coordinates due to disorder; only the coordinates with the highest occupation were retained in the data set. The side chain residue of Glu 87 which was missing from the PDB file was constructed by translating the coordinates of Glu 86 to the position of Glu 87. No poor contacts were detected between the constructed coordinates and the rest of the protein. The exact conformation of Glu 87 is unlikely to be critical in this work because this residue is > 20 Å from the side chain of His 162.

The effect of the entire protein structure (subsequently termed here the "full protein environment"; FULL) was considered by using all the atoms in the protein except those belonging to His 162 and Cys 25. To consider the effects of selected elements of the structure, three subsets of coordinates were also generated. One set (HX) consisted of the atoms belonging to the alpha helices as identified in the PDB file (i.e. helices A1 to A6). Another set (BETA) contained the beta sheets composed of the sheets B1 and B2 as identified in the PDB file. The third set (ACTIVE) contained only the atoms of Trp 184, Asn 182, and Gln 19, which, together with His 162 and Cys 25, form the active site of actinidin (Baker, 1980; Brocklehurst et. al., 1981; Lowe and Whitworth et. al., 1974).

The electrostatic effects of the inhomogeneous field from the above environments on the proton transfer process were computed through a scheme described in detail in the previous chapter. Briefly, McWeeny's Variation - Perturbation Theory of Group Functions (McWeeny and Sutcliffe, 1976) is applied to the semiclassical system composed of a quantum motif (i.e. the imidazolium/methanethiol complex; the "quantum group" or A group) and the classical motif (i.e. the macromolecule represented as a collection of point charges and polarizabilities; the "classical group" or B group). An iterative procedure is used to compute the polarization of a group due to the perturbation from the other. The electrostatic energy is decomposed into perturbed and unperturbed (i.e. polarization) contributions.

The first step in the iterative scheme (i.e. i=0) yields the unperturbed electrostatic interaction between the groups. The unperturbed interaction (UNPT) is computed from the sum of the VxQ and FxM energies as defined in the last chapter in section 2.2.7:

$$UNPT = VxQ + FxM \qquad (1)$$

The polarization of the macromolecule (IND B) by the unperturbed field from the quantum motif (i.e. the imidazolium/methanethiol complex) is also computed at the first step in the iterative scheme (i=0) using the effective polarizability supermatrix:

$$IND\ B = -\frac{1}{2}\sum_{k,l \in B} F_k^{(0)} \cdot \left\{ \bar{A}^{-1} + \bar{T} \right\}^{-1}_{k,l} \cdot F_l^{(0)} \qquad (2)$$

This energy term represents the response of the environment to the changes in the field from the quantum motif generated by the transfer of the proton. It is important to emphasize that IND B changes not only because the nuclear charge of the proton moves, but also because the change in position of this nuclear charge forces a rearrangement of the charge density of the entire quantum motif.

The contribution from the polarization of the quantum motif (POL QM) by the macromolecule is estimated from the i=1 step of the iterative scheme. Only the potential from the point charges q_k was included in the perturbed Hamiltonian, $H_A^{(1)}$.

$$POL\ QM = \langle \psi_A^{(1)} | H_A^{(1)} | \psi_A^{(1)} \rangle - \langle \psi_A^{(0)} | H_A^{(0)} | \psi_A^{(0)} \rangle \qquad (3)$$

where $\psi_A^{(1)}$ is the i=1 perturbed wavefunction and $\psi_A^{(0)}$ is the unperturbed wavefunction computed using the unperturbed molecular Hamiltonian for the quantum motif, $H_A^{(0)}$

Under the decomposition scheme described in the previous chapter, POL QM includes the contribution from the polarization of the quantum motif by the macromolecule, IND A, and the contribution from the polarization of the quantum motif to its self energy, SELF A:

$$IND\ A = \frac{1}{2}\sum_{k \in B}\left[V_k^{(1)} - V_k^{(0)}\right]q_k - \left[F_k^{(1)} - F_k^{(0)}\right] \cdot \vec{m}_k \qquad (4)$$

$$SELF\ A = \tfrac{1}{2}\langle \psi_A^{(0)} | \left[V_A^{(1)} - V_A^{(0)} \right] \psi_A^{(0)} \rangle \qquad (5)$$

where $V_k^{(1)}$ and $F_k^{(1)}$ are the electrostatic potential and the field generated by the charge distribution associated with $\psi_A^{(1)}$. $V_A^{(1)}$ and $V_A^{(0)}$ are the electrostatic potential on the nuclei and electrons of the quantum motif, and generated by the charge distributions associated with $\psi_A^{(1)}$ and $\psi_A^{(0)}$, respectively.

For the electrostatic interaction between the imidazolium/methanethiol complex and actinidin, the iterations were limited to i=0 and i=1 using the STO-3G and 6-31G basis set because the small magnitude of POL QM suggested that the results were close to convergence (See results.). In the previous chapter it was shown that the addition of polarization functions would not cause significant changes in the computed energies, and that convergence for the iterative scheme would be very rapid (McWeeny and Sutcliffe, 1976). The electrostatic potentials and fields were computed using the property package in Gaussian 82. The computations with the perturbed Hamiltonian were done using the HONDO package (Dupuis et al., 1976). For the computations with the FULL protein, the effective polarizability matrix would be too large to be tractable. Thus, the external field from the induced dipoles was neglected in the computation of IND B, i.e. ,the dipole interaction supertensor was set to zero. From test calculations on other fragments, this approximation overestimated the IND B by 20 to 30%, but introduced no qualitative

changes in the results. Overestimation of the computed energy is always expected because the polarization at one center in the macromolecule is entirely driven by the quantum group without opposition from the field of the induced dipoles at other centers in the macromolecule. Also, no FxM computation for the FULL protein case was possible because neglect of the dipole interaction supertensor (see chapter 2 for details) yields physically meaningless results. Thus, the UNPT energy term for the FULL protein environment was estimated from the VxQ energy.

3.2.4 CONTRIBUTION TO THE ELECTROSTATIC ENERGY FROM THE COMPONENTS OF THE QUANTUM MOTIF

Previous work suggested that the proton transfer in the PTM was modulated by the electrostatic effect of the ligand on the acceptor and donor molecules and not by a direct effect on the proton (Osman et al., 1987). To evaluate if a similar mechanism existed for the modulation by the protein environment of the proton transfer between imidazolium and methanethiol, the VxQ energy was decomposed into contributions from the imidazole (IMID), methanethiol (METS), and the proton (PTN). This decomposition was achieved by first approximating the VxQ energy by

$$QxQ = \sum_{\substack{j \in A \\ k \in B}} \frac{q_j q_k}{|\vec{r}_k - \vec{r}_j|} \qquad (6)$$

where q_i correspond to the net charges from the Mulliken Population analysis and then, collecting the contributions from the point charges centered on the imidazole, the methanethiol, and the proton to the QxQ energy. As shown below, the QxQ energy is a good approximation to the VxQ energy in this case, as found earlier for other types of molecular interaction (Weinstein et al., 1981a).

3.2.5 CONSIDERATION OF THE SOLVENT SCREENING EFFECTS

The polypeptide structure of actinidin is strongly basic and the full protein molecule is calculated to have a net charge of -15.0 when the ionization of acidic and basic groups is determined at pH 7 using the standard pKa's of free amino acids. When the positively charged quantum motif is excluded to construct the full protein environment, the net charge increases to -16.0. In solution, solvent accessible charges would be surrounded by water dipoles and counterions. The electrostatic effects of the large net charge of the protein environment would be expected to be attenuated by interaction with the solvent and ions, with the largest effect being registered for the atoms which are closest to the protein-solvent interface (Gilson et al., 1985; Warshel and Russell, 1984). To explore if the results of our computations are biased by the large net charge of the full protein environment and to mimic the attenuating effect of a polar environment, the total charge of -16.0 was reduced by scaling down the charge of solvent accessible atoms. This procedure is expected to provide a qualitative indication of the dependence of the computed results on the net charge of the protein

environment, but did not provide a quantitative measure of effects of the surrounding dielectric environment with its polyelectrolytes. Although methods for the inclusion of the effect of the dielectric environment and the surrounding polyelectrolytes are being developed (Gilson et al., 1988; Gilson and Honig, 1987; Rashin and Namboodiri, 1987; Zauhar and Morgan, 1988), no attempts were made to include these effects in a comprehensive scheme because no consensus has yet been reached regarding the most adequate method, especially when such schemes are coupled to quantum mechanical computations (see Warshel, 1987).

For the charge scaling procedure, the surface atoms of actinidin were identified with the use of a program supplied by Dr. Alexander Rashin (Rashin et al., 1986). In this procedure a sphere with a radius approximating that of a water molecule was rolled over the protein to identify "water accessible points" according to a criterion described by Connolly (Connolly, 1983). These points were then connected to form a surface around the protein and the atoms that belong to this surface were identified. For computational efficiency, the program used a collapsed representation for the hydrogen atoms. Therefore, it was assumed that if a heavy atom was on the surface, its corresponding hydrogen atoms were also on the surface. The attenuation of the charge in the full protein environment was then simulated by a multiplication factor that scaled down the net charge of the exposed atoms. When the charges of the atoms identified to be "solvent accessible" were reduced by a factor of 1.35

the total net charge of the full protein environment was reduced to -0.1 a.u..

3.3 RESULTS

3.3.1 ISOLATED QUANTUM MOTIF

Figure 3-2 shows the energy curve for the proton transfer in the imidazolium/methanethiol complex computed with the STO-3G basis set in the absence of the protein environment. At the Hartree-Fock level, the complex was stable with the proton on the imidazole side. The potential energy curve displayed a double well character with critical points located at ND1--1HD1 distances of 1.03 Å for the first minimum (M1), 1.63 Å for the transition state (TS), and 1.90 Å for the minimum on the methanethiol side (M2). The barrier for proton transfer from the imidazole side (TS-M1) was 39.0 kcal/mol and the driving energy (M2-M1) was 35.6 kcal/mol. (See Table 2.) Figure 3-2 also shows the effects of correlation energy calculated at the MP3 level on the proton transfer curve. As observed earlier for other systems (Scheiner et. al., 1983), the contribution from the correlation energy drastically reduced the barrier to proton transfer; it also reduced the the driving energy. Due to the impracticality of geometry optimizations when computing correlated wavefunctions, the critical points of the proton transfer curve were estimated from a quartic polynomial fit to the values plotted in Figure 3-2. The fit yielded critical points at 1.07 Å for the minimum closest to the imidazole

(M1), 1.63 Å for the transition state (TS), and 1.85 Å for the second minimum (M2), nearly identical to the values from the SCF level of computation. The barrier for proton transfer calculated from the fit was 26.3 kcal/mol and the driving energy was 24.1 kcal/mol.

Table 3-2 shows the effect of extending the basis set on the energetics of proton transfer between imidazolium and methanethiol; only the critical points were computed. Extending the basis set to split-valence retained the stability of the complex, but the barrier for proton transfer increased by 16.4 kcal/mol and the driving energy decreased by 9.4 kcal/mol from the STO-3G values. This result was again consistent with earlier observations regarding the effect of basis sets on calculated barriers for proton transfer (Scheiner, 1983). The addition of polarization functions reversed the trend observed with the split-valence basis set: relative to the split-valence basis set values, the barrier dropped by 11.3 kcal/mol and the driving energy increased by 14.5 kcal/mol.

Table 3-3 shows the internal coordinates for the proton (i.e. HD1) and the hydrogen bonded to the sulfur of methanethiol (i.e. 1HSG). These internal coordinates were optimized in determining the critical points of the proton transfer energy curve. The internal coordinates showed that the optimal path of the proton did not follow a straight line. Figure 3-3 shows the positions of the proton when computed with the STO-3G basis set. The energy curve constructed by moving the proton in a straight line between ND1 and SG (data not shown) was composed of considerably higher energies and had higher

barriers than the one shown in Figure 3-2. Table 3-3 also shows the basis set dependence for the optimized internal coordinates. In general, the bond lengths showed the least variation with changes in basis set while the angles varied more. It is noteworthy that the coordinates of the 1HSG exhibited a stronger basis set dependence than the proton (i.e. 1HD1) coordinates. This effect was probably due to a dependence of the internal coordinates of 1HSG on the description of the "lone-pairs" of the sulfur in methanethiol by the various basis sets.

3.3.2 INTERACTION WITH THE PROTEIN ENVIRONMENT

Table 3-4 lists the electrostatic energy of interaction between the protein environment and the imidazolium/methanethiol complex computed at the critical points using the STO-3G basis set. The electrostatic energy was decomposed into unperturbed (UNPT) and induction (IND B) terms. Also, into contributions from fragments of the protein structure as described above in Theoretical Approach. The full protein structure (FULL) interacted favorably with the quantum motif (i.e. the imidazolium/methanethiol complex) at the three critical points. A result noteworthy because the quantum motif beared a net positive charge not present in the model for the active site of actinidin used to study the catalytic mechanism of this enzyme, i.e., the imidazole/methanethiol complex. The full protein opposed the proton transfer by raising the barrier (TS-M1) by 9.3 kcal/mol and reducing the driving energy (M2-M1) by 10.8 kcal/mol from the results in Table 3-2. These effects were due to the unperturbed interaction as

approximated by the VxQ energy term because the polarization of the protein (IND B) lowered the barriers by 2.3 kcal/mol and increased the driving energy by 5.3 kcal/mol. These changes on the in vacuum proton transfer energy curve were more dramatic when shown graphically as done in Figure 3-4. In this figure the changes in the Hartree-Fock energy are shown by taking advantage of the QxQ approximation to the VxQ energy (see below). As explained in the discussion, it was noteworthy that as a model of the electrostatic effects of the unknown receptor structure, the full protein hindered the proton transfer. Otherwise, the protein electrostatic effects would have be able to trigger the proton transfer responsible for activation of the receptor in the absence of any ligand.

The analysis of the electrostatic contributions from the different elements of the protein structure showed that the changes in the proton transfer energy curve described above resulted from a complex interplay between opposite contributions from the fragments that compose the protein. The residues included in the active site, none of which are part of the alpha helices or beta sheets in actinidin, interacted favorably with the quantum motif at the critical points. Similar results applied to the contribution from the alpha helices and the beta sheets. However, these groups did not stabilize the critical points uniformly, and thus, affected the barrier and driving energy differently. The groups in the active site increased the barrier by 2.8 kcal/mol and lowered the driving energy by 4.1 kcal/mol, a result qualitatively consistent with the full protein effects. The beta sheets and the alpha helices had a different effect -- they aided the transfer of

the proton. The beta sheets and the alpha helices lowered the barrier by 8.5 kcal/mol and 8.9 kcal/mol, respectively, and increased the driving energy by 11.8 kcal/mol and 12.7 kcal/mol, respectively.

Table 3-4 shows that the relative contribution from the unperturbed and induction energy terms to the changes described above for the proton transfer energy curve varied among the protein fragments. For the groups of the active site the induction energy was primarily responsible for the changes in the barrier and driving energy. The interplay between unperturbed and perturbed contributions (i .e. UNPT and IND B, respectively) was more complex in the case of the beta sheets. The VxQ component of the unperturbed energy, given in parenthesis in Table 3-4, had a similar magnitude, but opposite effect on the barrier and driving energy to the one from the IND B term. Thus, their effects canceled and the net result was from the FxM component of the unperturbed interaction energy. The effect from the alpha helices also comes from the unperturbed interaction energy, but both the FxM and the VxQ components had similar effects on barrier and driving energy. It is noteworthy that for the alpha helices the VxQ energy computed at the critical points was two orders of magnitude greater than either the IND B or the FxM term, and gave results qualitatively consistent with the more complete computation for the changes in the barrier and driving energy.

Table 3-5 lists the polarization of the quantum motif (POL QM) computed with the 6-31G basis set. The polarization of the quantum

motif by the active site groups, the alpha helices, and the full protein was significantly smaller in magnitude than the UNPT and the IND B energy terms listed in Table 3-4. A more important observation is that the contribution from POL QM to the changes in the barrier and driving energy of the proton transfer energy curve was negligible.

3.3.3 ANALYSIS OF THE ELECTROSTATIC INTERACTION ENERGY

To test if the changes produced in the barrier and driving energy values calculated in vacuum (Table 3-4) were due to the inhomogeneous field along the path of the proton, the VxQ energy was approximated by the QxQ energy as described in Theoretical Approach. Then, it was decomposed into contributions from the proton donor (i.e. the imidazole, IMID), the proton acceptor (i.e. the methanethiol, METS), and the proton (PTN). This test was limited to the effects from the full protein and the alpha helices where the VxQ energy gave results qualitatively consistent with the more complete computations. The effects from the alpha helices were of considerably more interest than those from the beta sheets and the active site groups because the structural data available for neurotransmitter receptors and other membrane bound proteins suggested that alpha helices were prominent features in their secondary and tertiary structure (Engelman et al., 1982; Stevens, 1985; Dixon et al., 1986; Gocayne et al., 1987; Grenningloh et al., 1987; Hulme and Birdsall, 1986; Kobilka et al., 1987; Kubo et al., 1987; Stevens, 1987; Trowbridge, 1987).

The top of Table 3-6 lists the QxQ and VxQ energy terms for the alpha helices and the full protein. As expected the QxQ energy was a good approximation to the VxQ energy for the interaction energy at the critical points and for the changes in the barrier (TS-M1) and driving energy (M2-M1). The discrepancies were within 1 kcal/mol. Figure 3-5A and 3-5B show the contributions to the QxQ energy from the components of the quantum motif (i.e. IMID, METS, and PTN), computed for the full protein and alpha helices, respectively. The energy at point M1 was taken as zero, and the bottom of Table 3-6 lists points selected from the figures. The results showed that the stabilities of the proton donor (IMID) and acceptor (METS) were affected by the electrostatic interaction with the environment significantly more than the stability of the proton (PTN) as it was moved towards the acceptor. For both, the alpha helix and the full protein environments, the proton donor and acceptor were affected differently -- the donor was destabilized and the acceptor was stabilized. *Both* environments stabilized the proton as it was moved towards the acceptor, but only the alpha helix environment lowered the barrier and increased the driving energy for proton transfer (see top of Table 3-6). As shown in Figure 3-5A and in the bottom of Table 3-6, it was the large destabilization of the proton donor (i.e. IMID) as the proton was moved that kept the proton on the imidazole when the effects of the full protein were included.

The collection of alpha helices and the full protein structure had net charges of -6 and -16, respectively. In solution their electrostatic

effects would have been attenuated as discussed in Theoretical Approach. To explore the changes in the qualitative results described above by such attenuation, the surface charges were scaled as described in Theoretical Approach. Table 3-7 and Figures 3-6A and 3-6B show results analogous to the ones in Table 3-6 and Figures 3-5A and 3-5B, but computed with the scaled charges. Again the QxQ energy was a good approximation to the VxQ energy, and the major electrostatic effect from the protein environments was on the stability of the proton donor and acceptor. The most significant difference from the results with the unscaled charges was the *destabilization* of both the proton acceptor and the proton by the full protein environment as the proton was transferred (See Figure 3-6A).

3.4 DISCUSSION

The choice of actinidin as the protein that would allow the exploration of the electrostatic effects of the polypeptide structure on the potential energy curve for a model proton transfer event was guided by the main features of the *imidazolium/proton acceptor* complex that had been previously proposed as a receptor model for the activation mechanism at the 5-HT/LSD receptor (Osman et al., 1985; Osman et al., 1987). Thus, the simulated proton transfer, from the imidazolium moiety (ImH^+) on His 162 to the thiol (SH) of Cys 25, was in a direction opposite to that postulated for the function of thiol proteases (Baker and Drenth, 1987), i.e., from Cys 25 (SH) to neutral His 162 (Im) to form a zwitterion state (S^-/ImH^+). It

corresponded to a state of the enzyme at low pH. Although it was not possible to compare the proton transfer energy curve for the quantum motif considered here with the ones computed for the active site of actinidin, the results may be compared to the energy curve computed for an ammonium/hydrogen sulfide complex reported by Scheiner (Scheiner, 1984). In the potential energy curve for the proton transfer between ammonium and hydrogen sulfide in a linearly hydrogen bonded complex, Scheiner found the optimal distance between N and S to be 3.35 Å. This distance was similar to the 3.32 Å distance between the N and S atoms of the imidazolium/methanethiol complex that modeled the side chain residues of His 162 and Cys 25 in actinidin. The calculated barrier for proton transfer was 30 kcal/mol and the driving energy was 28.3 kcal/mol (Scheiner, 1984). The differences between these values and the ones computed here for the imidazolium/methanethiol complex (cf, 44.1 kcal/mol and 40.5 kcal/mol, respectively, using the 6-31G* basis set) may be attributed to the lack of full geometry optimization of the donor and acceptor molecules, the nonlinear orientation of the hydrogen bond in the complex (i.e. < 1HND1-ND1-SG = 55.5 degrees) as imposed by the protein structure, and the different proton affinities of the donor and acceptor molecules. The latter factor was expected to have a minimal effect on the changes in the barrier and driving energy because the *difference* in proton affinities between imidazolium and methanethiol and between ammonia and hydrogen sulfide was expected to be similar.

Structural considerations have been shown to play a key role in modifying the barrier and driving energy of proton transfer (Scheiner, 1986). The lack of optimized structures would increase the barrier and reduce the driving energy because the geometries of the donor (i.e. imidazolium) and the acceptor (i.e. methanethiol) molecules were optimal for the reactants, as opposed to the products of the proton transfer (i.e. imidazole and methanethiol cation). Although Scheiner found for the NH_4^+/H_2S complex that full geometry optimization did not significantly affect the proton transfer energy curve computed using the frozen molecule approximation at fixed intermolecular distance, previous work and my own preliminary computations have suggested that the barrier would decrease and the driving energy would increase by ca. 5 kcal/mol if the imidazolium/methanethiol complex were optimized, but constrained to the intermolecular orientation required by the protein (Topiol et al., 1985; Mercier, unpublished results). The major contribution to the changes in the barrier and the driving energy were due to the large deviation from linearity in the hydrogen bond of the imidazolium/methanethiol complex. Substitution of the imidazolium and the methanethiol by ammonia and hydrogen sulfide, respectively, while retaining the nonlinear orientation resulted in larger barriers and smaller driving energies than those computed by Scheiner, as discussed in chapter 2. These results were explained on the basis of the charge-dipole interaction model proposed by Scheiner for the stability of cationic hydrogen bonds (Scheiner, 1986). Briefly, the imidazole/methanethiol cation form of the complex (i.e. at point M2) was higher in energy in the angular form of the complex because the

charge-dipole interaction was unfavorable in this orientation. This interaction was essentially the same for both orientations of the complex when the proton lies on the imidazole, i.e., the imidazolium/methanethiol form of the complex at M1. Thus, the driving energy decreased (M2-M1); the barrier also increased because the geometry at the transition state, TS, is close to the M2 geometry and TS-M1 would increase.

Correlation energy was only computed at the minimal basis set level due to the size of the complex. The energies computed with correlation corrections showed a trend previously described for cationic hydrogen bonded complexes in which correlation energies were calculated with larger basis sets (Scheiner et al., 1983): correlation energy reduced the barrier for proton transfer from either the proton acceptor or from the donor. Reports in the literature would suggest that geometry optimizations including correlation effects would not be expected to modify the qualitative features of the observations obtained here (Jonsson et al., 1976; Karlstrom et al., 1976).

Because one goal of this study is to gain insight into the potential electrostatic effects of proteins for which no high resolution structural data is available (such as is the case with the 5-HT/LSD receptor), the electrostatic effects from the polypeptide structure of actinidin were computed in terms of the contributions from its secondary and tertiary structure. Such elements of protein structure have been recognized in all the proteins for which structural data are available

(Richardson, 1981), and recent evidence suggested that they are also prominent in the structure of membrane bound neurotransmitter receptors (Grenningloh et al., 1987; Kobilka et al., 1987; Schofield et al., 1987). Indeed, during the course of this work the primary structure of several subtypes of the serotonin receptor were determined (Fargin et al., 1988; Julius et al., 1988; Prichett et al., 1988; Hartig, 1989), and analysis of their primary sequences suggested the presence of seven transmembrane helices, a common motif in the neurotransmitter receptors that interact with G proteins. It must be emphasized that this strategy focuses on the effects from the higher order structure of proteins (i.e. alpha helices), as opposed to the effects from specific residues within a local structure of the active groups in an enzyme (e. g. the oxyanion hole in serine proteases). As Hwang and Warshel have discussed, these local effects may be optimized through strong evolutionary pressure for the particular function of the enzyme, and may be transferable only across those members of that family of proteins with the same function (Hwang and Warshel, 1988).

Results of the calculations presented here show that the protein environment of actinidin discriminated between the different critical points in the proton transfer energy curve. This was particularly significant for the complex studied here because it does not correspond to the complex suspected to exist in the protein at neutral pH (Baker, 1980; Brocklehurst et al., 1981; Polgar and Halasz, 1982), and also because the redistribution of net charge upon proton transfer in this system represented a charge shift (i.e from [+ 0] to [0 +]) as

opposed to the charge separation process (i.e. from [0 0] to [- +]) that has been considered to occur in the catalytic mechanism of actinidin (Angelides and Fink, 1978). The electrostatic effects from the protein structure of actinidin hindered the proton transfer. This effect included the contribution from the side chain of Trp 184 which as explained in Theoretical Approach was intended to mimick a ligand in the receptor. Thus, a priori, the full protein structure including the ligand mimicked by the side chain of Trp 184 was expected to aid in the proton transfer if the X-ray structure of actinidin were a good model for the electrostatic effects of the 5-HT/LSD receptor structure. Computations analogous to those listed in Table 3-4 showed that the side chain Trp 184 made a negligible contribution to the barrier and driving energy (i.e. TS-M1= 0.4 kcal/mol; M2-M1= 0.5 kcal/mol for the total electrostatic interaction energy). This was due most likely to the discrepancy between the orientation of the indole group in Trp 184 in the protein (i.e. nearly stacking over the imidazole ring of His 162) and the orientation suggested by Osman et al. to be responsible for lowering the barrier for proton transfer (i.e. stacking perfectly parallel to the imidazole and midpoint between the donor and acceptor molecules; Osman et al., 1987). Therefore, even though the side chain of Trp 184 was included in the full protein computations, this model environment was not analogous to the receptor with a ligand bound in a form capable of activation (i.e. triggering the proton transfer), and understandably the electrostatic effects from the full protein structure of actinidin opposed the proton transfer. Indeed, the increase in the barrier and decrease in the driving energy by the electrostatic interaction between the quantum motif and the full

protein environment was a desirable feature because the proton transfer should be triggered by certain ligands, i.e. the agonists, when in the proper orientation, and not by the surrounding protein environment. As shown in a subsequent chapter, chapter 5, the proton transfer between His 162 and Asn 182 was affected by the ligand mimick (Trp 184) and other congeners because the relative position was more favorable.

The decomposition of the electrostatic effects from the protein structure into contributions from the fragments that compose the protein indicated that different groups contributed differently to the modulation of the proton transfer energy curve. It was significant that the alpha helices and the beta sheets aided the proton transfer, and their effects was considerably larger than the contribution from the groups in the active site which opposed the transfer. Thus, the elements of the protein structure which were not included in the decomposition are presumably responsible for hindering the proton transfer when the full protein effects was considered. This finding suggested that computations of molecular processes in proteins in which the environment would be limited only to a fraction of the structure in the protein may not reflect the effects of the entire protein structure on the energetics of a reaction coordinate. Different parts of the protein may counteract each other's effects in yielding the net result observed when the entire protein structure is considered. Consequently, the use of a **distance criterion**, often applied to reduce the size of computations aimed at elucidating the role of electrostatics in the structure and function of proteins, may not be adequate.

Similarly, the significant modulatory effects from the different elements of the structure of proteins would be missed in computations that only consider a **single** element of structure or the entire protein structure alone. Such modulatory effects may be of significant value in efforts to design proteins with specific function. Consequently, the attribution of a particular physicochemical effect observed inside a protein, such as a shift in pKa, to a single element of the protein structure would be incorrect unless all the contributions from the different elements in the complex structure of the protein happen to cancel out.

The complex interaction between the protein environment and the quantum motif was further demonstrated by studying the interaction between the groups of the quantum motif and their environment. The changes in the potential energy curve for proton transfer when the electrostatic effects of the polypeptide environment was considered, resulted from opposite effects on the stabilization of not only the proton, but also its acceptor and donor molecules as the proton was moved. This implied that the modulatory effect from the protein originated from its electrostatic interaction with the charge distribution of the donor and acceptor molecules as it was redistributed by the moving proton and not by the field from the protein because the polarization of the quantum motif by the latter was small. Consequently, computational schemes that attempt to develop mechanistic hypothesis for enzyme catalysis or receptor activation events in which proton transfers occur need to go beyond the mere description of the electrostatic potential from the protein

environment *along* the reaction coordinate path (Lavery et al., 1983). Moreover, it suggested that electrostatic effects described here may have been missed in molecular mechanics or dynamic simulations that used potential functions that did not incorporate the charge redistribution associated with the proton transfer in a hydrogen bonded complex. Thus, quantum mechanical simulations or modification to the potential functions are necessary to study the modulatory role of the protein electrostatic environment on, at least, proton transfer reactions, and possibly chemical catalysis.

The breakdown of the electrostatic energy into perturbed (IND B and POL QM) and unperturbed (i.e. VxQ and FxM) contributions showed that the nature of the electrostatic interaction between the quantum motif and the different fragments of the protein varied among the fragments. Work by Holmes et al. (Holmes et al., 1985) showed that the polarization energy was nonnegligible between hydrogen bonded groups. His 162 was hydrogen bonded to Cys 25 and Asp 182. The former interaction was included in the quantum mechanical description of the groups. The latter was included in the semiclassical scheme by the classical representation of Asp 182, and hence was appropriately described because the hydrogen bond is largely electrostatic in nature. Nevertheless, the polarization of the quantum motif by the protein was small. As shown in the previous chapter, inclusion of polarization functions would not be expected to change this result. Such result may be explained by the small polarizability of cationic systems like the imidazolium/methanethiol complex. In contrast, the polarization of the active site groups was the

major component of its electrostatic interaction with the quantum motif. Polarization contributions were also nonnegligible for the beta sheets. Currently, the electrostatic properties inherent in the beta sheet structure are not clear (van Duijnen, et al., 1985) and the importance of this structural motif in the structure of neurotransmitter receptors is not known. The scarce data from the analysis of the sequence of a few receptors and the known structure of membrane-bound proteins do not suggest major roles for these elements of tertiary structure. In contrast, alpha helices play a prominent role, and their electrostatic properties have been considered (Hol et al., 1978). The unperturbed interaction energy was the major component to the electrostatic interaction between the imidazolium/methanethiol complex and the alpha helices. A similar conclusion applied to the interaction with the full protein. Thus, both the perturbed and unperturbed contributions to the electrostatic energy of interaction between the protein and the quantum motif were important. As Warshel pointed out, protein polarity may not be neglected in computations of electrostatic effects in proteins (Warshel, 1987). A detailed analysis of the electrostatic interaction between the alpha helices and the imidazolium/ methanethiol complex is the subject of the next chapter.

TABLE 3-1. Coordinates for the imidazolium/methanethiol complex [a].

ATOM	X	Y	Z
ND1	60.021	23.883	16.079
CE1	60.108	24.232	17.375
NE2	58.972	24.877	17.685
CG4	58.789	24.318	15.538
CD2	58.143	24.936	16.548
SG	60.507	20.605	16.260
CB	60.491	20.717	18.068
1HD1	60.753	23.373	15.565
1HE1	60.944	24.029	18.049
1HE2	58.751	25.264	18.614
1HG4	58.522	24.136	14.504
1HD2	57.174	25.417	16.583
1HSG	59.569	19.667	16.173
1HB	61.209	21.479	18.371
3HB	60.757	19.770	18.569

[a] In angstroms and in the coordinate frame of the PDB file 2ACT, actinidin.

TABLE 3-2. Proton transfer energy: imidazolium/methanethiol complex in isolation [a].

POINT	STO-3G	6-31G	6-31G*	STO-3G/MP3[b]
M1	-2.1	-3.3	-1.6	-2.0
TS	36.9	52.1	42.5	24.3
M2	33.5	51.7	38.9	22.1
TS-M1	39.0	55.4	44.1	26.3
M2-M1	35.6	55.0	40.5	24.1

[a] Energy in kcal/mol. Zero point energy is the sum of isolated STO-3G optimized imidazolium and Methanethiol, its geometry as described in Theoretical Approach. Imidazolium: -222.43930 hartrees, STO-3G; -225.09830 hartrees, 6-31G; -225.18905 hartrees, 6-31G*; -222.77066 hartrees, STO-3G/MP3. Methanethiol: -432.89504 hartrees, STO-3G; -437.64422 hartrees, 6-31G; -437.69923 hartrees, 6-31G*; -432.99498 hartrees, STO-3G/MP3.

[b] From quartic fit to points in Figure 3-2. Quartic fit equation: 2046.418 - 5877.605 X + 6141.368 X**2 - 2766.353 X**3 + 456.389 X**4.

TABLE 3-3. Internal coordinates for 1HND and 1HSG [a].

POINT	BASIS SET	R1	BETA1	TAU1	R2	BETA2	TAU2
M1	STO-3G	1.03	50.1	173.2	1.33	123.8	-16.8
	6-31G	1.00	51.6	175.0	1.35	139.4	-7.4
TS	STO-3G	1.63	5.5	120.9	1.34	97.8	-15.6
	6-31G	1.74	7.1	122.6	1.35	100.1	-11.8
M2	STO-3G	1.90	5.5	120.8	1.34	96.1	-14.3
	6-31G	1.89	7.2	122.7	1.35	100.0	-11.2

[a] In angstroms and degrees. R1 and R2 are the ND1- 1HD1 and the 1HSG- SG bond lengths, respectively. BETA1 and BETA2 are the 1HD1- ND1- SG and the 1HSG- SG- ND1 angles, respectively. TAU1 and TAU2 are the 1HD1- ND1- CG4- NE2 and the 1HSG- SG- ND1- CG4 dihedral angles, respectively.

TABLE 3-4. Protein electrostatic effects [a].

	M1	TS	M2	TS-M1	M2-M1
ACTIVE					
UNPT	-6.8	-6.5	-5.9	0.3	0.9
	(-11.5)	(-10.6)	(-9.7)	(0.9)	(1.7)
IND B	-8.7	-6.3	-5.5	2.5	3.2
TOTAL	-15.6	-12.8	-11.4	2.8	4.1
HX					
UNPT	-116.4	-123.5	-126.2	-7.1	-9.9
	(-110.7)	(-114.0)	(-115.0)	(-3.3)	(-4.3)
IND B	-3.6	-5.3	-6.4	-1.7	-2.8
TOTAL	-119.9	-128.8	-132.6	-8.9	-12.7
BETA					
UNPT	-7.7	-10.7	-11.0	-3.0	-3.3
	(3.5)	(8.9)	(11.0)	(5.3)	(7.5)
IND B	-6.4	-11.8	-14.9	-5.4	-8.6
TOTAL	-14.1	-22.5	-25.9	-8.5	-11.8
FULL					
UNPT [b]	-316.1	-304.5	-299.9	11.6	16.2
IND B [c]	-33.4	-35.7	-38.7	-2.3	-5.3
TOTAL	-349.5	-340.2	-338.7	9.3	10.8

[a] Computed with the STO-3G basis set. Values in parenthesis are VxQ energies. Energy in kcal/mol. See Theoretical Approach for definition of energy terms.

[b] Only VxQ term is included.

[c] Dipole interaction tensor is neglected.

TABLE 3-5. Polarization of the quantum motif [a].

	M1	TS	M2	TS-M1	M2-M1
ACTIVE	-0.8	-0.8	-0.9	0.0	-0.1
HX	-0.2	-0.2	-0.2	0.0	0.0
FULL	-1.9	-2.6	-2.4	-0.7	-0.5

[a] Computed with the 6-31G basis set. Energy in kcal/mol.

TABLE 3-6. Electrostatic QxQ energy [a].

	M1	TS	M2	TS-M1	M2-M1
HX	-109.3	-112.9	-114.0	-3.6	-4.7
	(-110.7)	(-114.0)	(-115.0)	(-3.3)	(-4.3)
FULL	-315.3	-304.6	-299.7	10.7	15.6
	(-316.1)	(-304.5)	(-299.9)	(11.6)	(16.2)

CONTRIBUTION FROM FRAGMENTS OF THE QUANTUM MOTIF [b]

		TS	M2	AT POINT 2.0
HX	IMID [c]	47	69	73
	METS [d]	-42	-60	-63
	PTN [e]	-9	-14	-15
FULL	IMID	140	202	214
	METS	-107	-154	-162
	PTN	-21	-33	-35

[a] Computed with the STO-3G basis set. Energy in kcal/mol. Values in parenthesis are VxQ energies.

[b] Zero point is at M1. For the helices (HX): IMID, -74 kcal/mol; METS, -38 kcal/mol; PTN 2 kcal/mol. For the full protein (FULL): IMID, -211 kcal/mol; METS, -108 kcal/mol; PTN, 4 kcal/mol.

[c] Imidazolium

[d] Methanethiol

[e] The proton

TABLE 3-7. Electrostatic QxQ energy after scaling [a].

	M1	TS	M2	TS-M1	M2-M1
HX	-29.3	-30.7	-31	-1.4	-1.7
	(-30.0)	(-31.3)	(-31.6)	(-1.3)	(-1.6)
FULL	-14.9	-0.6	5.6	14.3	20.5
	(-15.4)	(-0.8)	(4.8)	(14.6)	(20.2)

CONTRIBUTION FROM FRAGMENTS OF THE QUANTUM MOTIF [b]

		TS	M2	AT POINT 2
	IMID [c]	12	18	19
HX	METS	-11	-16	-17
	PTN	-3	-4	-4
	IMID	6	9	9
FULL	METS	6	8	9
	PTN	2	3	4

[a] Computed with the STO-3G basis set. Energy in kcal/mol. Values in parenthesis are VxQ energies.

[b] Zero point is at M1. For the helices (HX): IMID, -19 kcal/mol; METS, -11 kcal/mol; PTN 0 kcal/mol.. For the full protein (FULL): IMID, -5 kcal/mol; METS, -9 kcal/mol; PTN, 0 kcal/mol.

[c] Description of quantum motif fragments as in Table 3-6.

Figure 3-1. Alpha carbon chain of actinidin. Only the side chains of selected residues in the active site are shown: Cys 25, His 162, and Asn 182 in yellow; and Trp 184 in red.

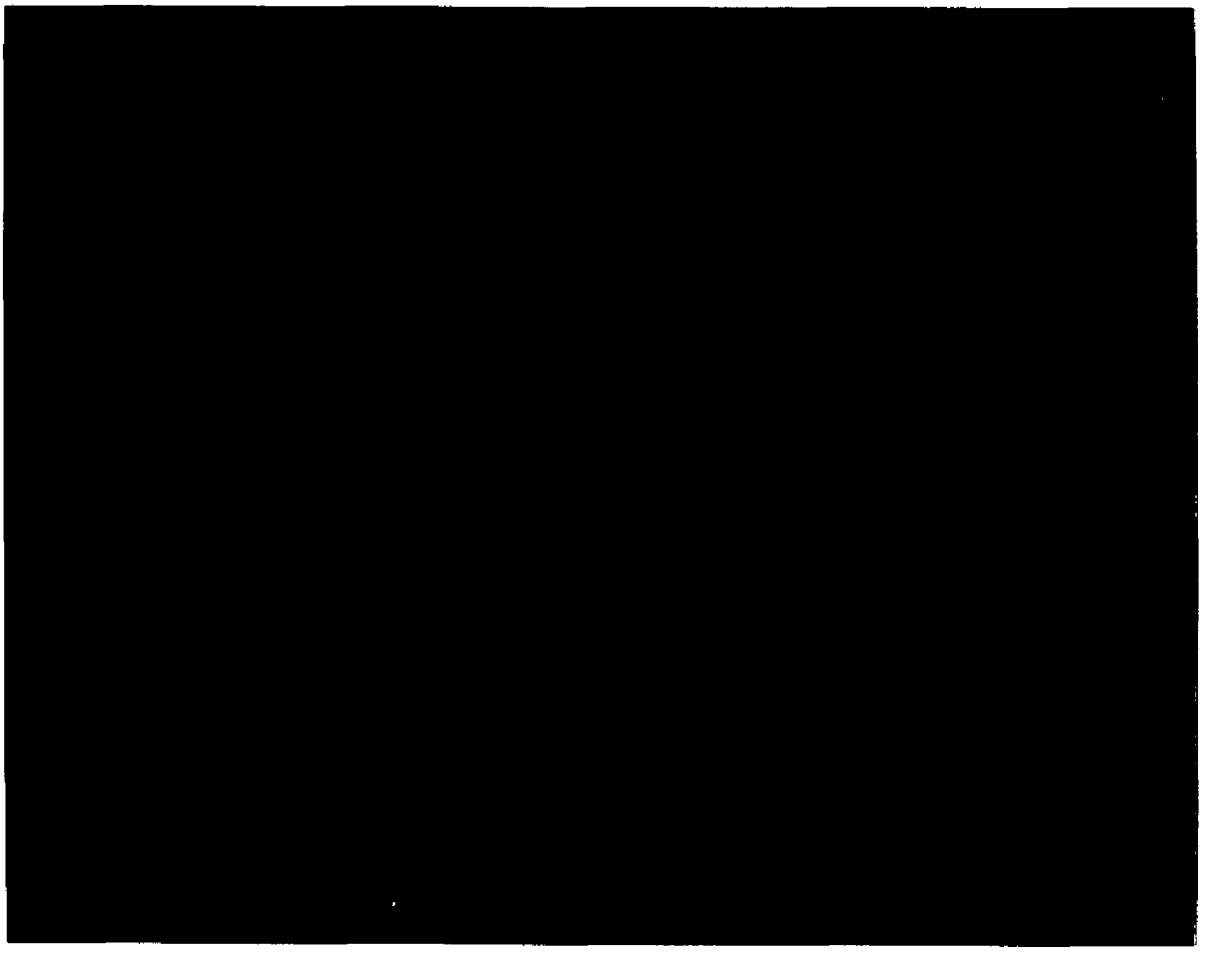

Figure 3-2. Proton transfer energy curve for the imidazolium/ methanethiol complex in the absence of protein effects. Circle: Hartree-Fock energy using the STO-3G basis set. Square: Hartree-Fock plus MP3 energy, same basis set Zero energy is the sum of the isolated imidazolium and methanethiol molecules; see Table 3-2.

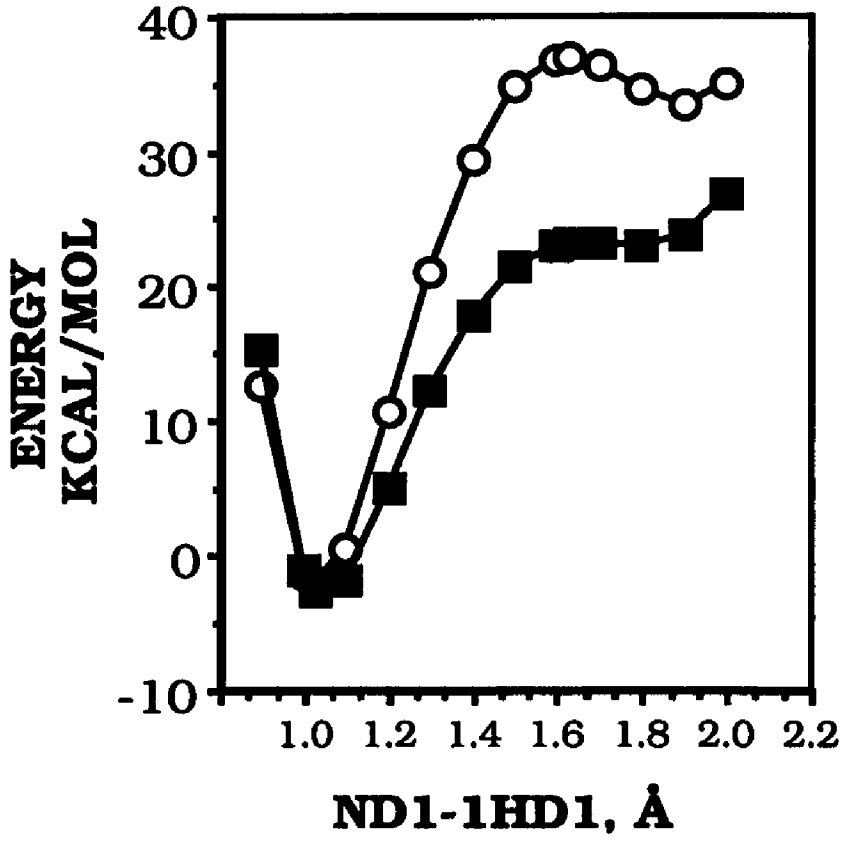

Figure 3-3. Geometry and proton path in the proton transfer between imidazolium and methanethiol. Orientation as in the coordinates of Table 3-1.

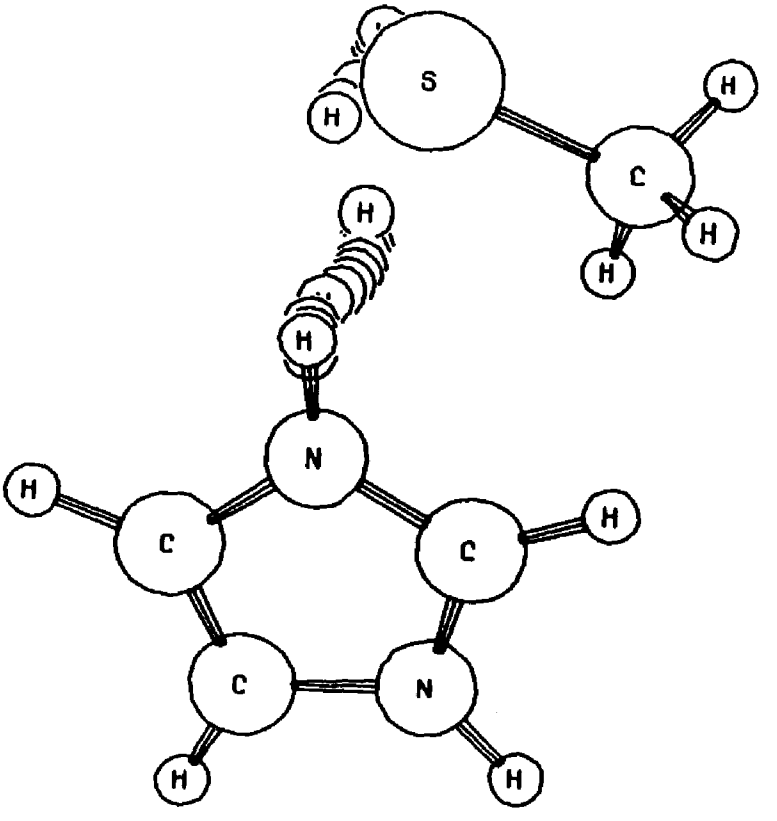

Figure 3-4. Proton transfer energy curve for the imidazolium/ methanethiol complex in the absence and presence of protein effects. Circle: Hartree-Fock energy using the STO-3G basis set. Zero energy is the sum of the isolated imidazolium and methanethiol molecules; see Table 3-2. Square: Hartree-Fock plus QxQ energy. QxQ energy is normalized to point M1 is zero. QxQ energy at point M1 is -315.3 kcal/mol.

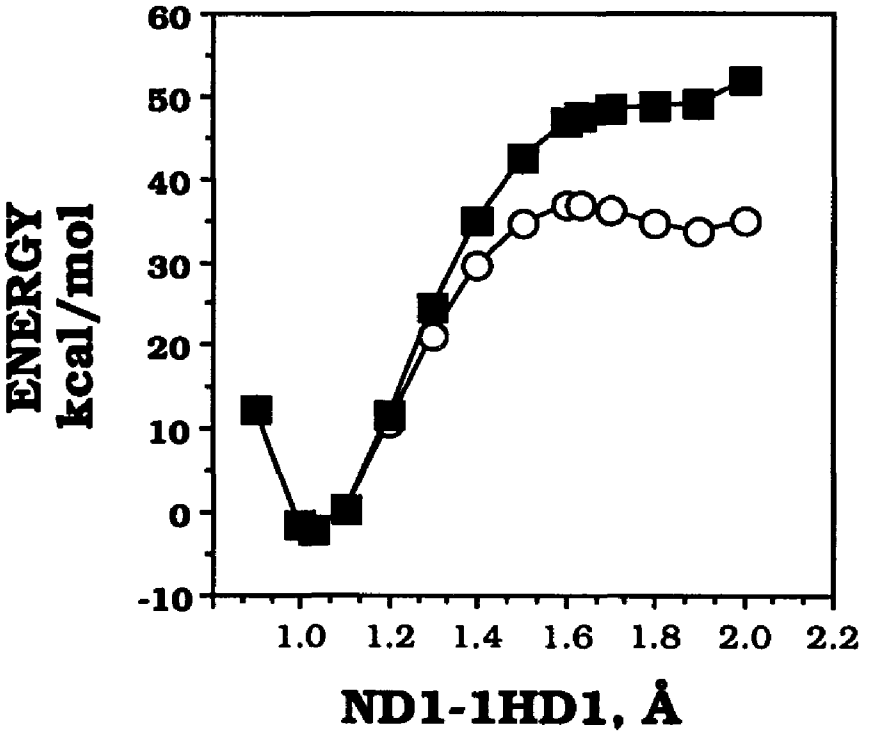

Figure 3-5. Electrostatic energy of interaction between the groups of the quantum motif and groups of the protein structure of actinidin. A, Full protein structure. B, Helices A1-A6. Squares, energy for imidazole; triangle, energy for methanethiol; circle, energy for the proton. Zero energy is at proton position 1.03 Å (i.e. M1); see Table 3-6. Energy in kcal/mol.

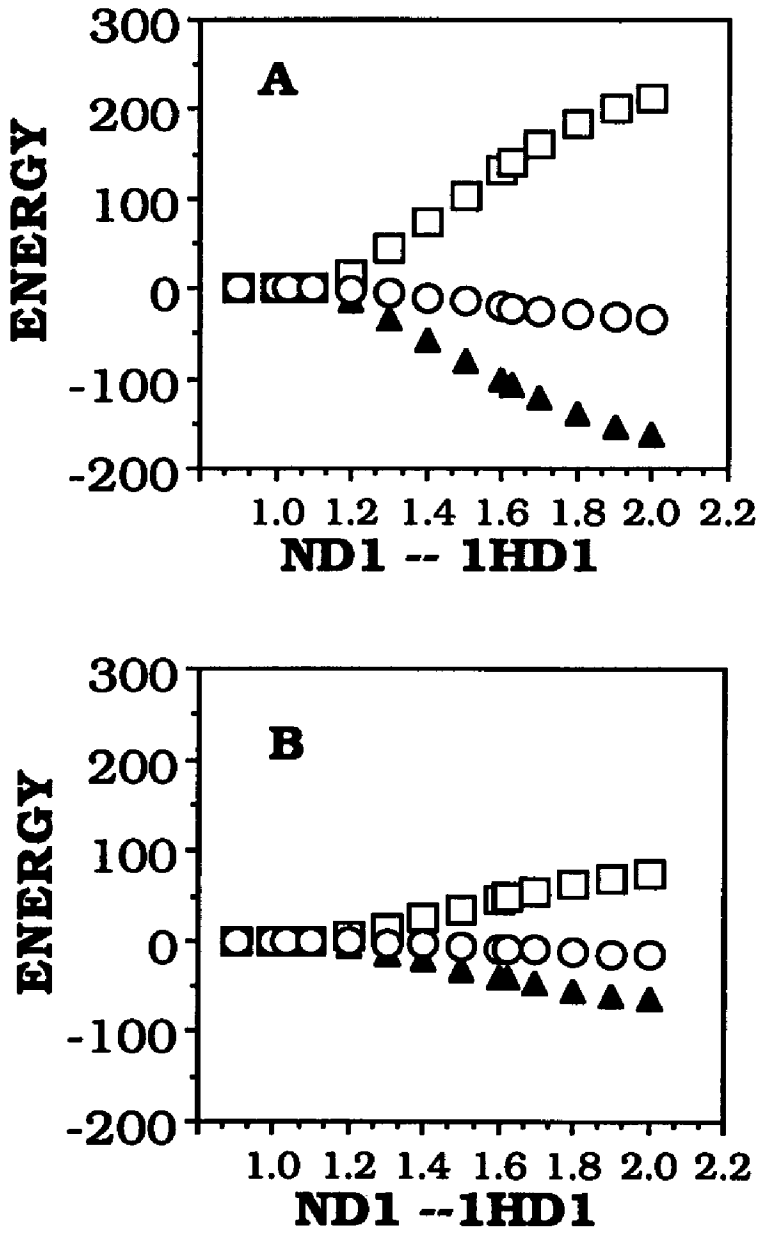

Figure 3-6. Electrostatic energy of interaction between the groups of the quantum motif and groups of the protein structure of actinidin using the scaled charges as described in Theoretical Approach. Details as in Figure 3-5 and Table 3-7.

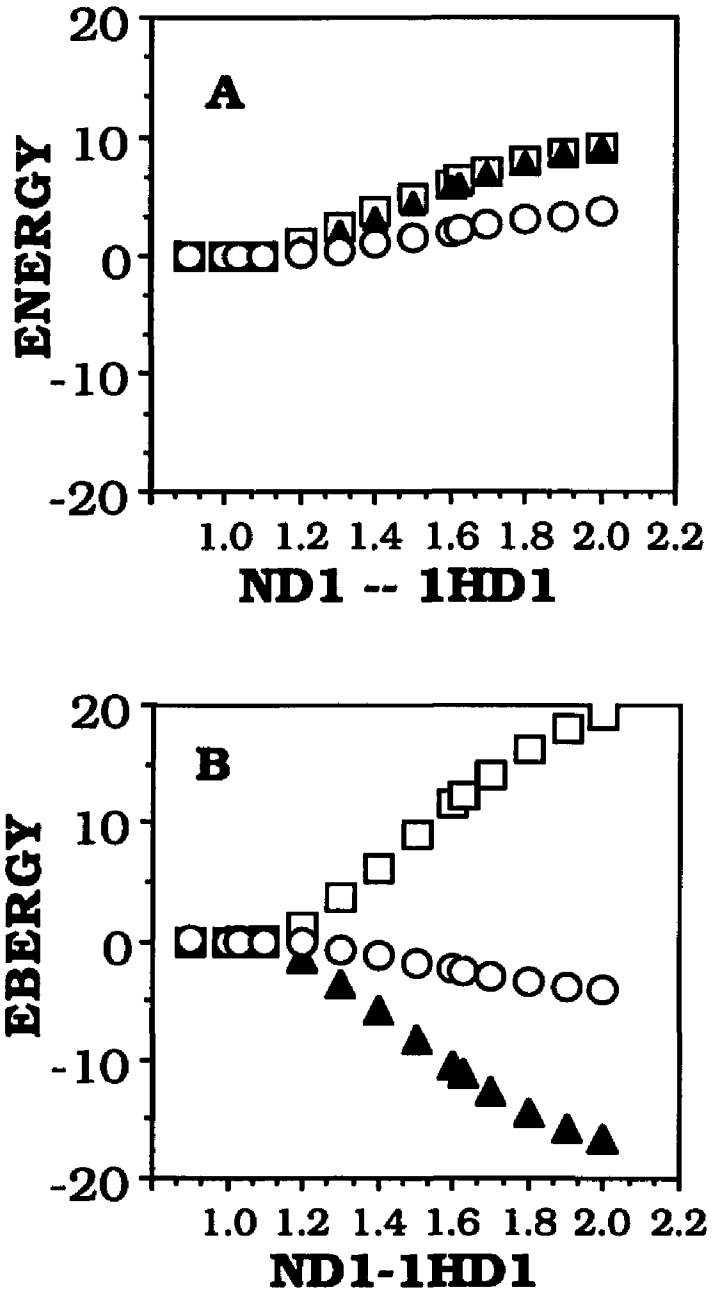

CHAPTER 4

ELECTROSTATIC EFFECTS FROM THE ALPHA HELICES

(from Mercier et al., 1988b)

4.1 INTRODUCTION

In the previous chapter the electrostatic effects of the protein structure of actinidin on the proton transfer between the His 162 and Cys 25 residues in the active site were computed and analyzed in terms of contributions from constitutive elements of the structure of the enzyme. Alpha helices contain special electrostatic properties (Hol et al., 1978) determined by their structure (i.e. the alpha helix dipole). These structures have been postulated to exist in many membrane-bound receptors, including the 5-HT receptors (Fargin et al., 1988; Julius et al., 1988; Prichett et al., 1988; Hartig, 1989). Thus, they deserve special attention. In this chapter I report on the effects of the six helices in the structure of actinidin and on their putative role in modulating the actions of a ligand in the receptor activation process.

4.2 THEORETICAL APPROACH

4.2.1 PROTEIN AND QUANTUM MOTIF STRUCTURES

The protein coordinates of actinidin (E.C. 3.4.22.14) were obtained from the PDB (file 2ACT) and modified as described in the previous chapter. Similarly, the quantum motif was constructed from imidazolium and methanethiol as discussed in the Theoretical Approach section of chapter 3.

4.2.2 PROTON TRANSFER ENERGY CURVE IN THE ABSENCE OF ACTINIDIN

The energy curve for proton transfer between imidazolium and methanethiol was computed as described in the previous chapter. These computations were limited to the LCAO-MO-SCF Hartree-Fock level of approximation and the STO-3G basis set (Hehre et al., 1970; Hehre et al., 1969) as implemented in the Gaussian 82 system of programs (Binkley et al., 1982). As shown already in previous chapters, qualitative results and inferences from the computations remain unchanged by improvements in the computational model or the basis set. A basis set dependence of the results was not completely unexpected because the proton transfer energy curve in the absence of the protein would depend on the difference in absolute acidities between the donor and acceptor molecules involved in the cationic hydrogen bond. The minimal basis set reproduces the

difference in experimental absolute acidities only within 3 kcal/mol (see Table 6.74 in Hehre et al., 1986).

The reaction coordinate for the energy curve for the transfer of the (1HD1) proton consisted of the ND1--1HD1 distance. The critical points (i.e., the minimum near ND1, termed M1, the transition state, termed TS, and the minimum near SG, termed M2) were calculated by full optimization of the internal coordinates of 1HD1 and 1HSG; all other internal coordinates remained fixed.

4.2.3 COMPUTATIONS WITH THE QUANTUM MOTIF EMBEDDED IN ACTINIDIN

As described in previous chapters, the effect of the entire protein structure (the "full protein environment"; FULL) was considered by using all the atoms in the protein except those belonging to His 162 and Cys 25. Hydrogen atoms were treated explicitly as generated by the program HYDRO from M. Levitt. To consider the effects of the alpha helices, seven subsets of coordinates were also generated from the FULL set. One set (HX) consisted of the atoms belonging to all the alpha helices as described in the PDB file (i.e. helices A1 to A6). The remaining six sets (A1, A2, A3, A4, A5, and A6) contained the individual helices A1 to A6, respectively. (See Figure 4-1.) To the atoms in these structures point charges were assigned as described in the previous chapter.

The electrostatic effects from the above environments on the proton transfer process were computed from the interaction of the point charges with the proton transfer model (Mercier et al., 1988a; Mercier et al., 1988b). This unperturbed interaction was shown in the last chapter to be the major component in the electrostatic interaction between the alpha helices and the quantum motif (i.e. the imidazolium/methanethiol complex). Moreover, this interaction term was the only strictly additive term in the electrostatic interaction between these groups (i.e. the interaction with the set HX will equal the sum of the interaction with the individual helices in sets A1 to A6). Additivity in the energy term computed for the interaction between fragments of the environment with the quantum motif would make the results easier to generalize from the test system such as actinidin to the system of interest such as the 5-HT/LSD receptor.

The accurate representation of the electrostatic properties of the quantum motif is given by the electrostatic potential, V(Rj), calculated from the wavefunction (Weinstein et al., 1981a). The electrostatic interaction energy (ES) with the protein environment is calculated from the sum of products

$$ES = \sum_j V(R_j) \times Q_j$$

where Qj is the point charge of an atom from the environment positioned at Rj. A useful approximation to this energy is obtained by using net charges from a Mulliken Population analysis

to represent the charge distribution of the quantum motif (Weinstein et al., 1981a). In this approximation, hereby referred to as the "QxQ" energy, the electrostatic interaction energy is given by

$$ES = \sum_{i,j} \frac{Q_i \times Q_j}{|R_i - R_j|}$$

where Qi is the net charge on an atom in the quantum motif, and Qj is the point charge representing an atom of the environment. This approximation to ES was shown to be very accurate for the calculations with actinidin and the imidazolium/methanethiol complex (See chapter 3, section 3.3.3).

4.2.3 CONSIDERATION OF THE SOLVENT SCREENING EFFECTS

For reasons described in chapter 3 solvent screening effects were explored by reducing the net charge in atoms that were solvent accessible. The method employed here was as described in the previous chapter.

4.3 RESULTS

4.3.1 ISOLATED QUANTUM MOTIF

Results from computations in the absence of the protein environment were extensively discussed in the previous chapter. For convenience, they are briefly summarized here. The proton transfer

in the imidazolium/methanethiol complex (i.e., the quantum motif) computed in the absence of the protein environment showed a stable complex with the proton on the imidazole side. The potential energy curve (shown in Figure 3-2) displayed the double well character typical of a hydrogen bonded system with critical points located at ND1--1HD1 distances of 1.03 Å for the first minimum (M1), 1.63 Å for the transition state (TS), and 1.90 Å for the minimum on the methanethiol side (M2). As shown in Table 3-2, the barrier for proton transfer from the imidazole side (TS-M1) was 39.0 kcal/mol, and from the methanethiol side it was 3.4 kcal/mol (TS-M2).

4.3.2 THE INTERACTION WITH THE PROTEIN ENVIRONMENT

Table 4-1 shows the effects of the electrostatic interaction between actinidin and the imidazolium/methanethiol complex computed at the critical points of the curve in Figure 3-2. The contributions of the entire protein (FULL), of the collection of helices (HX), and of the largest helix, A1, are given in the columns of Table 4-1. Helix A1 has been implicated in the catalytic activity of the sulfhydryl proteinases (van Duijnen et al., 1980; van Duijnen et al., 1979; Thole and van Duijnen, 1983), and its electrostatic properties have been considered (Hol et al., 1978; van Duijnen and Thole, 1982). The quantum motif interacted favorably with the full protein, independent of the proton position as seen in Table 4-1 under the heading "FULL".

Table 4-2 summarizes the changes in the barrier (i.e. TS-M1 and TS-M2) and driving energy (i.e. M2-M1) induced by the electrostatic effects of the protein. The full protein stabilized the complex at M1 more than at TS, and at TS more than at M2. This resulted in an increase in the barrier for proton transfer from the imidazolium side by 10.7 kcal/mol; it also eliminated the double well character of Figure 3-2 by raising the M2 point over the TS point by 4.9 kcal/mol.

The interaction of the A1 helix with the complex was unfavorable (Table 4-1), regardless of the position of the proton. This was not surprising because the His 162/Cys 25 complex was positively charged and lay next to the amino terminus of A1 which carried the positive end of the alpha helix dipole (Hol et al., 1978). The A1 helix had a significant effect on the proton transfer: for the barrier to transfer from the imidazole side this corresponded to an increase of 7.0 kcal/mol; for the barrier from the methanethiol side the decrease was 2.8 kcal/mol (see Table 4-2).

Notably, the effects of helices A2 to A6 were opposite in sign to those from A1. (See Table 4-1 column heading "HX".) Unlike A1 alone, the collection of helices A1 to A6 interacted favorably with the quantum motif. More significant was the effect of the helices on the barriers to proton transfer (Table 4-2). The tertiary structure composed of the alpha helices A1 to A6 contributed to retain the proton near the methanethiol, by reducing the barrier from the imidazole side by 3.6 kcal/mol and increasing the barrier from the

methanethiol side by 1.1 kcal/mol, compared to the results in vacuum.

To understand the source of the difference in the electrostatic effects of helices A2 to A6 compared to those of A1, the QxQ scheme was used to evaluate the individual contribution of each helix. Figure 4-2A shows the interaction energy between the quantum motif and each one of the helices. Helices A1 and A6 did not interact favorably with the positively charged complex, whereas helix A2 did. The changes in barriers and driving energy due to the electrostatic effects from the alpha helices are shown in Figure 4-3A. Helices A1 and A2 made large, but opposite contributions to the barrier from both the imidazole and methanethiol sides: A1 by increasing the barrier from the M1 side by 7.0 kcal/mol and reducing the barrier from the M2 side by 2.8 kcal/mol, and A2 by decreasing the first barrier by 5.9 kcal/mol and increasing the second by 2.3 kcal/mol.

Helices A2 to A5 had a net negative charge produced by the charged groups identified in the footnote of Figure 4-2A. Within the QxQ scheme, it was possible to separate the effect of the net charges on certain residues from that of the total charge distribution in the helical structures. After excluding the charged groups, the helix dipole should be the leading term in a multipole expansion of the remaining charge distribution. This separation made it possible to identify the part of the electrostatic interaction attributable to the special property (the dipole moment) of this element of secondary structure, i.e., the helix dipole. The contribution from the charged

groups to the electrostatic interaction energy between the quantum motif and the helices is shown in Figure 4-2B. Notably, most of the electrostatic interaction energy between the quantum motif and the helices A2 to A5 came from the charged residues, and not from the helix dipole. (Compare Figures 4-2A and 4-2B.) A similar conclusion applies to the driving energies for proton transfer as shown by the similarities between Figures 4-3A and 4-3B.

The results shown in Figure 4-2C correspond to the contribution from the alpha helix dipole (i.e. not including the net charged residues) to the interaction between the helices and the quantum motif. As expected from the full helix results, helices A1 and A6 which have no net charge, had rather significant positive energies of interaction with the quantum motif (Figure 4-2C). An interesting result was the positive energy of interaction obtained with the dipole of helix A3, because the net charges in this helix (i.e. the contribution from the primary sequence) had an opposite effect. (Compare Figures 4-2B and 4-2C.) The net effect from helix A3 resulted from the sum of the electrostatic properties arising from its secondary and primary structure. As shown below, scaling of the charges emphasized the difference between the contribution from the helix dipole and the charged groups.

Figure 4-3C shows the contribution from the helix dipoles to the changes in the barriers and driving energy for the proton transfer. Among helix dipoles, A1 made the largest contribution with an effect that was 5-10 times larger than that from any other helix dipole. The

alpha helix dipole in A1, the largest helix in actinidin, had a dipole moment of 21.1 Debye computed from the point charge model. The net effect from helix A3 resulted from the sum of the properties from its secondary and primary structures. (Compare Figures 4-3C to 4-3B, and these to Figure 4-3A.) The dipole contributions from A3 and A6 to the energy barriers nearly canceled each other, while the effect of the remaining helices was negligible. In contrast to the effects from the dipoles, helices A2 to A5 which had a net negative charge dominated the electrostatic effects on the barriers and driving energies of the proton transfer when the collection of alpha helices was taken as a group. This was due to the strong effects of the charged residues in these helices.

4.3.3 EFFECTS OF REDUCING THE SURFACE CHARGE

Table 4-1 shows the results of the computations after scaling the surface charges as described above. As expected, the scaling reduced significantly (i.e. by approximately 300 kcal/mol) the QxQ energy for the interaction between the quantum motif complex and the FULL protein environment. However, the energy differences responsible for changes in the barriers for proton transfer were much less sensitive to scaling of the surface charges. Table 4-2 shows that the values were quite close to the results from the unmodified charges shown in the same table: the barrier from the imidazole (i.e. M1 point) increased by 14.3 kcal/mol, and the barrier from the methanethiol side (i.e. M2 point) decreased by 6.2 kcal/mol.

With the modified charges, the A1 helix still interacted unfavorably with the quantum motif at all three critical points. This interaction was rather large, ranging from 17.1 kcal/mol at M1 to 27.7 kcal/mol at M2. Adding the contribution of the other helices, the interaction with the quantum motif became favorable at all critical points. At M1, Table 4-1 shows a stabilization by 29.3 kcal/mol; position TS was stabilized by 30.7 kcal/mol, and at M2 by 31.0 kcal/mol. Thus, the interaction with helices A2 to A6 compensated for the unfavorable interaction between the complex and the A1 helix, the same result as described above for the unmodified charges.

The effect of scaling the surface charges in the A1 helix or in the collection of helices A1 to A6, on the barriers is shown in Table 4-2. As described for the unmodified charges, the A1 helix still favored the proton near the imidazole by stabilizing the complex at M1 over TS, and TS over M2. Thus, the barrier increased on the imidazole side by 7.6 kcal/mol and decreased from the methanethiol side by 3.0 kcal/mol.

As with the unscaled model, helices A1 and A6 had positive interactions with the quantum motif after scaling the surface charges (Figure 4-4A). The negative energy of interaction of A2 to A4 was responsible for the overall negative interaction of the collection of helices A1 to A6 with the quantum motif when scaling was introduced. The largest contribution came from the charged groups in helices A2 to A4, as observed also with the unmodified charges (See Figure 4-4B). However, after scaling, helix A5 had a positive energy of

interaction with the quantum motif of approximately 3 kcal/mol for all three critical points (Figure 4-4A). This was different from the unscaled case. Because this interaction was small compared to that of other helices, and rather constant across the proton positions, helix A5 would still not be expected to have a significant role in modulating the proton transfer, a result consistent with the unscaled model. The most striking difference between the computations with the modified and unmodified charges was in the relative contribution from the alpha helix dipoles. As shown in Figure 4-4C, the contribution from the helix dipoles increased when computed with the modified point charges. This was expected because most of the charged groups, all of which carry negative charge, were preferentially located on the solvent accessible surface of actinidin, and were attenuated.

The reduction of the surface charges did not change the qualitative trend observed for the unscreened helices. (See Figures 4-5A to 4-5C.) Helix A1 was still found to have the largest contribution, and charged side chains in A2 to A5 were responsible for the total effect of the collection of helices (with the exception of A3) on the barrier. The dipole of helix A3 had an opposite effect on the barriers for proton transfer from that computed from its charged side chains: the helix dipole increased the barrier from the M1 side by 2.3 kcal/mol and decreased it from the M2 side by 0.9 kcal/mol, while its charged groups, Asp 72 and Asp 80, decreased the first barrier by 3.0 kcal/mol and increased the second barrier by 1.2 kcal/mol (Compare Figures 4-5A and 4-5B). Thus, the effect of helix A3 on the

barriers for proton transfer may be reproduced only when the effects of its charged groups (i.e. primary sequence) and its helix dipole (i.e. secondary structure) are taken together, and not just by considering the strong interaction from the charged groups. The scaling of the surface charges emphasized the helix dipole at the expense of the charged groups.

4.4 DISCUSSION

Results from the previous chapter showed that the elements of the highly complex structure of proteins achieve their effect through different contributions to the energetics of proton transfer occurring inside an active site pocket. This holds true even if only the collection of alpha helices is considered. Thus, helix A1 contributed to an increase in the total energy of the system with the movement of the proton towards Cys 25, thus forcing the proton to remain on the His 162 side of the complex, an effect qualitatively consistent with the effect from the full protein structure. In contrast, the charged groups in helices A2 and A3 had the opposite effect even after the charge from the atoms located on the protein surface was reduced. The detailed analysis of the electrostatic effect of the alpha helices revealed the complex interplay between the electrostatic properties of the elements in the secondary structure and the primary structure groups that compose them. Helices A2 to A5 have charged groups as part of their primary structure that add to a net negative charge, and these influence the proton transfer energy more strongly than

the alpha helix dipoles. This finding demonstrated that it would be inappropriate to think of helical structures as contributing only dipole moments to the electrostatic properties of the protein if the helices contain charged groups. This composite effect would hold even if the surface charges were attenuated.

Helix A3 offered an even more interesting example of the interplay between charged groups and the alpha helix dipole in the modulation of the proton transfer process. The effect from its helical structure was not reproduced by its charged groups after scaling of the surface charges, because these groups had an effect on the proton transfer energy curve opposite to the one from the alpha helix dipole. As shown recently (Gilson et al., 1985), and consistent with results in classical electrostatics (Edsall and Wyman, 1959; Lorrain and Corson, 1970), the electrostatic potential from charged groups would be reduced more than that from the helix dipole by the solvent dielectric and counterions. Thus, upon reducing the surface charges, the effect of the helix dipole would compete favorably with the charged groups and only their combination would account for the effect observed with the whole helical structure.

A noteworthy consequence of the results presented here is the suggestion that changes in the charged groups of a protein would produce not only the alteration of electrostatic properties expected from the change in primary structure, but also unexpected ones produced by the unmasking of the electrostatic properties of elements of the secondary structure. For example, in helix A3, the

effect from the alpha helix would be in the opposite direction if the charged groups in this helix were removed. In addition, the elimination of the charged groups in helices A2 to A5 would emphasize the effect of the helix A1 dipole. These considerations assume that the overall protein structure is unchanged by the mutations that eliminate the changes. That such mutations are possible has been shown recently (Wells et al., 1987).

Actinidin modulated the proton transfer proposed for the activation mechanism of one of the 5-HT receptors (Osman et al., 1985; Osman et al., 1987). Through their electrostatic properties different elements of its structure, such as the helices in actinidin, made different contributions to this effect. Moreover, the proton donor and acceptor molecules in the complex (i.e. the side chains of His 162 and Cys 25) responded differently to the electrostatic effect from the protein environment as discussed in chapter 3. Such a mechanism for modulation of the proton transfer (i.e. modulation of the energies by electrostatic effects on the donor and acceptor fragments) has been proposed as the action of the agonist at a 5-HT receptor (Osman et al., 1985; Osman et al., 1987), and the effect of the protein may follow the same pattern. Such details of mechanisms can be revealed only by quantum mechanical descriptions of the catalytic groups or groups involved in receptor activation because the electronic properties and, hence, the electrostatic properties of the donor and acceptor fragments change upon proton transfer. However, to complete the picture the computations must include not only a description of the electrostatic properties of the surrounding

polypeptide structure and the solvent, but also the steric effects from the protein. These effects would have important consequences on the final orientation that the ligand may achieve in the binding pocket, and hence indirectly modulate the electrostatic effects from the ligand on the activation process. These issues are addressed in the next chapter.

TABLE 4-1. Effects of the protein structure: QxQ energy [a].

POINT	FULL[b]	HX[b]	A1[b]
M1	-315.3	-109.3	9.4
TS	-304.6	-112.9	16.4
M2	-299.7	-114.0	19.2
	AFTER SCALING		
M1	-14.9	-29.3	17.1
TS	-0.6	-30.7	24.7
M2	5.6	-31.0	27.7

[a] Energy in kcal/mol. Electrostatic energy of interaction between the imidazolium/methanethiol complex and actinidin, computed with the STO-3G basis set. Similar computations after introducing scaling as described in the text are reported in the lower part. Proton positions correspond to the critical points as defined in the text. QxQ refers to the computational scheme as defined in the text.

[b] The fragments of the protein defined as follows: FULL- full protein as defined in the text; HX- collection of alpha helices A1 to A6; A1- helix A1. Total charges of protein fragments are as follows: unscaled full protein -16.0; scaled full protein -0.1; unscaled alpha helices -8.0; scaled alpha helices -3.2; unscaled A1 helix 0.0; scaled A1 helix 0.6.

TABLE 4-2. Electrostatic effects from the protein structure on the barriers and driving energies [a].

POINT	FULL	HX	A1
TS-M1	10.7	-3.6	7.0
TS-M2	-4.9	1.1	-2.6
M2-M1	15.6	-4.7	9.8
	AFTER SCALING		
TS-M1	14.3	-1.4	7.6
TS-M2	-6.2	0.3	-3.0
M2-M1	20.5	-1.7	10.6

[a] Protein effects on the barriers and driving energies computed from results in Table 4-1. Points of calculations and protein structure fragments are defined in Table 4-1. Energy in kcal/mol.

Figure 4-1. Alpha carbon chain of actinidin with helices and active site color coded. Active site shown as in Figure 3-1, including Gln 19 in red. Alpha helices are color coded: A1, red; A2, cyan; A3, bright green; A4, orange; A5, magenta; A6, dark green.

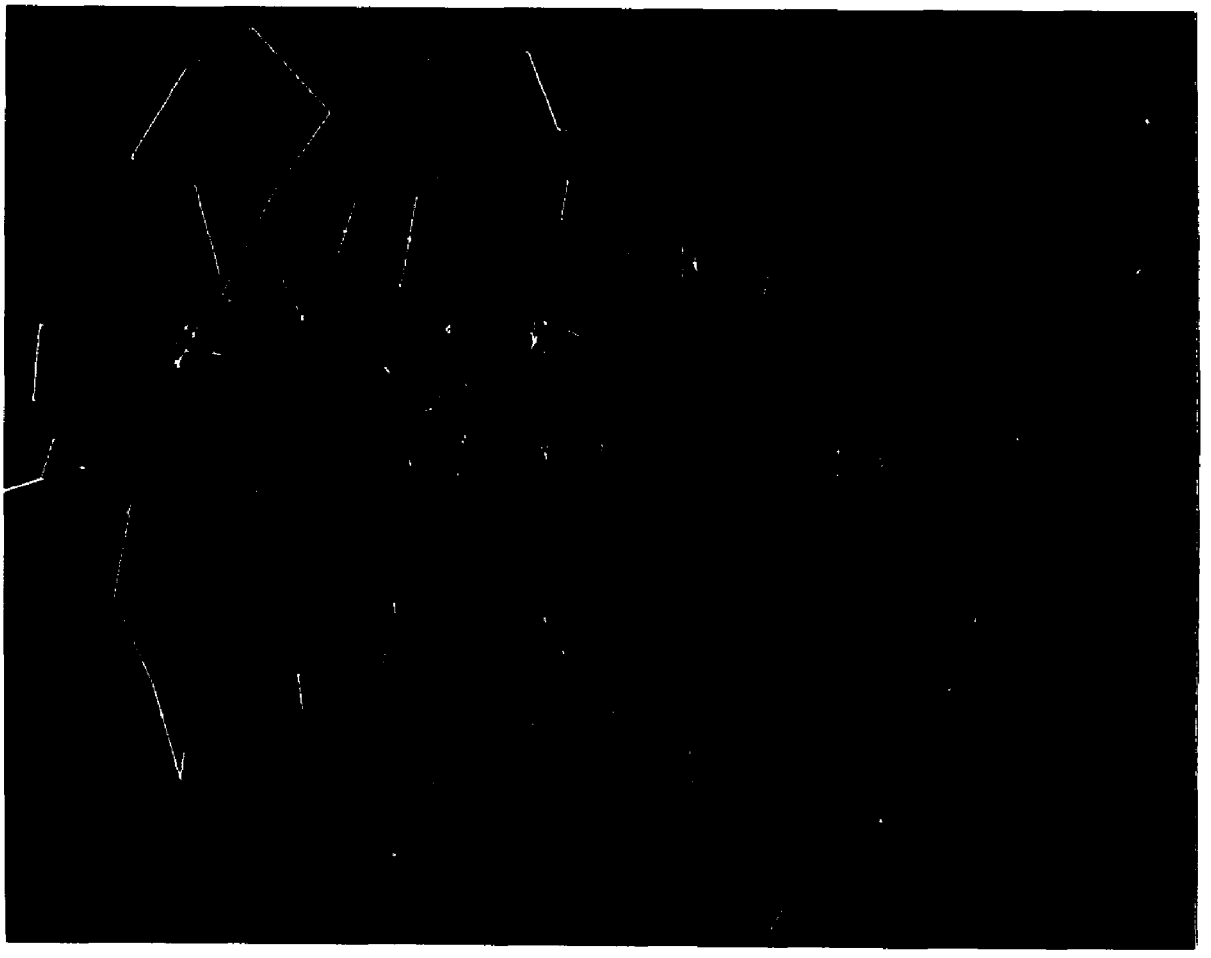

Figure 4-2. QxQ electrostatic interaction energy between the imidazolium /methanethiol complex and the alpha helices in actinidin. Black, at point M1; vertical stripes, at point TS; and horizontal stripes, at point M2. A: Full helices. B: Side chains of charged groups in the helices with a net charge. C: The helix dipole contribution, i.e. like A, but not including the side chains included in B. Energy in kcal/mol.

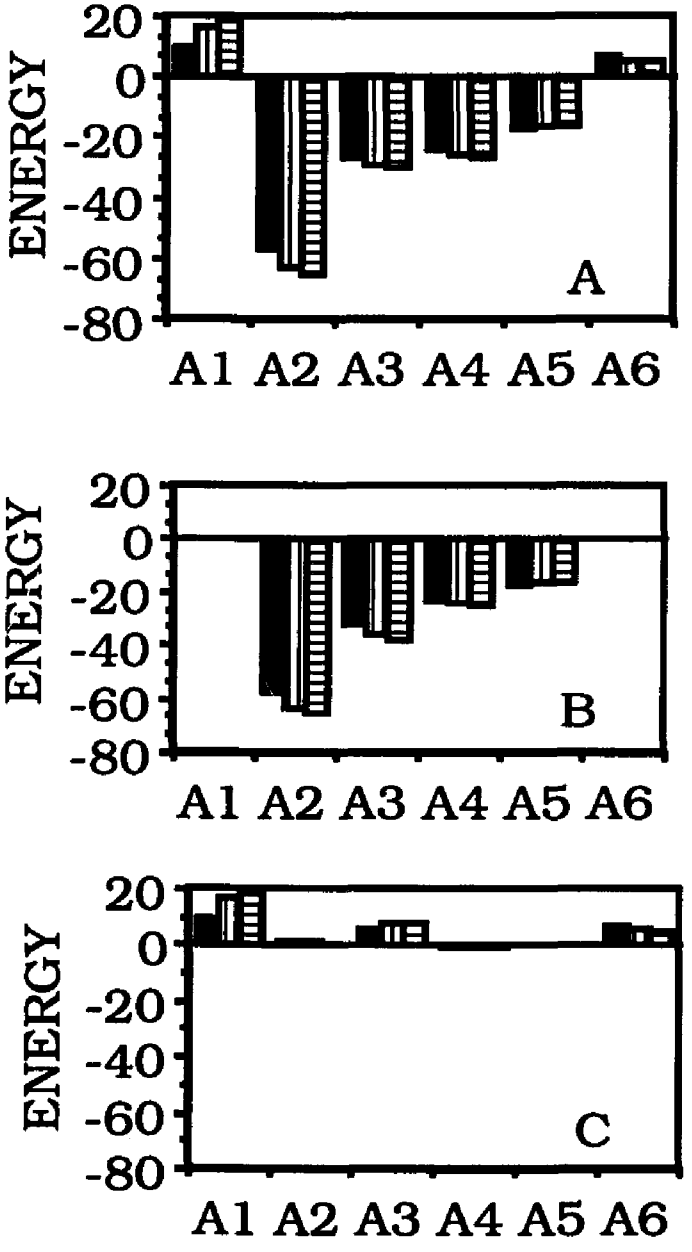

Figure 4-3. The changes in the barriers and driving energy for the proton transfer of Figure 3-2 by the electrostatic interaction energies given in Figure 4-2. Black, TS-M1; vertical stripes, M2-M1. The difference corresponds to TS-M2. A, B, and C as defined in Figure 4-2. Energy in kcal/mol.

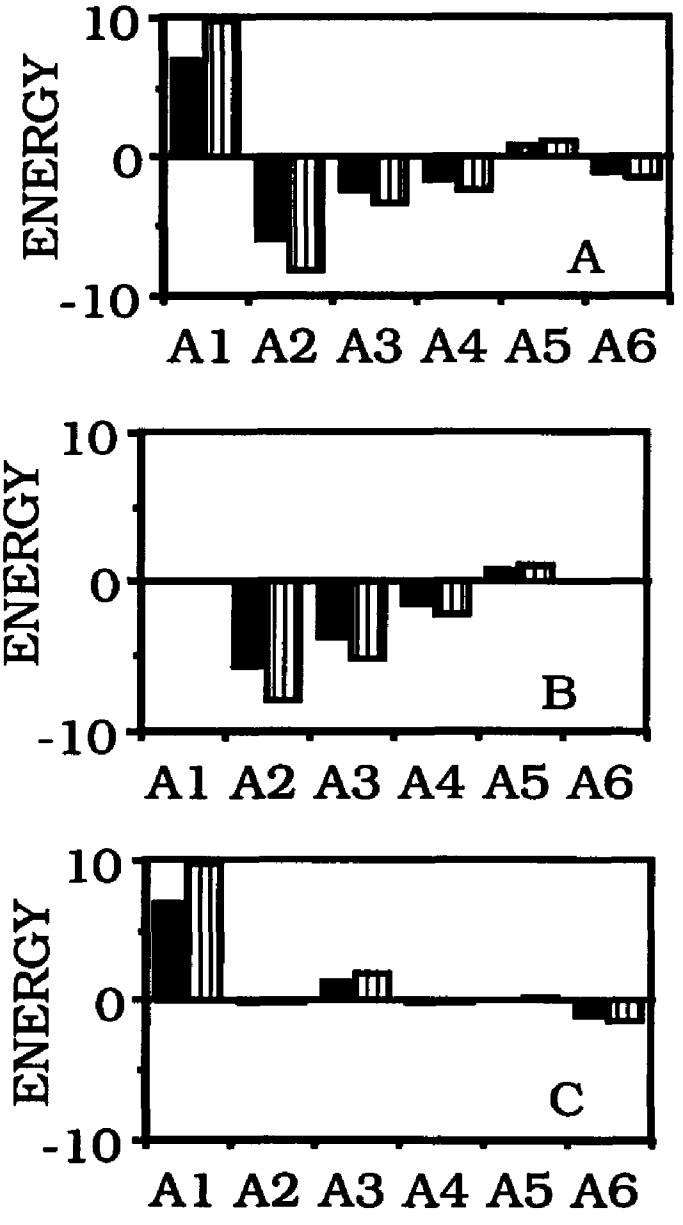

Figure 4-4. QxQ (scaled) electrostatic interaction energy between the imidazolium/methanethiol complex and the alpha helices in actinidin. Point charges are scaled as described in the Theoretical Approach. Details in Figure 4-2.

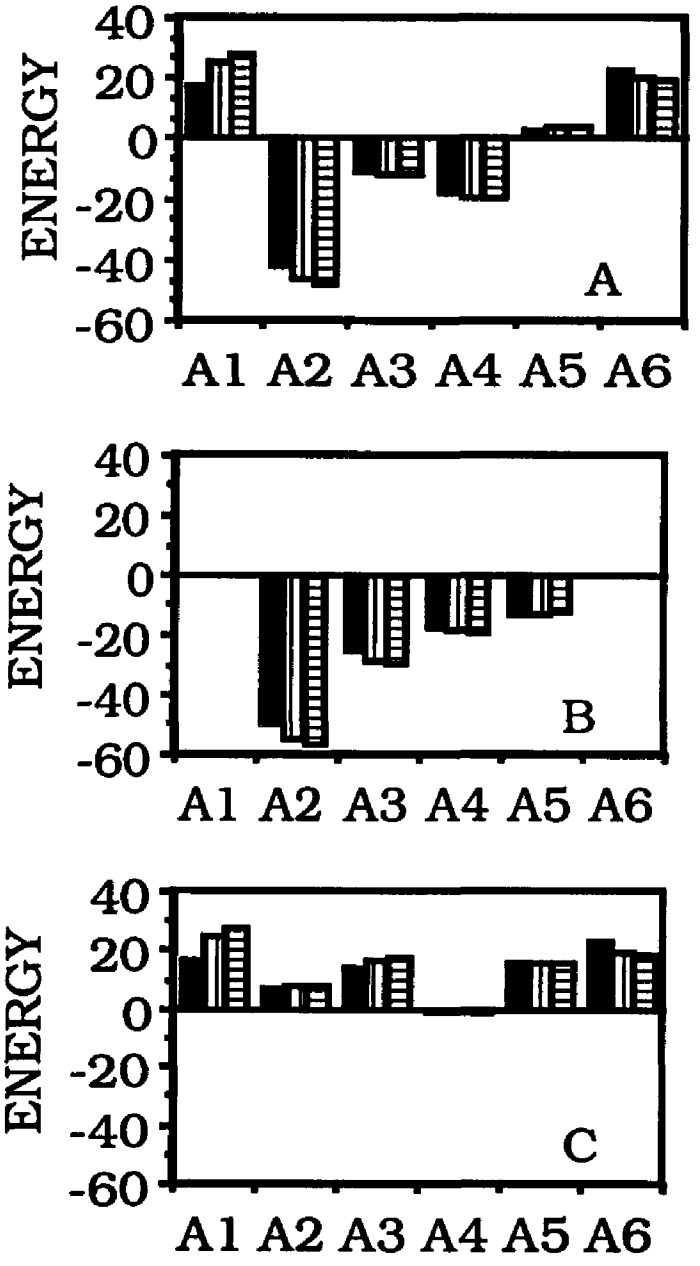

Figure 4-5. The changes in the barriers and driving energy for the proton transfer of Figure 3-2 by the electrostatic interaction energies in Figure 4-4. Details in Figure 4-3.

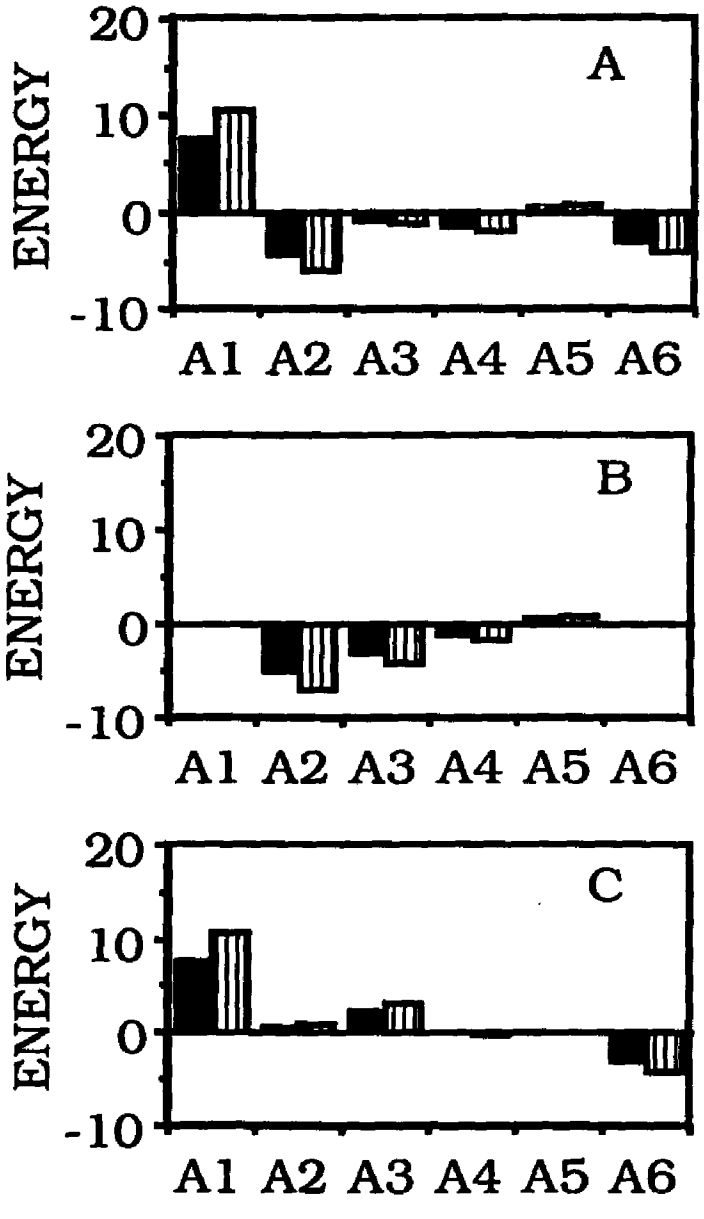

CHAPTER 5

CONSTRAINTS FROM THE RECEPTOR-MACROMOLECULE ON THE ACTIVATION MECHANISM

5.1 INTRODUCTION

The environment from the receptor-macromolecule is expected to introduce electrostatic and steric effects in the process of ligand recognition and receptor activation. The electrostatic effects on the activation process were explored in previous chapters. Briefly, the protein environment of actinidin was able to modulate the proton transfer between His 162 and Cys 25 through the electrostatic interaction of the protein with the proton donor and acceptor molecules as opposed to the interaction between protein and proton. The latter mechanism for modulating the proton transfer has also been described for the modulation of the PTM by the endogenous ligand 5-HT (Osman et al., 1987). Moreover, the effect from the full protein structure was the result of opposite electrostatic effects from the various elements of the primary and secondary structure. A noteworthy point was that the full protein structure did not favor proton transfer. Such behavior is expected from a suitable **model for the environment** of the receptor-macromolecule because the latter is not active in the **absence** of the ligand. Thus, the work suggests that

the ligand initiates the activation process by overcoming the electrostatic barrier imposed by the receptor-macromolecule on the proton transfer process that leads to receptor activation.

To address the role of steric constraints from the receptor-macromolecule on the proton transfer process that initiates activation, this study used the hydrogen bonded complex between *His 162 and Asn 182* in actinidin. In the crystal structure these groups are near Trp 184 which has its indole side chain in almost stacking conformation over the ring of His 162. This arrangement of groups was similar to the one suggested to represent the ligand in the process of activation (Osman et al., 1987). By replacing the side chain of Trp 184 with derivatives of indole which are known ligands at the 5-HT/LSD receptor, it has been possible to introduce the constraints from the steric effects from the protein in the process of identifying orientations of the ligands suitable for triggering proton transfer. The His 162/Cys 25 complex used in previous work regarding the electrostatic effects of the protein structure on the activation process is too far from the indole of Trp 184 to be affected by ligands at this position. Therefore, it was not useful to study the effects from steric constraints. Thus, the work on electrostatic effects from the protein structure on a proton transfer process was extended by studying the proton transfer between His 162 and Asn 182 in the same manner as described in the previous chapters for the His 162/Cys 25 complex.

5.2 THEORETICAL APPROACH

5.2.1 PROTEIN STRUCTURE

The three dimensional coordinates of actinidin (E.C. 3.4.22.14) were those used in the work reported in previous chapters. For details refer to the Theoretical Approach section of chapter 3. The position of the hydrogen on Cys 25, not required in our previous studies in which Cys 25 was the proton acceptor, was obtained from quantum mechanical computations. The 1HSG degrees of freedom in the imidazolium/methanethiol complex of chapter 3 were optimized. This was accomplished by an optimization of the Hartree-Fock SCF wavefunction using the Gaussian 82 system of programs and the STO-3G basis set as implemented in the program.

5.2.2 CONSTRUCTION OF THE QUANTUM MOTIF AND PROTON TRANSFER CURVES

The proton transfer between His 162 and Asn 182 was modeled by a modification of a scheme previously described by us for the computation of proton transfer energy curves (Topiol et al., 1985). In this scheme the proton acceptor and donor molecules were optimized independently in their protonated and unprotonated forms then oriented as the side chains of His 162 and Asn 182 and, the proton transfer energy curve was generated by computations in which the

donor and acceptor molecules remained fixed while the proton moved. In the computations the side chain of His 162 was represented by imidazole (or imidazolium) and the side chain of Asn 182 by formamidinium (or formamide). This complex was labeled IMID/FOR. The intermolecular orientation of the hydrogen bonded species was maintained as in the protein structure. Because the protonation of formamide or formamidinium could be in a direction that is colinear either with the C-O bond (i.e. linear form) or with the direction of the lone pair (i.e. bent form), three possible complexes were studied: imidazolium/ formamide, imidazole/ formamidinium (bent), and imidazole/ formamidinium (linear). Scheiner and co-workers have shown that the proton transfer between the carbonyl oxygen atom of formaldehyde and H_3O^+ was very sensitive to the orientation of the hydrogen bond, i.e., along the C-O axis or along the lone pair of the carbonyl oxygen atom (Scheiner and Hillenbrand, 1985). Their work showed that the orientation of the hydrogen bond could dictate if the products of the proton transfer would yield a bent or linear structure for the cationic form of aldehyde. Thus, in this chapter both structures for the protonated form of formamidinium are considered.

Proton transfer curves were computed for each of the three complexes (IMID+/FOR, IMID/FOR+(linear), IMID/FOR+(bent)) following the scheme described earlier (Topiol et al., 1985). But, it was modified to include full optimization of the angular degrees of freedom of the proton and of the distance of the proton from the donor within the constraint of fixed donor and acceptor geometries. Angular

degrees of freedom were optimized because the proton path was not known a priori. An accurate proton transfer energy curve was constructed by combining the lowest energy points in the curves computed using the three geometries (See Figure 5-1). The critical points where computed by adding the donor-to-proton distance to the optimized variables. Critical point M1 corresponded to the proton on His 162 and was generated using the IMID/FOR complex. Critical point M2 corresponded to the proton on Asn 182 and was generated by using the IMID/FOR+ (bent) complex. Two potential transition state geometries were generated. One corresponding to the IMID/FOR+ (bent) complex (i.e. the TSP point) and another to the IMID/FOR+ (linear) complex (i.e. the TSL point); the imidazolium/ formamide structure did not have a transition state for the proton transfer with the basis sets used in our studies. The second minimum generated from the IMID/FOR+ (linear) was clearly higher in energy than the one generated by the bent form. Thus, it was disregarded as a possible M2 point in the proton transfer energy curve. For the STO-3G basis set the TSL point was lower than the TSP point, but extension to the 6-31G basis set reduced this difference.

All computations were done using the GAUSSIAN 82 system of programs (Binkley et al., 1982) and its default optimization options. The STO-3G, 6-31G, and 6-31G* basis sets as implemented in the system were used in the computations. In the computation of transition states the constraint of one negative eigenvalue in the Hessian matrix was included in the optimization.

5.2.3 GEOMETRIES OF LIGANDS AND THEIR COMPLEXES WITH THE QUANTUM MOTIF

Indole was the basic nucleus of the ligands used in this study. The geometry of indole was generated from the side chain of Trp 184 in the structure of actinidin. This structure was very similar to an STO-3G optimized indole and did not differ significantly from the Falkenberg averaged geometry used in previous work from this laboratory (Osman et al., 1987; Weinstein et al., 1976). The hydroxy derivatives of indole were generated from the corresponding tryptamine derivatives reported in previous work (Weinstein et al., 1976). The Falkenberg averaged structure for indole was used as a template to which the hydroxy group was added to the appropriate carbon atom. The hydroxy hydrogen was always in the plane of the molecule. Except for the 5-OH derivative, it was always *trans* to the N1 nitrogen due to considerations from modeling the 5-hydroxytryptamine recognition pattern described earlier (Weinstein et al., 1976; Weinstein et al., 1981b). For the 5-OH derivative, the hydrogen was *cis* to the N1 nitrogen. The structure of the methylenedioxy derivatives of indole had been reported in previous studies (Reggio et al., 1981). Again, the indole template was retained and the methylenedioxy group at standard bond length and angles was added in the appropriate position.

The indole derivatives were oriented with respect to the quantum motifs by superposition of the indole ring onto the ring of Trp 184 in actinidin. Figure 3-1 shows the orientation of this group

with respect to the side chains of His 162, Cys 25, and Asn 182. The indole was closest to the NE2 nitrogen in His 162 and the OD1 oxygen of Asn 182, and lay in a plane slightly tilted from the plane of the imidazolium ring of His 162 at a distance of roughly 4-5 Å.

5.2.4 COMPUTATION OF ELECTROSTATIC INTERACTIONS

The energetic stabilization of the IMID/FOR complexes inside the protein and the interaction between these complexes with the ligands were computed using the iterative scheme described in detail in chapter 2 which were applied to computations using actinidin in chapter 3. The reader is referred to these chapters for details.

The electrostatic computations were limited to the first step in the iterations because previous work and computations indicated that the polarization of the quantum motif was less than 0.5 kcal/mol (see results in chapters 2 and 3). Thus, the first step in the iterative scheme was a good approximation to the converged solution.

The point charges and atomic polarizabilities necessary for the representation of the classical motifs were the same used in the work described in chapter 3. Specific computations with the Mehler-Paul basis set (Mehler and Paul, 1979) were necessary to generate the dipole conserving point charges for the ligands. These computations were done using a version of the program HONDO that was modified with this option. The atomic polarizabilities for the atoms in the ligands were taken from the same library of polarizabilities used in

chapter 3. The fields and potentials generated by the quantum motif were computed from an Hartree-Fock SCF wavefunction computed using the STO-3G basis set and the property package from GAUSSIAN 82 (Binkley et al., 1982). Work described in earlier chapters showed that this basis set was adequate for the computation of the electrostatic interaction using the iterative scheme described above.

The effect of the entire protein structure (the "full protein environment"; FULL) was considered by using all the atoms in the protein except those belonging to His 162 and Asn 182. To consider the effects of selected elements of the structure, three subsets of coordinates were also generated. One set (HX) consisted of the atoms belonging to the alpha helices as described in the PDB file (i.e. helices A1 to A6). Another set (BETA) contained the atoms of the beta sheet structures in the protein, including the sheets B1 and B2 identified in the PDB file. The third set (ACTIVE) contained only the atoms of the residues Trp 184, Cys 25, and Gln 19, which, together with His 162 and Asn 182, formed the active site of actinidin (Baker, 1980; Brocklehurst et. al., 1981).

5.2.5 SOLVENT EFFECTS

The effect of the solvent surrounding the protein structure was estimated as done in chapter 3 by computing the electrostatic interaction energy using a modified set of point charges for the macromolecule. In this modified set, the atoms exposed to the solvent had their charge scaled down by a constant value of 1.35. Because the

major contribution to the electrostatic interaction energy (see Results) was from the VxQ energy term in UNPT, computations with the set of scaled point charges was limited to this energy term. No attempts were made to explore polarization effects with these new set of point charges since the three-body effects involved in the polarization of the solvent, protein matrix, and the quantum motif would be too complex to be estimated by using the scaled charge approximation.

5.2.6 SPATIAL CONSTRAINTS ON THE ORIENTATION OF THE LIGANDS

In an effort to orient the drug molecules around the IMID/FOR and IMID/MET (i.e. imidazolium/methanethiol) complexes to optimize their effect on the proton transfer energy curves, the spatial constraints introduced by the protein structure of actinidin on the indole group of Trp 184 were explored using the CHARMM package of programs (Brooks et al., 1983) as implemented in the QUANTA system of programs (POLYGEN Corp., 1988). Using the default potential function and parameter file in CHARMM, the self energy of actinidin was computed as a function of rotating the indole of Trp 184 around the Cα -- Cβ (TAU 1) and Cβ -- Cγ (TAU 2) bonds in 20 degree steps. The results yielded a preliminary scan of the potential surface. For values of TAU 1 greater than -20 degrees the energy surface was over several hundred to thousands of kilocalories higher in energy than the crystal structure geometry (data not shown). For this reason a second more detailed scan with step size of 5 degrees was limited to

$-180 \leq$ TAU 1 ≤ -20 and $-180 \leq$ TAU 2 ≤ 180; the results are shown in Figure 5-2 where they were plotted in isoenergetic contours as a function of the angles, and with the energy for the crystal structure geometry as the zero point of energy. Although it did not represent a true measure of the interaction of the indole group with the protein structure due to the nature of the potential functions and the neglect of structural adjustment of the protein macromolecule, this approach gave a qualitative estimate of the freedom of movement around the region of the side chain of Trp 184 in the catalytic site of actinidin, Additional analysis of the spatial constraints introduced by the protein structure on the possible orientations for the ligand molecules was done using the molecular graphics package available through QUANTA and its default parameters for van der Waal radii.

5.3 RESULTS

5.3.1 THE PROTON TRANSFER

5.3.1.1 IMID/FOR Complex in the absence of the protein or ligands

Figure 3-1 shows the orientation of the indole from Trp 184 and the imidazolium/ formamide in the IMID/FOR complex, and Figure 5-1 shows that proton transfer energy curve for the IMID/FOR system computed with the STO-3G basis set as described in the Theoretical Approach section. The double well character of the curve was typical

for proton transfer between hydrogen bonded systems (Scheiner, 1985). Table 5-1 lists the stabilization energy of the critical points, barriers, and driving energy for proton transfer in the IMID/FOR system. The complex was stable at the M1 point with a stability of 19.2 kcal/mol computed with the 6-31G* basis set and the 6-31G geometry. With the same basis set the barrier for proton transfer was 26.8 kcal/mol when the TSL transition state structure was considered and 28.5 kcal/mol when computed at the TSP transition state point. The driving energy (i.e. M2-M1) was 22.0 kcal/mol. Table 5-1 also shows the basis set dependence for these computations. The STO-3G basis set overestimated the stability of the IMID/FOR complex when the proton moves to formamide while results obtained with the 6-31G basis set were in reasonable agreement with the 6-31G* results. In comparison to the computations with the 6-31G* or 6-31G basis sets, the minimal basis set underestimated the barrier for proton transfer and overestimated the driving energy (i.e. less negative M2-M1).

5.3.1.2 Protein electrostatic effects on the proton transfer

Table 5-2 shows the electrostatic energy of interaction between fragments of the structure of actinidin and the IMID/FOR complex at the critical points of the proton transfer energy curve. The full protein structure interacted favorably with the complex at all critical points and the stabilization overcame the destabilization calculated in vacuum for the complex with the proton near formamide. As pointed out also for the His 162/ Cys 25 complex, the elements of the protein structure considered here had different contributions to this effect.

The groups in the active site stabilized the complex by less than 2 kcal/mol while the collection of alpha helices A1 to A6 made a major contribution to the stabilization of the complex. The effect from the beta sheet structures was significant because at the M2 point these structures *destabilized* the complex by 0.7 kcal/mol. These effects were mediated through a combination of the unperturbed and polarization energies of interaction (UNPT and IND B, respectively). For the full protein structure and the collection of alpha helices the polarization energy was a small component of the total interaction energy. For the groups in the active site and the beta sheet structure the polarization energy was a major component of the favorable interaction between these groups and the IMID/FOR complex.

Table 5-3 shows the effect from the protein on the barrier and driving energy for proton transfer between imidazolium and formamide. Because the difference between the TSL and TSP forms of the IMID/FOR complex was negligible (e. g. Table 5-2) only the results for TSL are listed. The full protein structure increased the barrier and reduced the driving energy by approximately 3 kcal/mol. The groups in the active site had negligible effects on the barrier and driving energy (i.e. approximately < 0.5 kcal/mol), thus they had little effect in modulating the proton transfer. The alpha helices aided the transfer of the proton by reducing the barrier and increasing the driving energy, but their effect was also very small. The beta sheets had a significant influence on modulating the in vacuum proton transfer energy curve. This element of supersecondary structure increased the barrier for proton transfer by 5.5 kcal/mol. The driving

energy was decreased by 9.7 kcal/mol. It is noteworthy that most of these effects were due to the unperturbed interaction energy; the only exception was the polarization contribution from the groups in the active site. The latter were the closest groups to the IMID/FOR complex, and the result was reasonable.

As described in Theoretical Approach, I estimated the consequence of solvent screening on the calculated effect of the protein on the proton transfer curve. Table 5-4 compares the barriers (TSL-M1) and driving energies (M2-M1) estimated from the computation of VxQ energies using scaled charges and non-scaled charges as described in Theoretical Approach. As expected with the modified charges, the electrostatic interaction between the FULL protein structure and the IMID/FOR was reduced. Similar reductions were not expected with fragments of the protein because the scaling factor was constructed by considering the full set of charges. In modulating the activation process it was the barrier (i.e. TSl-M1) and driving energy (i.e. M2-M1) which were the relevant terms. Scaling of the charges introduced no changes on these terms suggesting that addition of solvent effects would not make qualitative changes in the results described above. Moreover, for the β sheets eliminating the charged groups did not make significant changes to the effect from these structures to barrier and driving energy.

5.3.2 THE EFFECTS OF THE LIGANDS ON THE PROTON TRANSFER ENERGY

5.3.2.1 Spatial constraints imposed by the protein structure

Because of their agonistic activity at the 5-HT/LSD receptor tryptamine derivatives as represented by their model structures (e.g. hydroxy and methylenedioxy indoles) were expected to have modulatory effects on any proton transfer process responsible for activation of the receptor. However, both binding of ligands to the proton transfer complex, and the electronic effect of complexation were shown to be dependent on the mutual orientation of the ligand and the complex (Osman et al., 1987). The steric constraints imposed by the protein structure would affect the measured affinity of the ligands. Figure 5-2 shows a contour plot of the energy of actinidin as a function of the orientation of the indole in Trp 184. In the crystal structure the indole in Trp 184 was in nearly stacking conformation over the hydrogen bond between His 162 and Asn 184, an orientation similar to the one shown to be important in modulating the proton transfer responsible for activation of the 5-HT/LSD receptor (Osman et. al., 1987). The calculations showed the orientation in the crystal structure to be the most favorable one because all other regions lay higher in energy. Only two small windows existed between τ(Cα -- Cβ) of -50 to -180 degrees and τ(Cβ -- Cγ) of -180 to -20 and 180 to 20 degrees with energies within 50 kcal/mol from the crystal structure. The strong spatial constraints imposed by the protein structure was evident in Figure 5-3 which showed a 5-hydroxyindole molecule ori-

ented as the indole in Trp 184 and with the surrounding protein structure. The surface surrounding the molecule at a distance equal to the van der Waal radii of the atoms is shown as a dot surface. Small displacements from the original crystal structure orientation yielded poor steric contacts as evidenced by the overlap between the dot surfaces.

5.3.2.2 Electrostatic effects on the proton transfer

Given the strong spatial constraints introduced by this model protein structure, the electrostatic effects of the ligands on the proton transfer in the IMID/FOR complex were studied with the ligands in the orientation of the indole group of residue Trp 184. This was done as an exploration of the ability of such ligands to modulate the proton transfer even in the absence of an optimal orientation with respect to the hydrogen bonded complex responsible for activation. Table 5-5 shows the calculated electrostatic interaction between the IMID/FOR complex at each one of the critical points for the various indole derivatives. and the effect of these ligands on the barrier and driving energy for proton transfer. Notably, the interaction of all ligands reduced the barrier and increased the driving energy, but to different extents thus giving rise to a definite rank order in which 5-HT was calculated to have the greatest effect.

5.4 DISCUSSION

The results from this work illustrated the two major effects of protein structure on the mechanism of ligand recognition at the receptor, and on the process of triggering a response to binding. One was the result of steric constraints imposed by the protein structure. The other was the electrostatic effect of the structure on the activation mechanism -- in this case a proposed proton transfer.

The proton transfer between His 162 and Asn 182 was affected by the electrostatic effects from actinidin in a manner similar to that discussed for the His 162/Cys 25 system (See chapters 3 and 4.). In both systems the proton transfer was hindered by the protein structure. This total effect was composed of several, sometimes opposite contributions from different elements of the protein structure. For examples, the effects of various helices, and the opposite nature of the effect of all helices compared to the effect of the rest of the structure. A noteworthy difference between the way in which the two proton transfer systems are affected was the large effect the beta sheet structure had on the proton transfer between His 162 and Asn 182. For the His 162/Cys 25 system the alpha helices had a more significant role in modulating the proton transfer. Unfortunately, the extent to which beta sheets may be prominent in the structure of neurotransmitter receptors is presently unknown. The general electrostatic properties arising from the secondary

structure of beta sheets remains unclear (van Duijnen et al., 1985). The nature of the electrostatic interaction energy with the protein was also similar for both complexes. When a net charge was present as was the case with the alpha helices and the full protein structure, the UNPT energy term made the greatest contribution to the energy due to the VxQ energy. For the interaction with groups lacking a net charge as was the case with the beta sheets and the active site, the polarization energy was of similar magnitude to the UNPT term. The electrostatic contribution to the barrier and driving energy responsible for modulation of the proton transfer came primarily from the UNPT term in both systems.

In the simulation of 5-HT interacting with the proton transfer model in vacuum (Osman et al., 1987), full freedom was allowed in identifying the optimal orientation for 5-HT to interact with the imidazolium molecule in a plane parallel to the plane of the imidazolium molecule. This freedom made possible the identification of the optimal orientation that was likely to be built into a receptor structure if this were the recognition process. But it was not expected to exist in the macromolecular receptor model due to steric effects from the protein structure. Indeed, the simulations and molecular graphics analysis of the area surrounding the indole of Trp 184 indicated that the packing within the protein was tight, and there was little room for modifying the orientation of this group within the active site of actinidin from the original crystal structure orientation. These constraints hindered the ability to optimize the indole of Trp 184 over either the His 162/Cys 25 complex studied before or the His 162/Asn

182 complex studied here. Thus, it was not possible to maximize the effects from indole or its congeners on the barrier and driving energy for proton transfer. Because the crystal structure orientation for the indole of Trp 184 was close to the optimal orientation suggested from the simulations in vacuum, and the molecular mechanics computations and graphics analysis suggested little freedom of movement for this group, it is reasonable to assume that the crystal structure orientation for the indole represents its preferred orientation within the constraints of the surrounding protein structure.

The present findings concerning the electrostatic effect of congeners of 5-hydroxyindole (representing 5-HT) on the proton transfer between His 162 and Asn 182 extended the conclusions on the electrostatic effects that the receptor-macromolecule itself has on the activation of the 5-HT/LSD receptor. The His 162/Asn 182 complex was chosen here because the proton donor and acceptor moieties in this complex were closer to the indole of Trp 184. Thus, the proton transfer energy curve was directly affected by the presence of the indole as oriented in the crystal structure. The models for all the congeneric drugs, when oriented as the indole of Trp 184, lowered the barrier for proton transfer and increased the driving energy for the process. These changes in the proton transfer energy curve were expected for ligands with agonist activity such as the 5-HT congeners studied here. The effects on the barriers and driving energy were of the same magnitude, but in the opposite direction as those already described for the protein structure (compare Tables 5-3 and 5-5). Thus, while the protein structure inhibited activation by

hindering the proton transfer, the drugs lowered the barrier and increased the driving energy for transfer hence contributing to activation. These effects follow a specific rank order as shown in Table 5-5 with 5HIND (5-hydroxyindole) having the greatest effect. Such results were not obtained by using an optimization of the ligands around the His 162/Asn 182, but by choosing an orientation that appeared optimal within the steric constraints in actinidin. Thus, this heuristic modelling suggests that the receptor-macromolecule may have a structure that *selects* for an orientation of ligands with agonistic activity that optimizes the interaction energy and lowers the barrier for the proton transfer so as to trigger receptor activation. This selection would result from steric constraints that fine tune the interaction between ligands and the receptor. In this context, it may be noteworthy that recent QSAR work by Taylor and co-workers has identified the molecular volume of tetrahydropyridylindoles as a significant parameter in the nonlinear regression model that predicts pK_i's at the 5-HT_{1a} receptor (Taylor et al., 1988).

The structure-activity studies of ligands at neurotransmitter receptors have emphasized an analysis of those structural features that are relevant for binding and biological activity. Activity has been addressed primarily as an all or none feature, but receptor theory and experimental evidence has indicated that there is a spectrum of binding affinities and biological activities as represented by the maximum effect and potency of an agonist (Kenakin, 1987). The *intrinsic efficacy* (τ) of a ligand has been a measure of the biological activity of a drug which was dependent only on properties of the

ligand (Kenakin, 1987). Hence, it was different from the binding affinity which depended on both the ligand and its binding site. Within the Ternary Complex Theory of Black and Leff (Kenakin, 1987), the intrinsic efficacy depended on the equilibrium constant (K_E) for the binding of the drug-receptor complex with the effector protein to form a ternary complex whose concentration was proportional to the stimulus responsible for the pharmacologic response. Because the proton transfer described here was postulated to generate an active form of the receptor capable of binding the effector and generating a response, the driving energies listed in Table 5-5 should correlate with the intrinsic efficacies of the drugs under conditions in which the rate of formation of the ternary complex is fast. Otherwise, the intrinsic efficacy should correlate with the barrier for proton transfer (TS-M1). The intrinsic efficacy for all the tryptamine derivatives has not been reported, but it is of significance that 5-carboxyamido tryptamine, modeled here by 5CIND, is a partial agonist at the 5-HT_{1a} receptor (Shenker et al., 1985; Shenker et al., 1987), the pharmacologically correct name for the 5-HT/LSD receptor, whereas 5-HT is a full agonist. This observation is in agreement with the rank order in Table 5-5 for either the barrier or driving energy effects.

The analysis presented here for the interplay between the steric and the electrostatic effects from the receptor macromolecule on the interaction of the ligands with the elements of the activation mechanism, represented the first attempt to address the physicochemical basis of the intrinsic efficacy of ligands in terms of properties generated by their molecular structure. The work has

shown how the intrinsic efficacy of a ligand at the 5-HT/LSD receptor depends on its electrostatic properties and on its steric fit in the receptor site. The simulations have shown that the electrostatic properties would be responsible for lowering the barrier and increasing the driving energy for proton transfer and the steric properties would be responsible for the proper orientation of the ligand within the binding site. Without the proper orientation, a ligand with an electrostatic potential that mimics that of 5-HT would be unlikely to trigger the proton transfer that activates the receptor. Thus, a potent full agonist at the 5-HT/LSD receptor would have three properties: 1) an electrostatic orientation vector topologically oriented with respect to its equivalent of the amine group in the ethylamine side chain of 5-HT (see Chapter 1 for details) so that tight binding is achieved, 2) steric properties that will enable its electrostatic field to be in the proper orientation to trigger activation once it binds to the recognition site, and 3) an electrostatic field capable of triggering a proton transfer in a hydrogen bonded system such as the one of the PTM. The properties of antagonists emerge from this definition as compounds that would fail to have either the steric and/or the proton transfer triggering properties, but that would maintain the specific binding properties.

Most importantly, the studies provided for the first time a specific mechanistic hypothesis, at the molecular level, for the properties of partial agonists. Thus, partial agonists are revealed as compounds in which the combination of specific steric and/or electrostatic requirements defined by the model are not sufficient to

affect the driving energy (or the barrier -- see above) for proton transfer. Fully compatible with the operational definition in modern receptor theory (see Black and Leff, 1983), these molecular mechanisms provide the first definition of pharmacological efficacy at the discrete molecular level.

TABLE 5-1. Formamide/imdazolium complex in vacuum.

STABILIZATION ENERGY [a]				
BASIS SET	M1	TSL	TSP	M2
STO-3G	-20.2	-3.3	0.0	-8.5
6-31G	-20.8	6.5	7.0	4.0
6-31G*// 6-31G	-19.2	7.6	9.3	2.8

BARRIERS AND DRIVING ENERGY			
	STO-3G	6-31G	6-31G*//6-31G
TSL-M1	16.9	27.4	26.8
TSP-M1	20.2	27.8	28.5
M2-M1	11.7	24.8	22.0

[a] Energy values in kcal/mol. Zero point energy is the sum of isolated and optimized imidazolium and formamide. For STO-3G, imidazolium energy is -222.43956 a.u. and formamide energy is -166.68822 a.u.. For 6-31G, imidazolium energy is -225.10345 a.u. and formamide energy is -168.85507 a.u.. For 6-31G*, imidazolium energy is -225.19580 a.u. and formamide energy is -168.92938 a.u..

TABLE 5-2. Protein electrostatic effects [a].

	M1	TSL	TSP	M2
FULL PROTEIN				
UNPT [b]	-306.3	-302.7	-303.6	-299.7
IND B [c]	-30.2	-29.9	-30.2	-33.5
TOTAL	-336.5	-332.6	-333.8	-333.2
ACTIVE SITE FRAGMENT				
UNPT	5.0	4.0	4.0	3.0
	(0.1)	(-0.1)	(-0.1)	(-0.4)
IND B	-6.0	-4.8	-4.8	-4.6
TOTAL	-1.0	-0.8	-0.8	-1.6
ALL HELICES				
UNPT	-108.7	-110.3	-109.9	-111.4
	(-108.2)	(-110.4)	(-109.9)	(-112.0)
IND B	-6.1	-5.1	-5.2	-4.7
TOTAL	-114.8	-115.4	-115.2	-116.1
ALL BETA SHEETS				
UNPT	-3.7	1.2	0.8	5.4
	(5.9)	(10.3)	(9.9)	(14.1)
IND B	-5.3	-4.7	-4.6	-4.7
TOTAL	-9.0	-3.5	-3.8	0.7

[a] Computed with the STO-3G basis set. Values in parenthesis are VxQ energies. Energy in kcal/mol. See Theoretical Approach for definition of energy terms.

[b] Only VxQ term is included.

[c] Dipole interaction tensor is neglected.

TABLE 5-3. Protein electrostatic effects: barrier and driving energy [a].

	M1-TSL	M2-M1
FULL PROTEIN		
UNPT [b]	3.6	6.6
IND B [c]	0.3	-3.3
TOTAL	3.9	3.3
ACTIVE SITE FRAGMENTS		
UNPT	-1.0	-2.0
	(-0.2)	(-0.5)
IND B	1.2	1.4
TOTAL	0.2	-0.6
ALL HELICES		
UNPT	-1.6	-2.7
	(-2.2)	(-3.8)
IND B	1.0	1.4
TOTAL	-0.6	-1.3
ALL BETA SHEETS		
UNPT	4.9	9.1
	(4.4)	(8.2)
IND B	0.6	0.6
TOTAL	5.5	9.7

[a] Computed with the STO-3G basis set. Values in parenthesis are VxQ energies. Energy in kcal/mol. See Theoretical Approach for definition of energy terms.

[b] Only VxQ term is included.

[c] Dipole interaction tensor is neglected.

TABLE 5-4. Protein electrostatic effects: solvent effects [a].

POINT	FULL	HX	ACTIVE	BETA [b]
M1	-306.3	-108.2	0.1	5.9 (-8.3)
TSL	-302.7	-110.4	-0.1	10.3 (-5.0)
TSP	-303.6	-109.9	-0.1	9.9 (-5.1)
M2	-299.7	-112.0	-0.4	14.1 (-2.0)
TSL-M1	3.6	-2.2	-0.2	4.4 (3.3)
M2-M1	6.6	-3.8	-0.5	8.9 (6.3)
		AFTER SCALING		
M1	-5.6	-26.2	-4.1	28.9 (8.0)
TSL	-3.2	-28.2	-4.9	33.5 (11.3)
TSP	-4.1	-27.8	-4.8	33.0 (11.1)
M2	-1.3	-29.7	-5.6	37.4 (14.2)
TSL-M1	2.4	-2.0	-0.8	4.6 (3.3)
M2-M1	4.3	-3.5	-1.5	8.5 (6.2)

[a] From VxQ energy computations using the STO-3G basis set as described in Theoretical Approach. Energy in kcal/mol.
[b] Values in parenthesis correspond to computations with the side chains of charged groups excluded: Asp 6, Glu 172, Asp 176, Lys 181, Arg 195, Arg 198. His 162 is never included because it is part of the quantum motif.

TABLE 5-5. Electrostatic interaction: ligands vs. formamide /imidazolium complex [a].

LIGAND	M1		TSL		M2	
	UNPT	IND B	UNPT	IND B	UNPT	IND B
FHIND	2.5	-2.3	0.2	-2.1	-1.6	-2.5
INDOL	0.7	-2.2	-1.5	-2.0	-3.2	-2.4
4HIND	2.2	-2.3	0.2	-2.1	-1.1	-2.5
45MDX	3.2	-2.4	1.6	-2.3	0.4	-2.8
56MDX	2.7	-2.5	1.2	-2.3	0.0	-2.7
5CIND	3.5	-2.5	2.1	-2.3	1.1	-2.8
6HIND	1.0	-2.3	-0.4	-2.1	-1.4	-2.5
7HIND	-1.7	-2.4	-2.6	-2.1	-3.5	-2.5

	TSL-M1 [b]	M2-M1 [b]
5HIND	-2.3	-4.1
INDOL	-2.2	-3.9
4HIND	-2.0	-3.3
45MDX	-1.6	-2.8
56MDX	-1.5	-2.8
5CIND	-1.4	-2.4
6HIND	-1.4	-2.4
7HIND	-0.9	-1.8

[a] Energy in kcal/mol. 5HIND: 5-hydroxyindole. INDOL: indole. 4HIND: 4-hydroxyindole. 45MDOX: 4,5-methylenedioxyindole. 56MDOX: 5,6-methylenedioxyindole. 5CIND: 5-carboxy-amidoindole. 6HIND: 6-hydroxyindole. 7HIND: 7-hydroxyindole.
[b] Values only for UNPT interaction energy.

Figure 5-1. Proton transfer energy curve for the IMID/FOR complex computed using the STO-3G basis set as described in methods.

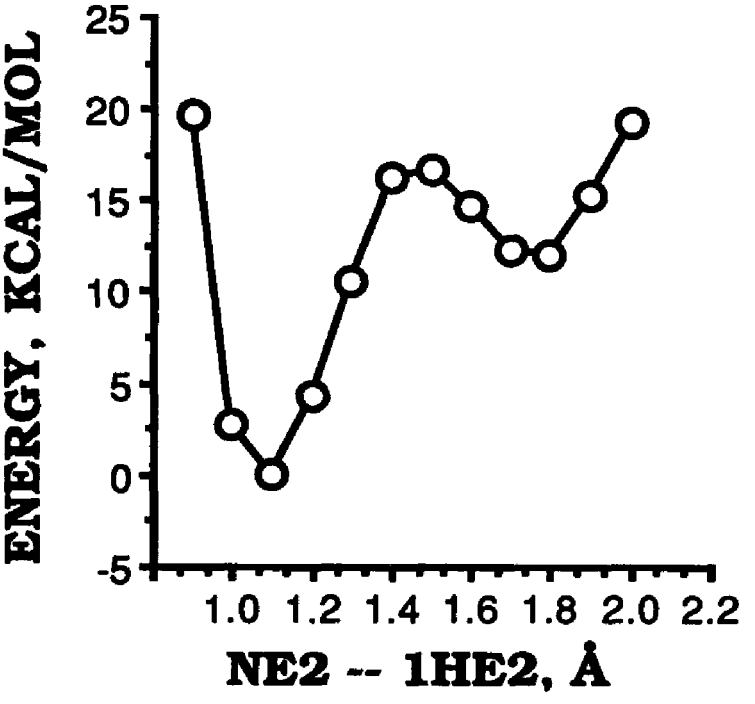

Figure 5-2. Contour plot of the self energy of actinidin as a function of the dihedral angles N--Cα--Cβ--Cγ and Cα--Cβ--Cγ—Cδ2. Zero of energy is -5363.48 kcal/mol.

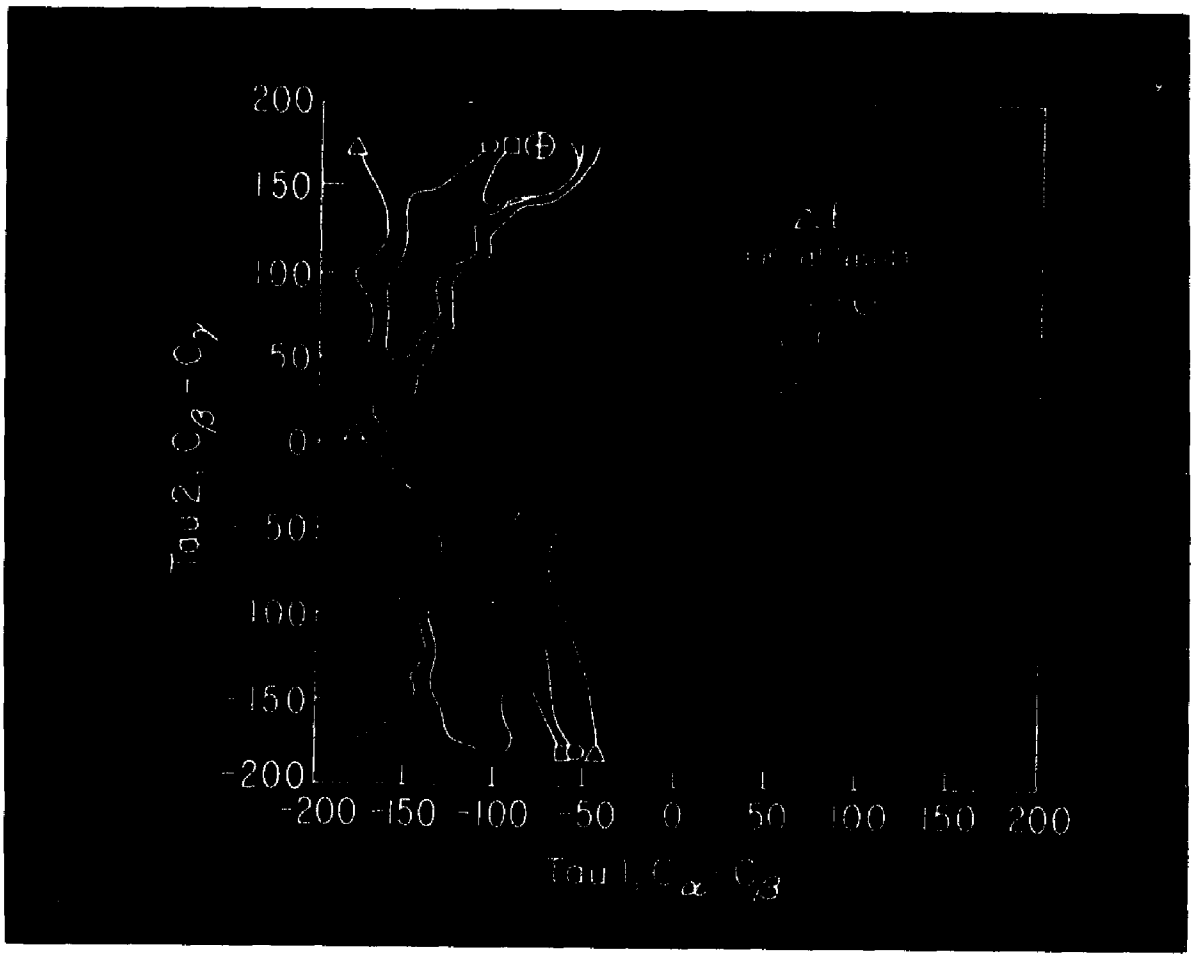

Figure 5-3. 5-hydroxyindole oriented as the side chain of Trp 184 and surrounding groups in actinidin: van der Waal surface shown as colored dots. 5-hydroxyindole colored yellow.

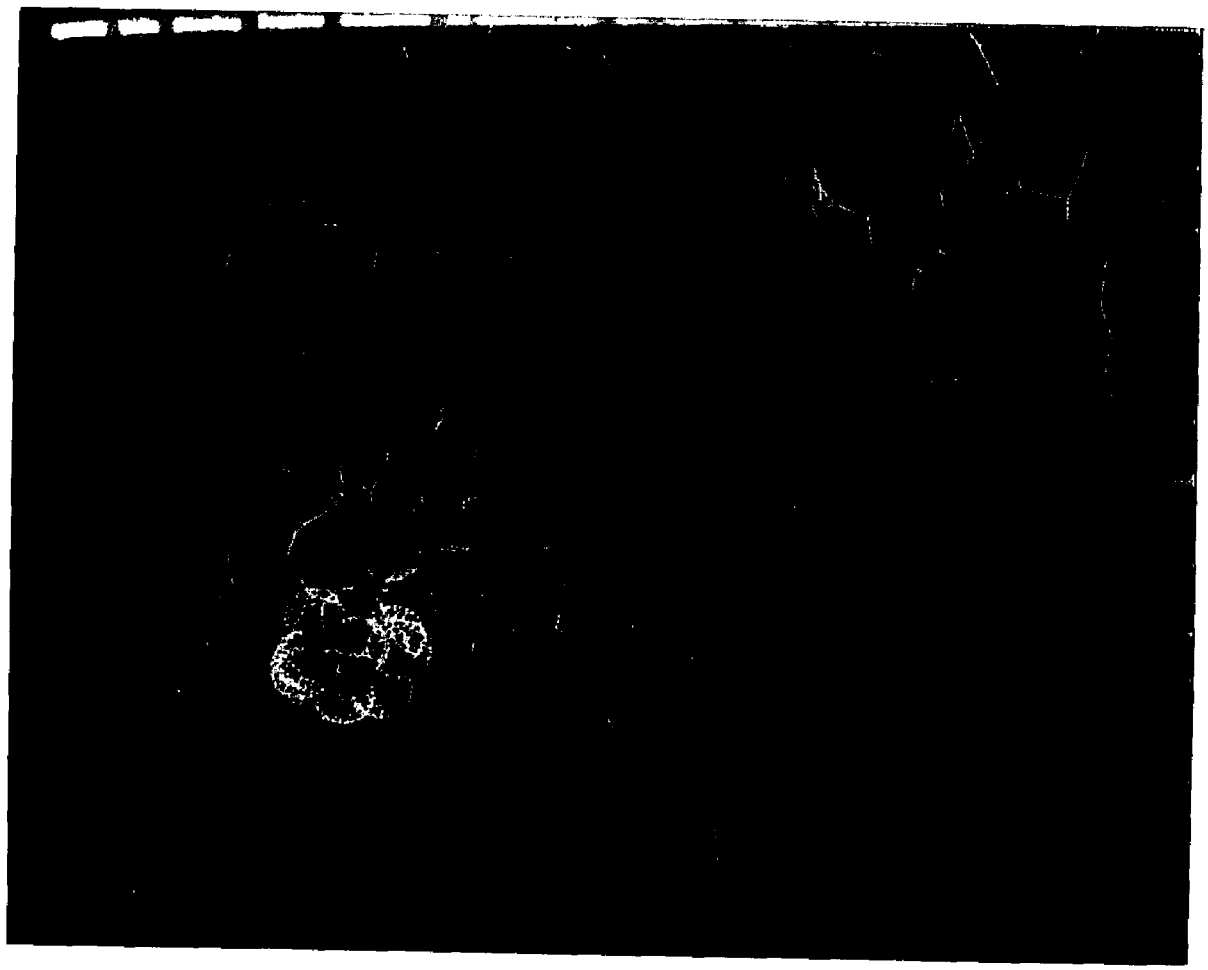

CHAPTER 6

CONCLUSION

Advances in biochemistry and molecular biology have opened the door for evaluating the structure-function relationship of neurotransmitter receptors (Lester, 1988; Hartig, 1989). The new information complements the structure-activity studies that are the subject of traditional pharmacological research (Kenakin, 1987). Unfortunately, the lack of detailed atomic structures for membrane bound neurotransmitter receptors limits the scope of structure-function and structure-activity investigations. This thesis presented an approach to structure-function relationship research designed to circumvent this limitation. This **new** approach resulted from identifying a protein with known three dimensional structure (i.e. the enzyme actinidin) as a polypeptide with structural elements recognized by previous research to be relevant in the binding of ligands and activation of the 5-HT/LSD receptors. With actinidin as a **model for the environment** of the receptor, the **electrostatic** and **steric** effects that the receptor structure may have on the process of **activation** were explored for the first time. The results from the studies using actinidin were expressed as contributions from elements in the secondary and tertiary structure of the protein (e.g. alpha helices). These structural elements were known to exist in other

systems, including the membrane bound proteins, the protein subset that includes neurotransmitter receptors (Richardson, 1981; Allen et al., 1987; Hartig, 1989). This decomposition scheme and the assumption that effects generated by a structural element would be inherent to its structure formed the basis for generalizing the results from the structure of actinidin to the unknown structure of the 5-HT/LSD receptor. Thus, this approach to the structure-function relationship of neurotransmitter receptors aimed at exploring the long-range effects from large elements of the protein structure. This work did not explore the local interactions (i.e. oxyanion hole) described by Hwang and Warshel that may be subjected to strong evolutionary pressures and that may generate families of macromolecules (Hwang and Warshel, 1988).

The electrostatic effects from actinidin on the model for activation of the 5-HT/LSD (i.e. the Proton Transfer Model) (Osman et al., 1987) illustrated the effects that may be expected from the receptor structure. *First*, the protein structure through its electrostatic effects was capable of discriminating between the His 162/Cys 25 complex with the proton on the donor side, i.e., the non-activating state versus the proton on the acceptor side, i.e., the activating state. As would be expected from any reasonable model for the environment of the receptor, the protein structure hindered the proton transfer. Otherwise, the receptor would be activated in the absence of agonist ligands. *Second*, these electrostatic effects were the result of a complex interplay between contributions from different elements in the primary, secondary, and tertiary structure. For

example, the collection of alpha helices helped the proton transfer between His 162 and Cys 25, but some helices individually opposed the proton transfer. The collection of helices (tertiary structure) did not affect the proton transfer in the His 162/Asn 182 complex. *Third*, the effects from individual alpha helices resulted from a combination of the ionized groups in their primary structure and the helix macro-dipole generated by its secondary structure. As shown clearly by the effects of helix A3 on the proton transfer between His 162 and Cys 25, the electrostatic contribution from the secondary structure (i.e. helix dipole) may be **opposite** to that from the primary structure (i.e. ionized residues). The solvent environment had profound influence on the balance between these opposite effects; therefore, it would be expected to be important to the net electrostatic effect from the alpha helices in the receptor structure. *Fourth*, the electrostatic effects from the elements of the protein structure resulted from both unperturbed and polarization interactions with the proton transfer complex. In general, polarization effects were significant even when the structural elements were distant from the PTM (e. g. beta sheets). It was only when several ionized groups contributed to a net charge (e. g. alpha helices) that the unperturbed interaction term overwhelmed the electrostatic effects. *Fifth*, the effect of the protein on the energy curve for proton transfer was not the result of the electrostatic effects from the protein on the proton, but on the donor and acceptor molecules whose electron distribution changed as the proton was transferred. A similar interaction had been described for the modulation of the PTM by ligands of the receptor (Osman et al., 1987). These results implied that it would not be sufficient to explore only

the potential from the macromolecule along the path of a proton when studying biochemical reactions. The electronic rearrangement of the donor/acceptor complex upon proton transfer must be considered as can be done in a quantum mechanical description of the process.

The proton transfer between His 162 and Asn 182 was used to explore steric effects from the protein structure on the activation mechanism and to evaluate the effects of congeners of 5-HT on the proton transfer model. Thus, the **first** description of the molecular basis for the *intrinsic efficacy* of a drug was possible. An investigation of the steric hindrance around the indole of Trp 184 revealed major limitations to deviations in the orientation of this group from its crystal structure position within the active site. Nevertheless, indole and its derivatives in this orientation lowered the barrier to proton transfer between His 162 and Asn 182. The congeners showed a definite rank order for this effect. A rank order that appears to correlate with their intrinsic efficacy. Consequently, the strong steric constraints found within actinidin suggested that the receptor structure may select for an orientation of agonist ligands such that their electrostatic field is properly oriented to generate the proton transfer that would initiate activation. As a corollary, competitive antagonists would be expected to meet the electrostatic criteria necessary for binding (Weinstein et al., 1981). But they would lack the steric properties necessary to orient their electrostatic field in a position capable of lowering the barrier for proton transfer. The design of antagonists could be achieved by either eliminating the steric properties met by agonists **or** the electrostatic properties of

agonists that are needed to activate but not bind the receptor. It is noteworthy that the work with actinidin emphasized the importance of steric constraints in identifying molecular determinants of relevance to receptor activation. An experimental test for this hypothesis would require further developments in receptor theory and biochemical pharmacology because it demands classification of competitive antagonist by the physicochemical origin of their antagonism (i.e. steric vs. electrostatic). Under the best circumstances, the detailed structure of the receptor would be available. Spectroscopic tools guided by theoretical methodology would then be applied to probe the interaction between competitive antagonist and the receptor.

The approach presented in this thesis to the study of structure-function relationships in neurotransmitter receptors yielded new information and insight regarding drug-receptor interactions. Nevertheless, it is important to identify its limitations.

First, the description of the solvent is inadequate. The environment surrounding the receptor-macromolecule is important to the function of the macromolecule. This is known to be true for soluble enzymes (i.e. denaturation by the solvent) and may be true of membrane bound enzymes as recent reconstitution and transfection experiments suggest (see Fig. 9 in Falke and Koshland, 1987). Indeed, the modulation of the electrostatic effects of helix A3 by the solvent suggest that the same might be true of neurotransmitter receptors if the helices are exposed to polar environments. Solvent

effects cannot be properly addressed by modeling membrane bound proteins with soluble ones because the lipid bilayer environment of the former is absent in the latter. Thus, even if the methodological problems of representing solvent effects are solved (Zauhar and Morgan, 1988; Gilson et al., 1988), the incorporation of such methods into the heuristic approach used in this thesis is not straightforward.

Second, the need to decompose the effects of the model protein environment into contributions from its components imposes severe constraints in the computational methodology. Though in the last several years major advances in theoretical chemistry (e.g. thermodynamic perturbation methods, see McCammon, 1987 or Warshel et al., 1988) have permitted the computation of accurate differences in free energy. The application of such methodology to the heuristic approach described in this thesis would have been inadequate. These theoretical developments rely on the computation of complex interactions which are nonadditive. Thus, to associate specific elements of the protein structure with a specific contribution to the interaction energy computed using the full protein is not straightforward. Even when simple electrostatic interactions are considered nonadditive effects are present such as the polarization energy. In this thesis, the polarization contribution from an element of the protein structure (e.g. alpha helix) is arbitrarily defined as that computed when that element was the only one interacting with the quantum motif (for details, see chapter 3). It is clear that contributions from the polarization of the structural element of interest by other elements (e. g. beta sheets) which are excluded from

the computation are neglected, though such contribution to the total energy comes from the electron distribution of the structural element of interest. Thus, the sum of individual polarization terms do not add up to the polarization interaction with the full protein structure. The need to decompose nonadditive terms into contributions from individual structural elements that add to the full protein effect is critical in the application of the new theoretical methodologies to structure-function studies. It is only through theoretical analysis that such limitation may be overcome.

Third, the analysis of structure-function relationships in neurotransmitter receptors as presented here is inadequate to identify the issues of local electrostatic interactions such as those represented by the oxyanion-hole of serine proteases and the **specific** steric effects from residues in the binding site. This limitation may be addressed by using models that are as close to the receptor as possible. The information necessary to identify such models would come from the molecular biology of neurotransmitter receptors. For example, during the course of this thesis the primary structure of the 5-HT_{1a}, 5-HT_{1c}, and 5-HT_2 receptors were identified (for a review, Harting, 1989). All these receptors belong to the superfamily of neurotransmitter receptors that interact with G proteins. Comparison with other receptors of the same family and the generation of mutants of the adrenoreceptors permitted the identification of an amino acid sequence that may be relevant to **binding** of the ligands. This sequence contains a conserved Asp residue believed to interact with the ethylamine side chain of serotonin. Moreover, the 5-HT_2 and 5-

HT_{1c} receptors have a Met residue on the C side of the conserved Asp while the 5-HT_{1a} receptor has a Thr on the N side of the conserved residue. These residues are believed to impart specificity to the recognition of ligands by the receptors. Such residues may also be relevant to receptor activation. If they are in the binding site, they may be responsible for local electrostatic and steric interactions. By incorporating this information into future models for the receptor environment, it may be possible to have a more accurate description that would allow the theoretical investigation of local effects prior to the identification of the detailed structure of the receptor. Nevertheless, *a posteriori* finding has been the presence of a His residue unique to transmembrane helix V in the sequence for the 5-HT_{1a} receptor subtype and placed between a Asn and a Cys, the latter surprisingly located at the beginning of an alpha helix, the transmembrane helix VI (Weinstein, personal communication). It is also significant that experiments with chimeric receptors have identified the same two transmembrane helices as relevant to the binding of the β_2 receptor to its effector (Kobilka et al., 1988). 5-HT_{1a} receptor belongs to the same family of receptors as the β_2 receptor. Both have seven transmembrane helices and have the G proteins as effector systems. Thus, it is reasonable to assume that a proton transfer between groups in transmembrane helices V and VI may be responsible for the binding of the receptor to its effector. As discussed in the literature (Peroutka, 1988), the 5-HT/LSD receptor corresponds to the 5-HT_{1a} subtype, and the arrangement of its Asn, His, and Cys groups is similar to the one found in actinidin and used here as a proton transfer model.

Finally, ligand binding and receptor activation are dynamic processes in a complex environment (Falke and Koshland, 1987). These dynamic effects are relevant to the function of the macromolecules (Warshel, 1984; Brooks and Karplus, 1985; Karplus and McCammon, 1986; Elber and Karplus, 1987) and are ignored in the heuristic approach used here. It is hard to envision any approach to receptor dynamics that uses model systems, such as soluble enzymes. Not only are molecular motions the results of many complex nonadditive interactions, but also the effects from the lipid bilayer that surrounds the receptor on such motion is poorly understood and hard to include in computations with current computer technology. Receptor dynamics will address such issues as coupling to transducer systems, but its theoretical analysis most likely will have to wait for the elucidation of the three dimensional structure of the receptors of interest.

Current pharmacological research addresses the issues of structure-function relationships in neurotransmitter receptors. The literature already discusses the impact of molecular biology in the design of new therapeutic agents (Lester, 1988). One may hope that in the future the specific chemical steps responsible for receptor function will be determined, as has been done for enzymatic catalysis. The application of sophisticated NMR methodology, new techniques for the collection of time-dependent X-ray diffraction data, and the generation of crystals of membrane bound proteins are needed to give three dimensional structure to the sequence data readily produced by

molecular biologists. The heuristic approach to structure-function relationships in neurotransmitter receptors followed here provides an indirect view of receptor function. Until membrane-bound receptor structures are readily determined, it will be necessary to use models for the effects of the protein environment such as the use of actinidin in this thesis. Nevertheless, even after the three dimensional structure of the receptors are known, the heuristic approach demonstrated here may be extended to the receptors as a powerful approach to research in molecular pharmacology.

BIBLIOGRAPHY

Allen, L. C.: The Catalytic Function of Active Site Amino Acid Side Chains in Well Characterized Enzymes, in: H. Weinstein and J. P. Green (Eds.), Quantum Chemistry in Biomedical Sciences. Annals of the New York Academy of Sciences. The New York Academy of Sciences, New York, NY, 367: 383-406, 1981.

Allen, J. P., Feher, G., Yeates, T. O., Komiya, H., and Rees, D. C.: Structure of the reaction center from Rhodobacter sphaeroides R-26: The protein subunits. Proc. Natl. Acad. Sci. USA. 84: 6162-6166, 1987.

Angelides, K. J., and Fink, A. L.: Cryoenzymology of Papain: Reaction Mechanism with an Ester Substrate. Biochemistry. 17:2659-2668, 1978.

Arvidsson, L., Hacksell, U., and Glennon, R. A.: Recent advances in central 5-hydroxytryptamine receptor agonist and antagonist. In: Progress In Drug Research. vol. 30. ed. by Jucker, E.. Boston, 365-471, 1986.

Baker, E. N.: Structure of Actinidin, after Refinement at 1.7 A Resolution. J. Mol. Biol.. 141: 441-484, 1980.

Baker, E. N., Boland, M. J., Colder, P. C., and Hardman, M. J.: The Specificity of Actinidin and its Relationship to the Structure of the Enzyme. Biochim. Biophys. Acta. 616: 30-34, 1980.

Baker, E. N., and Drenth, J.: The Thiol Proteases: Structure and Mechanism. In: Active Sites of Enzymes. Biological Macromolecules and Assemblies. edited by Jurnak, F. A., and McPherson, A.. pub. John Wiley and Sons, NY.. 3: 313-368, 1987.

Barkowski, S. L., Hedberg, L., and Hedberg, K.: Conformational Analysis. 10. Ethane-1,2-dithiol. Electron-Diffraction Investigation of the Molecular Structure, Conformational Composition, and Anti-gauche

Energy and Entropy Differences. Evidence for an Intramolecular S-H-S Hydrogen Bond. J. Am. Chem. Soc., 108: 6898-6902, 1986.

van Belle, D., Couplet, I., Prevost, M., and Wodak, S. J.: Calculations of Electrostatic Properties in Proteins, Analysis of Contributions from Induced Protein Dipoles. J. Mol. Biol., 198: 721-735, 1987.

Bernstein, F. C., Koetzle, T. F., Williams, G. J. B., Meyer, E.F., Brice, M. D., Rogers, J. R., Kennard, D., Simanouchi, T., and Tasumi, M.: The Protein Data Bank: A Computer-base Archival File for Macromolecular Structure. J. Mol. Biol., 112: 535-542, 1977.

Black, J. W. and Leff, P.: Operational models of pharmacological agonism. Proc. Roy. Soc. Lond. (Biol.) 220: 141-162, 1983.

Binkley, J. S., Frisch, M. J., DeFrees, D. J., Rahgavachari, K.,Whiteside, R A., Schlegel, H. B., Fluder, E. M., and Pople, J. A.: Gaussian 82, IBM version, Department of Chemistry, Carnegie-Mellon University, Pittsburgh, PA.

Binkley, J. S., Pople, J. A., and Hehre, W. J.: Self-Consistent Molecular Orbital Methods. 21. Small Split Valence Basis Set for First-Row Elements. J. Am. Chem. Soc., 102, 939-947, 1980.

Brocklehurst, K., Baines, B. S., and Malthouse, P. G.: Differences in the interactions of the catalytic groups of the active centres of actinidin and papain. Biochem. J., 197: 739-746, 1981.

Brooks, B. R., Bruccoleri, R. E., Olafson, B. D., Swaminathan, S., and Karplus, M.: CHARMM: A Program for Macromolecular Energy Minimization and Dynamics Calculations. J. Comp. Chem., 4: 187-217, 1983.

Brooks, B. and Karplus, M.: Normal modes for specific motions of macromolecules: Application to the hinge-bending mode of lysozyme. Proc. Natl. Acad. Sci. USA, 82: 4995-4999, 1985.

Bunzow, J. R., Van Tol, H. H. M., Grandy, D. K., Albert, P., Salon, J., Christie, M., Machida, C. A., Neve, K. A., and Civelli, O.: Cloning and expression of a rat D2 dopamine receptor DNA. Nature, 336: 783-787, 1988.

Burley, S. K. and Petsko, G. A.: Aromatic-Aromatic Interaction: A Mechanism of Protein Structure Stabilization. Science, 229: 23-28, 1985.

Dixon, R. A. F., Kobilka, B. K., Strader, D. J., Benovic, J. L., Dohlman, H. G., Frielle, T., Bolanowski, M. A., Bennett, C. D., Rands, E., Diehl, R. E., Mumford, R. A., Slater, E. E., Sigal, I.S., Caron, M. G., Lefkowitz, R. J., and Strader, C. D.: Cloning of the gene and cDNA for mammalian B-adrenergic receptor and homology with rhodopsin. Nature, 231: 75-79, 1986.

Drummond, M. L. J.: Quantum Calculations On Proteins: The Incorporation of Environmental Effects in Quantum Chemistry. Prog. Biophys. Molec. Biol., 47: 1-29, 1986.

van Duijnen, P. Th. and Thole, B. T.: Cooperative Effects in a-Helices: An *AB INITIO* Molecular-Orbital Study. Biopolymers, 21:1749-1761, 1982.

van Duijnen, P. Th., de Jager, J. and Thole, B. T.: Do Parallel B - Strands Have Dipole Moments? An *AB INITIO* Molecular - Orbital - Direction Reaction Field Study. Biopolymers, 24:735-745, 1985.

van Duijnen, P. Th., Thole, B. T., Broer, R., Nieuwpoort, W. C.: Active-Site α-Helix in Papain and the Stability of the Ion Pair RS-...ImH+. *AB INITIO* Molecular Orbital Study. Intl. J. Quantum Chem., XVII: 651-671, 1980.

van Duijnen, P. Th., Thole, B. Th., Hol, W. G. J.: On the Role of the Active Site Helix in Papain, An *AB INITIO* Molecular Orbital Study. Biophys. Chem., 9: 273-280, 1979.

Dupuis, M., Rys, J., and King, H. F.: Evaluation of molecular integrals over Gaussian basis functions. J. Chem. Phys., 65: 111, 1976.

Elber, R. and Karplus, M.: Multiple Conformational States of Proteins: A Molecular Dynamics Analysis of Myoglobin. Science, 235: 318-321, 1987.

Engelman, D. M., Goldman, A., and Steitz, T. A.: The Identification of Helical Segments in the Polypeptide Chain of Bacteriorhodopsin. In Packer, L. (ed.), Methods in Enzymology, Academic Press, New York, 88, pp.81-88, 1982.

Falke, J. J. and Koshland, Jr., D. E.: Global Flexibility in a Sensory Receptor: A Site-Directed Cross-Linking Approach. Science, 237: 1596-1600, 1987.

Fargin, A., Raymond, J. R., Lohse, M. J., Kobilka, B. K., Caron, M. G., and Lefkowitz, R. J.: The genomic clone G-21 which resembles a β receptor sequence encodes the 5-HT_{1a} receptor. Nature, 335: 358-360, 1988.

Fersht, A., Enzyme Structure and Mechanism, W.H. Freeman and Co., New York, 1985.

Francl, M. M., Peitro, W.J., Hehre, W. J., Binkley, J. S., Gordon, M. S., DeFrees, D. J., and Pople, J. A.: Self-Consistent Molecular Orbital Methods. 23. A Polarization-Type Basis Set for 2nd-Row Elements. J. Chem. Phys., 77: 3654-3665, 1972.

Gilson, M. K., Sharp, K. A., and Honig, B. H.: Calculating the Electrostatic Potential of Molecules in Solution. Method and Error Assessment. J. of Comp. Chem., 9: 327-335, 1988.

Gilson, M. K., Rashin, A., Fine, R., Honig, B. H.: On the Calculation of Electrostatic Interactions in Proteins. J. Mol. Biol., 183: 503-516, 1985.

Gocayne, J., Robinson, D. A., Fitzgerald, M. G., Chung, F., Kerlavage, A. R., Lentes, K., Lai, J., Wang, C., Fraser, C. M., and Venter, J. C.: Primary structure of rat cardiac B-adrenergic and muscarinic cholinergic receptors obtained by automated DNA sequence analysis: Further evidence for a multigene family. Proc. Natl. Acad. Sci. USA, 84: 8296-8300, 1987.

Goodford, P. J.: The haemoglobin molecule: is it a useful model for a drug receptor? TIPS, pp. 307-312, July, 1980.

Goodford, P. J., Louis, J. St., and Wootton, R.: The Interaction of Human-Hemoglobin with Allosteric Effectors as Model for Drug-Receptor Interactions. Br. J. Pharmac. 66: 741-748, 1980.

Gordon, M. S., Binkley, J. S., Pople, J. A., Pietro, W. J., and Hehre, W. J.: Self-Consistent Molecular-Orbital Methods. 22. Small Split-Valence Basis Sets for Second-Row Elements. J. Am. Chem. Soc., 104: 2797-2803, 1982.

Green, J. P., Johnson, C. L., Weinstein, H., Kang, S., and Chou, D.: Molecular Determinants For Interaction with the LSD Receptor: Biological Studies and Quantum Chemical Analysis. In: The Psychopharmacology of Hallucinogens, eds. Stillman, R. C. and Willette, R. E.. Pergamon Press, NY, 28-60, 1978.

Grenningloh, G., Rienitz, A., Schmitt, B., Methfessel, C., Zensen, M.,Beyreuther, K., Gundelfinger, E. D., and Betz, H.: The strychnine-binding subunit of the glycine receptor shows homology with nicotinic acetylcholine receptors. Nature, 328: 215-220, 1987.

Hariharan, P. C. and Pople, J. A.: Effects of D-Functions on Molecular Orbital Energies for Hydrocarbons, Chem. Phys. Lett., 66: 217-219, 1972.

Hartig, P. R.: Molecular biology of 5-HT receptors. TiPS, 10: 64-69, 1989.

Hehre, W. J., Ditchfield, R., and Pople, J. A.: Self-Consistent Molecular-Orbital Methods. XII. Further Extensions of Gaussian-Type Basis Sets of Use in Molecular Orbital Studies of Organic Molecules. J. Chem. Phys., 56: 2257-2261, 1972.

Hehre, W. J., Ditchfield, R., Stewart, R. F., and Pople, J. A.: Self-Consistent Molecular-Orbital Methods. IV. Use of Gaussian Expansions of Slater-Type Orbitals. Extension to Second-Row Molecules, J. Chem. Phys., 52: 2769-2773, 1970.

Hehre, W. J., Random, L., Schleyer, P. v. R., and Pople, J. A. *Ab initio* Molecular Orbital Theory, pub. John Wiley and Sons, New York, NY, pp. 311, 1986.

Hehre, W. J., Stewart, R. F., and Pople, J. A.: Self-Consistent Molecular-Orbital Method. I. Use of Gaussian Expansions of Slater-Type Atomic Orbitals, J. Chem. Phys., 51: 2657-2664, 1969.

Hinkle, P. C. and McCarty, E.: How Cells Make ATP, Scientific American, 238: 104-123, 1978.

Hol, W. G., van Duijnen, P. T., Berendsen, J. C.: The a-Helix dipole and the properties of proteins. Nature, 273: 443-446, 1978.

Holmes, R. E., Richards, G. W., and Lambros, S. A.: The Polarization of an Enzyme by an Inhibitor. The Influence of Boronic Acid on Residues in a-Chymotrypsin A. J. Mol. Struc. (THEOCHEM), 121: 273-279, 1985.

Hulme, E., and Birdsall, N.: Distinctions in acetylcholine receptor activity. Nature, 323: 396-397, 1986.

Hwang, J.-K. and Warshel, A.: Why Ion Pair reversal by protein engineering is unlikely to succeed. Nature, 334: 270-272, 1988.

Jonsson, B., Karlstrom, G., Wennerstrom, H., Roos, B.: *AB INITIO* Molecular Orbital Calculations on the Water-Carbon Dioxide System: Carbonic Acid. Chem. Phys. Let., 41: 317-320, 1976.

Karlstrom, G., Jonsson, B., Roos, B., Wennerstrom, H.: Correlation Effects on Barriers to Proton Transfer in Intramolecular Hydrogen Bonds. The Enol Tautomer of Malondialdehyde Studied by *AB INITIO* SCF-CI Calculations. J. Am. Chem. Soc., 98: 6851-6854, 1976.

Karplus, M. and McCammon, J. A.: The Dynamics of Proteins. Scientific American, 254: 42-51, 1986.

Kenakin, T. P.: Pharmacologic Analysis of Drug-Receptor Interaction. Raven Press, New York, NY. 1987.

Kobilka, B. K., Kobilka, T. S., Daniel, K., Regan, J. W., Caron, M. G., and Lefkowitz, R. J.: Chimeric α_2-β_2-Adrenergic Receptors: Delineation of

Domains Involved in Effector Coupling and Ligand Binding Specificity. Science. 240: 1310-1316, 1988.

Kobilka, B. K., Matsui, H., Kobilka, T. S., Yang-Feng, T. L.,Francke, U., Caron, M. G., Lefkowitz, R. J., and Regan, J. W.: Cloning, Sequencing, and Expression of the Gene Coding for the Human Platelet A(2)-Adrenergic Receptor. Science. 238: 650-656, 1987.

Kollman, P. A., Hayes, D. M.: Theoretical Calculations on Proton-Transfer Energetics: Studies of Methanol, Imidazole, Formic Acid, and Methanethiol as Models for the Serine and Cysteine Proteases. J. Am. Chem. Soc., 103: 2955-2961, 1981.

Kubo, T., Fukuda, K., Mikami, A., Maeda, A., Takahashi, H., Mishina,M., Haga, T., Haga, K., Ichiyama, A., Kangawa, K., Kojima, M., Matsuo, H., Hirose, T., and Numa, S.: Cloning, sequencing and expression of complementary DNA encoding the muscarinic acetylcholine receptor. Nature. 323: 411-416, 1986.

Kurnig, I. J., and Scheiner, S.: Additivity of the Effects of External Ions and Dipoles upon the Energetics of Proton Transfer. Intl. J. of Quantum Chem. Quantum Biolo. Symp., 13: 71-79, 1986.

Lester, H. A.: Heterologous Expression of Excitability Proteins: Route to More Specific Drugs? Science. 241: 1057-1063, 1988.

Leung, D. W., Spencer, S. A., Cachianes, G. Hammonds, R. G., Collins, C., Henzel, W. J., Barnard, R., Waters, M. J., and Wood, W. I.: Growth hormone receptor and serum binding protein: purification cloning and expression. Nature. 330: 537-543, 1987.

Liang, J., Lipscomb, W. N.: Transferability of Atomic Multipoles in Atomic Multipole Expansions. J. Phys. Chem., 90: 4246-4253, 1986.

Liebman, M. N., and Weinstein, H.: Heuristic studies of structure-function relationships in enzymes: carboxypeptidase and thermolysin, In: Structure and Motion: Membranes, Nucleic Acids, and Proteins, ed. by Clementi, E., Corongiu, G., Sarma, M. H., and Sarma, R. H.. pub. Adenine Press, N.Y., pp. 339-359, 1985.

Lipscomb, W. N.: A Survey of X-Ray Diffraction Studies of Enzyme-Other Molecule Interactions as Possible Models for Receptor Sites. In: Quantum Chemistry in Biomedical Sciences. H. Weinstein, and J. P. Green, eds., Annals of The New York Academy of Sciences. 367: 326-339, 1981.

Marx, J. L.: Receptors Highlighted at NIH Symposium. Science. 238: 615-616, 1987.

Masu, Y., Nakayama, K., Tamaki, H., Harada, Y., Kuno, M., and Nakanishi, S.: cDNA cloning of bovine substance-K receptor through oocyte expression system. Nature. 329: 836-838, 1987.

Mazurek, A. P., Weinstein, H., Osman, R., Topiol, S., and Ebersole, B. J.: Theoretical and Experimental Studies of Drug-Receptor Interactions: Determinants for Recognition of 5-Hydroxytryptamine Analogs. Int. J. of Quantum Chem. Quantum Biolo. Symp., 11: 183-194, 1984.

McCammon, J. A.: Computer-Aided Molecular Design. Science. 238: 486-491, 1987.

McWeeny, R. and Sutcliffe, B. T.: Methods of Molecular Quantum Mechanics, Academic Press, London and New York, 1976.

Mehler, E. L., and Paul, C. H.: Small Gaussian-Basis Sets for *AB INITIO* Calculations on Large Molecules. Chem. Phys. Let., 63:145-150, 1979.

Mercier, G. A., Dijkman, J. P., Osman, R., and Weinstein, H.: Effects of Macromolecular Environments on Proton Transfer Processes: The Calculation of Polarization. In: Quantum Chemistry: Basic Aspects, Actual Trends, edited by R. Carbo. Elsevier Scientific Publ., Amsterdam, The Netherlands., in press 1989.

Mercier, G. A., Osman, R., and Weinstein, H.: A Molecular Theoretical Model of Recognition and Activation at a 5-HT receptor. In: Proceedings of the OHOLO Conference on Computer Assisted Modeling of Receptor-Ligand Interactions, Alan R. Liss, Publ., NY, NY. pp. 399-410, 1988 (a).

Mercier, Jr., G. A., Osman, R., and Weinstein, H.: Role of primary and secondary protein structure in neurotransmitter receptor activation mechanisms. Prot. Eng., 2: 261-270, 1988 (b).

Middlemiss, D. N., Hibert, M., and Fozard, J. R.: Drugs Acting at Central 5-Hydroxytryptamine Receptors. Chapter 5 in: Annual Reports of Medicinal Chemistry - 21, edited by D. M. Bailey, editor-in-chief, and B. Hesp, section editor. Academic Press, Inc. NY, NY. pp. 41-50, 1986.

Osman, R., Topiol, S., Rubenstein, L., and Weinstein, H.: A Molecular Model for Activation of a 5-Hydroxytryptamine Receptor. Molec. Pharmc., 32: 699-705, 1987.

Osman, R., Topiol, S., and Weinstein, H.: Electron Density Redistribution in the Stabilization of a Molecular Stacking Complex: The Nature and Correction of Basis Set Superposition Error. J. of Comput. Chem., 2: 73-82, 1981.

Osman, R., Topiol, S., Weinstein, H., and Eilers, J. E.: Theoretical Studies of Molecular Complexes: A Probe Into Basis Set and Correlation Effects. Chem. Phys. Lett., 73: 399-403, 1980.

Osman, R., Weinstein, H., and Green, J. P.: Parameters and Methods in Quantitative Structure-Activity Relationships. In: Olson, E. C. and Christoffersen, R. E., eds., ACS Symposium Series, No. 112, Computer-Assisted Drug Design, 1979.

Osman, R., Weinstein, H., Topiol, S., and Rubenstein, L.: A Molecular Theory of Recognition and Activation at a 5-HT Receptor Based on a Quantum Chemical Approach to Structure Activity Relationships. Clin. Physiol. Biochem., 3: 80-88, 1985.

Peroutka, S. J.: 5-hydroxytryptamine Receptor Subtypes. Ann. Rev. Neurosci., 11: 45-60, 1988.

Pietro, W. J., Francl, M. M., Hehre, W. J., DeFrees, D. J., Pople,J. A., and Binkley, J. S.: Self-Consistent Molecular Orbital Methods. 24.

Supplemented Small Split-Valence Basis Sets for Second-Row Elements. J. Am. Chem. Soc., 104: 5039-5048, 1982.

Polgar, L. and Halasz, P.: Current Problems in mechanistic studies of serine and cysteine proteinases. Biochem. J., 207: 1-10, 1982.

Pritchett, D. B., Bach, A. W., Wozny, M., Taleb, O., Dal Toso, R., Shih, J. C., and Seeburg, P. H.: Structure and functional expression of cloned rat serotonin 5-HT_2 receptor. The EMBOL J., 7: 4135-4140, 1988.

Rashin, A., Iofin, M., and Honig, B.: Internal Cavities and Buried Waters in Globular Proteins. Biochemistry, 25: 3619-3625, 1986.

Rashin, A., and Namboodiri, K.: A Simple Method for the Calculation of Hydration Enthalpies of Polar Molecules with Arbitrary Shapes. J. Phys. Chem., 91: 6003-6012, 1987.

Richardson, J. S.: The Anatomy and Taxonomy of Protein Structure. In: Advances in Protein Chemistry, eds. C. B. Anfinsen, J. T. Edsall, and F. M. Richards. pub. Academic Press, New York. vol. 34, pp. 167-339, 1981.

Reggio P. H., Weinstein, H., Osman, R., and Topiol S.: Molecular Determinants for Binding of Methylenedioxytryptamines at 5-HT/LSD Receptors. Intl. J. Quantum Chem.: Quantum Biolo. Symp., 8: 373-384, 1981.

Scheiner, S.: Proton transfer between first and second-row atoms: $(H_2OHSH_2)^+$ and $(H_3NHSH_2)^+$. J. Chem. Phys., 80: 1982-1987, 1984.

Scheiner, S.: Theoretical studies of proton transfer. Acc. Chem. Res., 18: 174-180, 1985.

Scheiner, S. and Hillenbrand E. A.: Comparison between Proton Transfers Involving Carbonyl and Hydroxyl Oxygens. J. Phys. Chem., 89: 3053-3060, 1985.

Scheiner, S., Redfern, P., and Szczesniak, M. M.: Effects of External Ions on the Energetics of Proton Transfer across Hydrogen Bonds, J. Phys. Chem., 89: 262-266, 1985.

Scheiner, S., Redfern, P., and Hillebrand, E. A.: Factors Influencing Proton Positions in Biomolecules, Intl. J. Quantum Chem., XXIX: 817-827, 1986.

Schofield, P. R., Darlison, M. G., Fujita, N., Burt, D. R.,Stephenson, F. A., Rodriguez, H., Rhee, L. M., Ramachandran, J.,Reale, V., Glencorse, T. A., Seeburg, P. H., and Barnard, E. A.: Sequence and functional expression of the GABA(A) receptor shows a ligand-gated receptor super-family. Nature, 328: 221-227, 1987.

Shenker, A., Maayani, S., Weinstein, H., and Green J. P.: Two 5-HT Receptors Linked to Adenylate Cyclase in Guinea Pig Hippocampus are Discriminated by 5-Carboxyamidotryptamine and Spiperone. Eur. J. of Pharmacol., 109: 427-429, 1985.

Shenker, A., Maayani, S., Weinstein, H., and Green J. P.: Pharmacological Characterization of Two 5-Hydroxytryptamine Receptors Coupled to Adenylate Cyclase in Guinea Pig Hippocampal Membranes. Mol. Pharm., 31: 357-367, 1987.

Shinitzky M. and Katchalski, E.: Complexes between Indole and Imidazole Derivatives of the Charge-Transfer Type. In: Molecular Associations in Biology, edited by Pullman, B., Academy Press, NY, NY., pp-361-376, 1968.

Stevens, C. F.: AChRs: five-fold symmetry and the e-subunit. TINS, 8: 335-336, 1985.

Stevens, C. F.: Channel families in the brain. Nature, 328:198-199, 1987.

Stryer, L.: Biochemistry, 2nd Ed., W.H. Freeman and Co., San Francisco, 1981.

Szczesniak, M. M., Scheiner, S.: Effects of External Ions on the Dynamics of Proton Transfer across Hydrogen Bonds. J. Phys. Chem., 89: 1835-1840, 1985.

Tapia, O. and Goscinski, O.: Self-consistent reaction field theory of solvent effects. Mol. Phys., 29: 1653-1661, 1975.

Tapia, O. and Johannin, G.: An inhomogeneous self-consistent reaction field theory of protein core effects. Towards a quantum scheme for describing enzyme reactions, J. Chem. Phys., 75: 3624-3635, 1981.

Tapia, O., Stamato, F. M. L. G., and Smyers, Y. G.: Modelling Active site Response Towards Changes in the Protein-Core Serine Proteases. A CNDO/2-INDO SCRF Study of Subtilisin and Thiosubtilisin. J. Mol. Struc. (THEOCHEM), 123: 67-84, 1985.

Thole, B. T.: Molecular Polarizabilities Calculated with a Modified Dipole Interaction. Chemical Physics., 59: 341-350, 1981.

Thole, B. T., and van Duijnen, P. T.: On the Quantum Mechanical Treatment of Solvent Effects. Theoret. Chim. Acta (Berl.), 55: 307-318, 1980.

Thole, B.T. and van Duijnen, P. T.: The Direct Reaction Field Hamiltonian: Analysis of The Dispersion Term and Application to the Water Dimer. Chemical Physics., 71: 211-220, 1982.

Thole, B. T., van Duijnen, P. T.: Reaction Field Effects on Proton Transfer in the Active Site of Actinidin. Biophys. Chem., 18: 53-59, 1983 (a).

Thole, B. T., van Duijnen, P. Th.: A General Population Analysis Preserving the Dipole Moment. Theoret. Chim. Acta (Berl.), 63: 209-221, 1983 (b).

Thole, B.T. and van Duijnen, P. T.: Reaction Field Effects on Proton Transfer in the Active Site of Actinidin, Theoret. Chim. Acta (Berl.), 63: 209-221, 1983.

Topiol, S., Mercier, G., Osman, R., and Weinstein, H.: Computational Schemes for Modeling Proton Transfer in Biological Systems:

Calculations on the Hydrogen Bonded Complex $[CH_3OH . H . NH_3]^+$. J. Comp. Chem., 6: 581-586, 1985.

Trowbridge, I.: Interleukin-2 receptor proteins. Nature, 327:461-462, 1987.

Yeates, T. O., Komiya, H., Rees, D. C., Allen, J. P., and Feher, G.: Structure of the reaction center from Rhodobacter sphaeroides R-26: Membrane-protein interactions. Proc. Natl. Acad. Sci., USA, 84: 6438-6442, 1987

Umeyama, H., Hirono, S., and Nakagawa, S.: Charge state of His-57 - Asp 102 couple in a transition state analogue-trypsin complex: A molecular orbital study. Proc. Natl. Acad. Sci. USA, 81: 6266-6270, 1984.

Warshel, A.: Electrostatic Basis of Structure-Function Correlation in Proteins. Acc. Chem. Res., 14: 284-290, 1981 (a).

Warshel, A.: Dynamics of enzymatic reactions. Proc. Natl. Acad. Sci. USA, 81: 444-448, 1984.

Warshel A.: What about protein polarity? in News and Views Section. Nature, 330: 15-16, 1987.

Warshel, A.: Calculations of Enzymatic Reactions: Calculations of pKa, Proton Transfer Reactions, and General Acid Catalysis Reactions in Enzymes. Biochemistry, 20: 3167-3177, 1981 (b).

Warshel, A. and Levitt, M.: Theoretical Studies of Enzymic Reactions: Dielectric, Electrostatic and Steric Stabilization of the Carbonium Ion in the Reaction of Lysozyme. J. Mol. Biol., 103: 227-249, 1976.

Warshel, A., and Russell, S. T.: Calculations of electrostatic interactions in biological systems and in solutions. Q. Rev. of Biophys., 17: 283-422, 1984.

Warshel, A., Sussman, F., and Hwang, J.: Evaluation of Catalytic Free Energies in Genetically Modified Proteins. J. Mol. Biol., 201: 139-159, 1988.

Weinstein, H., Chou, D., Kang, S., Johnson, C. L., and Green, J. P.: Reactivity Characteristics of Large Molecules and Their Biological Activity: Indolealkylamines on the LSD/Serotonin Receptor. Intl. J Quantum Chem. Quantum Biolo. Symp., 3: 135-150, 1976.

Weinstein, H., Eilers, J. E., and Chang, S.: A Modified Hamiltonian Method For the Study of Multiple Site Reactivity: Comparison with Perturbation Results. Chem. Phys. Let., 51: 534-539, 1977.

Weinstein, H., Green, J. P., Osman, R., and Edwards, W. D.: Recognition and Activation Mechanisms on the LSD/Serotonin Receptor: The Molecular Basis of Structure Activity Relationships. In: 'QuaSAR' Research Monograph 22, edited by Barnett, G., Trsic, M., and Willette, R.. National Institute on Drug Abuse. pp. 333-358, 1978 (a).

Weinstein, H., Liebman, M. N., and Venanzi, C. A.: Theoretical principles of drug action: The use of enzymes to model receptor recognition and activity. In Makriyannis, A. (ed.), New Methods in Drug Research, J. R. Prous, S. A. Publishers, Barcelona, pp. 233-246, 1985.

Weisntein, H. and Osman, R: Models for Molecular Mechanisms in Drug-Receptor Interactions. Serotonin and 5-Hydroxyindole Complexes with Imidazolium Cation. Int. J. of Quantum Chem. Quantum Biolo. Symp., 4:253-268, 1977.

Weinstein, H., Osman, R., Edwards, W. D., and Green, J. P.: Theoretical Models for Molecular Mechanisms in Biological Systems: Tryptamine Congeners Acting on an LSD-Serotonin Receptor. Int. J. of Quantum Chem. Quantum Biolo. Symp., 5:449-461, 1978 (b).

Weinstein, H., Osman, R., Green, J. P., and Topiol, S.: Electrostatic Potentials as Descriptors of Molecular Reactivity: The Basis For Some Successful Predictions of Biological Activity. In: Chemical Applications of Atomic and Molecular Electrostatic Potentials, edited by Peter Politzer and Donald G. Truhlar, Plenum Publishing Corporation, NY, NY. pp 309-323, 1981 (a).

Weinstein, H., Osman, R., and Mazurek, A. P.: Simulations of molecular stereoelectronic mechanisms for the interaction of hallucinogens and indole derivatives at 5-HT receptors. In Naray-Szabo, G. and Kalman, S. eds., Steric Aspects of Biomolecular Interactions, CRC Press, Boca Raton Florida, pp. 199-210, 1987.

Weinstein, H., Osman, R., and Mercier, Jr., G. A.: Recognition and Activation of a 5-HT Receptor by Hallucinogens and Indole derivatives. In: NIDA Research Monograph no. 90, Proc. 50th Annual Meeting, Problems of Drug Dependence, edited by L. S. Harris, U.S. Dept. of Health and Human Services, pp. 243-255, 1988.

Weinstein, H., Osman, R., Topiol, S., and Green, J. P.: Quantum Chemical Studies on Molecular Determinants for Drug Action. In: Quantum Chemistry in Biomedical Sciences, edited by Weinstein, H. and Green, J. P. Annals of the New York Academy of Sciences, vol. 367, pp. 434-451, 1981 (b).

Wells J. A., Powers, D. B., Bott, R. R., Graycar, T. P., and Estell, D. A.: Designing substrate specificity by protein engineering of electrostatic interactions. Proc. Natl. Acad. Sci. USA, 84: 1219-1223, 1987.

Yeates, T. O., Komiya, H., Rees, D. C., Allen, J. P., and Feher, G.: Structure of the reaction center from Rhodobacter sphaeroides R-26: Membrane-protein interactions. Proc. Natl. Acad. Sci., USA, 84: 6438-6442, 1987

Zauhar, R. J., and Morgan, R. S.: The Rigorous Computation of the Molecular Electrostatic Potential. J. of Comp. Chem., 9: 171-187, 1988.